| VOLUMEN 44 | NUMBER 2 | **MAY-AUGUST 2023**

ib

Una publicación de:
SOMIB
Sociedad Mexicana
de Ingeniería Biomédica

Revista Mexicana de Ingeniería Biomédica

Modalidad de publicación

***Publicación continua*:**
una vez que se acepta y prepara un manuscrito, se publicará en línea

Publication Modality

***Continuous publication*:**
once a manuscript is accepted and prepared, it will be released online

http://www.rmib.mx

ISSN 2395-9126

SOMIB
Sociedad Mexicana
de Ingeniería Biomédica

Sociedad Mexicana de Ingeniería Biomédica

La Mesa Directiva de la Sociedad Mexicana de Ingeniería Biomédica hace una extensa invitación a las personas interesadas en participar, colaborar y pertenecer como Socio Activo de la SOMIB. La SOMIB reúne a profesionistas que se desarrollan en áreas de Ingeniería Biomédica, principalmente ingenieros biomédicos, así como otros profesionistas afines con el desarrollo de tecnología para la salud.

Membresía Estudiante
$1,400.00 ***PESOS MXN***
15% de descuento para grupos de 5 o más personas.

Membresía Profesionista
$2,400.00 ***PESOS MXN***
15% de descuento para grupos de 5 o más personas.

Membresía Institucional
$11,600.00 ***PESOS MXN***
No aplica descuento.

Membresía Empresarial
$20,000.00 ***PESOS MXN***
No aplica descuento.

EL PAGO CUBRE UN AÑO DE CUOTA. EN CASO DE REQUERIR FACTURA
FAVOR DE SOLICITARLA, ADJUNTANDO COMPROBANTE DE PAGO Y ESPECIFICANDO CONCEPTO,
AL CORREO ELECTRÓNICO: ***gerencia@somib.org.mx***

Revista Mexicana de Ingeniería Biomédica

AUTORES

Los trabajos a publicar en la RMIB, deben ser originales, inéditos y de excelencia. Los costos de publicación para autores son los siguientes:

NO SOCIOS:	***$200*** ***DÓLARES AMERICANOS***
SOCIOS:	***$150*** ***DÓLARES AMERICANOS***

PUBLICIDAD

A las empresas e instituciones interesadas en publicitar su marca o productos en la RMIB, los costos por número son los siguientes:

MEDIA PLANA:	***$4,999.00*** ***PESOS MXN*** *(INCLUYE I.V.A.)*
UNA PLANA:	***$6,799.00*** ***PESOS MXN*** *(INCLUYE I.V.A.)*
CONTRAPORTADA:	***$7,799.00*** ***PESOS MXN*** *(INCLUYE I.V.A.)*
FORROS INTERIORES:	***$7,799.00*** ***PESOS MXN*** *(INCLUYE I.V.A.)*

DESCUENTO DEL **20%** AL CONTRATAR PUBLICIDAD EN DOS O MÁS NÚMEROS.

Para ser socio

- Realiza el pago de derechos, de acuerdo a la categoría que te corresponde.
- Ingresa a *www.somib.org.mx/membresias* y elige el tipo de membresía por el cual realizaste el pago de derechos.
- Completa el formulario correspondiente y envíalo.
- Se emitirá carta de aceptación y número de socio por parte de la mesa directiva (aprobada la solicitud).
- Para mayor información sobre beneficios, ingresa a *www.somib.org.mx*; o escribe a *gerencia@somib.org.mx*.

Datos bancarios

- **Beneficiario:** *Sociedad Mexicana de Ingeniería Biomédica A. C.*
- **Banco:** *Scotiabank*
- **Referencia:** *1000000333*
- **Cuenta:** *11006665861*
- **CLABE Interbancaria:** *044770110066658614*

INFORMES

Juan Vázquez de Mella #481,
Polanco I Sección,
Alc. Miguel Hidalgo, C. P. 11510,
Ciudad de México, México,
(555) 574-4505
rib.somib@gmail.com

Revista Mexicana de Ingeniería Biomédica

Índices
La Revista Mexicana de Ingeniería Biomédica aparece en los siguientes índices científicos:
Sistema de Clasificación de Revistas Científicas y Tecnologías del CONACYT - Q4, SCOPUS, SciELO, EBSCO, LATINDEX, Medigraphic Literatura Biomedica, Sociedad Iberoamericana de Información Científica - SIIC.

www.rmib.mx
ISSN 2395-9126

Asistente Editorial
Carla Ivonne Guerrero Robles

Editor Técnico y en Internet
Sandra Sánchez Jáuregui

SOMIB Sociedad Mexicana de Ingeniería Biomédica

Sociedad Mexicana de Ingeniería Biomédica
Juan Vázquez de Mella #481, Polanco I Sección, Alc. Miguel Hidalgo, C. P. 11510, Ciudad de México, México, (555) 574-4505

Afiliada a:
International Federation of Medical and Biological Engineering (IFMB-IUPSM-ICSU)
Federación de Sociedades Científicas de México, A.C. (FESOCIME)
Consejo Regional de Ingeniería Biomédica para América Latina (CORAL)

SOMIB
Juan Vázquez de Mella #481, Polanco I Sección, Alc. Miguel Hidalgo, C. P. 11510, Ciudad de México, México (555) 574-4505
www.somib.org.mx

REVISTA MEXICANA DE INGENIERÍA BIOMÉDICA, Vol. 44, No. 2, Mayo-Agosto 2023, es una publicación cuatrimestral editada por la Sociedad Mexicana de Ingeniería Biomédica A.C., Juan Vázquez de Mella #481, Polanco I Sección, Alc. Miguel Hidalgo, C. P. 11510, Ciudad de México, México, (555) 574-4505, www.somib.org.mx, rib.somib@gmail.com. Editora responsable: Dra. Dora-Luz Flores. Reserva de Derechos al Uso Exclusivo No. 04-2015-041310063800-203, ISSN (impreso) 0188-9532; ISSN (electrónico) 2395-9126, ambos otorgados por el Instituto Nacional del Derecho de Autor. Responsable de la última actualización de este número: Lic. Sandra Sánchez Jáuregui, Juan Vázquez de Mella #481, Polanco I Sección, Alc. Miguel Hidalgo, C. P. 11510, Ciudad de México, México, (555) 574-4505, fecha de última modificación, 31 de agosto del 2023.

Disponible en línea:
www.rmib.mx

CONTENTS
CONTENIDO

RESEARCH ARTICLE

VOL. 44 | NO. 2 | **MAY - AUGUST 2023** | PP 6-15

Revista Mexicana de Ingeniería Biomédica

dx.doi.org/10.17488/RMIB.44.2.1

E-LOCATION ID: 1338

Type of Feet in a Mexican Population: Analysis of the Footprint Morphology and Literature Review

Tipos de pies en una Población Mexicana: Análisis de la Morfología de la Huella Plantar y Revisión de la Literatura

Jorge Armando Ramos-Frutos[1], *Israel Miguel-Andrés*[2], *Miguel León-Rodríguez*[3], *Luis Angel Ortiz-Lango*[2], *Sergio Luis Orozco-Villaseñor*[2], *Agustín Vidal-Lesso*[4].

[1]Posgrado Interinstitucional en Ciencia y Tecnología PICYT-CONACYT - México

[2]Centro de Innovación Aplicada en Tecnologías Competitivas (CIATEC, A.C.) - México

[3] Universidad Politécnica de Guanajuato, Campus Cortazar - México

[4] Universidad de Guanajuato - México

ABSTRACT

There is no specific age when the vault of the feet is completely formed. The objective of this study was to analyze the footprint morphology and obtain the Chippaux-Smirak Index in a Mexican population to identify the type of feet and its prevalence. A database of images of the soles of both feet was analyzed. The database contained images of 1,014 persons between 2 and 73 years old from Guanajuato state, Mexico. Moreover, a literature review was performed to identify the type of feet in the Mexican population. It was observed that less than 17 % of the population have cavus foot (p= 0.018). Furthermore, less than 25 % of the population between 17 and 73 years have flatfoot 3 (p= 0.0079) in the left foot. Also, only nine articles related to the type of foot in the Mexican population were found, but most of them were performed on young population. The formation of the medial arc could be beyond the first decade of life and the relatively high prevalence of flatfoot in adult life should be studied. Finally, the results found can be useful for orthopedists, physiotherapists, clinicians, and parents who are concerned about the foot health of their childre.

KEYWORDS: Flatfoot, cavus foot, normal foot, footprint, Chippaux-Smirak Index

RESUMEN

No hay una edad específica en la que la bóveda de los pies esté completamente formada. El objetivo de este estudio fue analizar la morfología de la huella de los pies y obtener el Índice de Chippaux-Smirak en una población mexicana para identificar el tipo de pie y su prevalencia. Se analizó una base de datos de imágenes de las plantas de ambos pies. La base de datos contenía imágenes de 1,014 personas de entre 2 y 73 años del estado de Guanajuato, México. Además, se realizó una revisión bibliográfica para identificar el tipo de pie en la población mexicana. Se observó que menos del 17 % de la población tiene pie cavo (p= 0,018). Además, menos del 25 % de la población entre 17 y 73 años tiene pie plano 3 (p= 0,0079) en el pie izquierdo. Además, se encontraron 9 artículos relacionados con el tipo de pie en población mexicana, pero la mayoría de ellos fueron desarrollados en población joven. La formación del arco medial podría estar más allá de la primera década de vida. Se encontró una prevalencia relativamente alta de pie plano en la vida adulta que debe ser estudiada. Finalmente, los resultados encontrados pueden ser útiles para ortopedistas, fisioterapeutas, médicos y padres preocupados por la salud de los pies de sus hijos.

PALABRAS CLAVE: Pie plano, pie cavo, pie normal, huella plantar, Índice Chippaux-Smirak

Corresponding author

TO: **Israel Miguel Andrés**

INSTITUTION: **Centro de Innovación Aplicada en Tecnologías Competitivas (CIATEC, A.C.)**

ADDRESS: **Omega 201, Col. Industrial Delta, C.P. 37545, León, Guanajuato, México.**

CORREO ELECTRÓNICO: **imiguel@ciatec.mx**

Received:

10 February 2023

Accepted:

12 April 2023

INTRODUCTION

The foot is one of the most complex parts of the human body, its structure integrated by ligaments, tendons, muscles, and bones, allows it to meet the demands of support and locomotion of the human [1]. The vault of the feet plays an important role in gait biomechanics, it reduces the impact loads from the ground to the body and keeps the correct alinement of the foot. Therefore, the modification to this structure will modify these functions [2]. The collapse of this vault is known as flatfoot. All children are born with flat feet [3], the formation of the medial plantar arc occurs naturally and it is generally until 5 or 6 years of age when the medial arch is adequately defined [4]. However, in some cases, the flatfoot deformity can stay until the first decade of life or after [2] [5] [6]. The etiology or the specific causes that produce flatfoot are unknown, and it is still a topic of debate nowadays [2] [5] [6] [7]. It has not been found a specific age when the vault of the feet is completely formed. In addition, when the formation of the vault of the feet in children is delayed becomes a common concern of parents.

On the other hand, the cavus foot (hollow foot) is the enlargement of the vault of the feet, increasing the contact on the anterior and posterior regions of the foot. This deformity is not a common pathology in the population. However, it has been reported an increment in the prevalence of cavus foot in athletes, especially in women [8] [9] [10] [11].

Although there are different studies about the morphology of the soles of the feet [2] [12] [13] [14] [15] [16] [17], to the best of our knowledge there is no research about the type of feet in a Mexican population from an early stage to adulthood. The true prevalence of the morphology of the feet in a Mexican population of all ages is unknown. It is known that the modification of any part of the structure of the foot will modify its biomechanics and generate injuries in the same structure and other parts of the body [2] [18] [19]. Therefore, the objective of this study is to analyze the morphology of the soles of the feet and obtain the Chippaux-Smirak Index (CSI) in a Mexican population to identify the type of feet and the prevalence of musculoskeletal disorders of the foot.

Literature review of the type of foot in the Mexican population

In order to validate the lack of knowledge about the type of feet in the Mexican population from the early stage to adulthood, a search of information related to the type of feet in a Mexican population was conducted. Search engines such as, Google scholar (n= 157), Scopus (n= 0), ScienceDirect (n= 6), and Scielo (n= 0) were used with the following search equation in English and Spanish: "Type of foot" AND "Footprint" AND "Mexican". The literature review was performed up to the 11th of January 2023. The equation gave a total of 163 studies, but not all of them related to the analysis of the soles of the feet to detect the morphology of the foot in a Mexican population. After reviewing the articles, duplicated manuscripts, theses, books, studies from different countries, and conference proceedings were excluded from the analysis, having a final number of 9 articles, [2] [3] [8] [10] [14] [15] [20] [21] [22]. Most of the studies are performed in a limited period of time and most of them are performed in young population [2] [3] [10] [14] [15] [20].

It is known that the increase or reduction of the medial arch of the foot could affect the biomechanics of the foot. The maturation of the vault of the foot occurs naturally and most of the time this happens in the first decade of life. Moreover, it is a common concern of parents when they notice that the medial longitudinal arch of the foot remains collapsed after the first decade of life. In Mexico, different studies have been performed to identify the type of foot, but most of them were developed in a young population, 2-5 and 6-12 years [3], 6-14 years [14], 9-11 years [20], 6-15 years [15], 6-13 years [10], and 3-6 years [2]. Although there are different studies of the type of foot in the Mexican

population, most of them are performed when the vault of the foot seems to be not completely matured. There were just two studies performed on athletes with a larger range of ages from 9 to 20 years old [8] [22]. In the study performed by Miguel *et al.*, it was found a high prevalence of cavus foot in women [8].

MATERIALS AND METHODS

A database of images of the soles of both feet was analyzed. The database contained images of one thousand and fourteen persons between 2 and 73 years old, all of them from Guanajuato state, Mexico. The images were acquired between April 2017 and February 2022. The soles of the feet of the participants were digitized with a 2D foot scanner (Sensormedica, Guidonia Montecelio, Rome, Italy). There were 544 (53.6 %) females and 470 (46.4 %) males in the database.

To classify the type of foot, the CSI was obtained in both feet [23], as shown in Figure 1a. The digitized images of the soles of the feet were analyzed in MATLAB R2015a version 8.5.0.197613. Matlab specific tools (ginput, GUI, imread) were used to locate the coordinate points in the image plane [8] [24] [25]. This process was performed manually by the same author to secure repeatability.

Once the soles of the feet were measured (medial and forefoot region), they were classified based on the Chippaux-Smirak Index (CSI) into six different types of feet, cavus foot, extreme cavus, normal foot, flatfoot 1°, flatfoot 2° and flatfoot 3°. For the cavus foot, the CSI was $0 < CSI < 0.25$, for the extreme cavus the CSI was 0, for the normal foot the CSI was $0.25 \leq CSI < 0.45$, for the flatfoot 1° the CSI was $0.45 \leq CSI < 0.5$, for the flatfoot 2° the CSI was $0.5 \leq CSI \leq 0.6$ and for the flatfoot 3° the CSI was $CSI > 0.6$ [8] [13] [23] [26] [27].

The database images were classified into groups of three years starting from 2 years until 73 years, as shown in Figure 1b. The minimum number of participants per group was 22 and the maximum was 68.

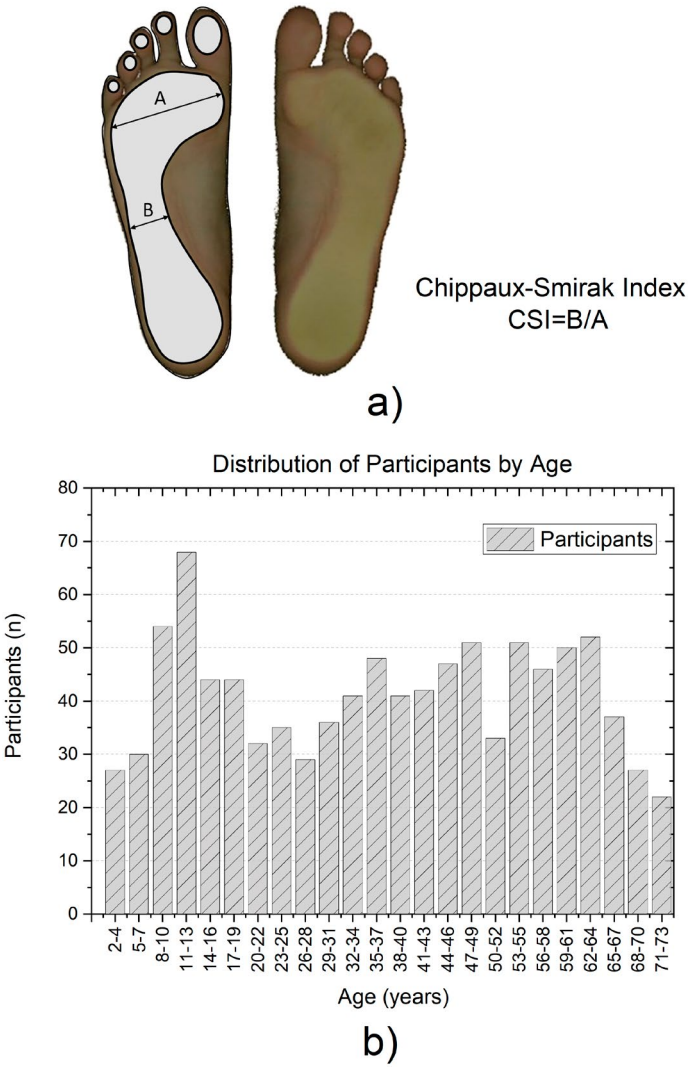

FIGURE 1. Morphology of the soles of the feet: a) Chippaux-Smirak Index and b) Distribution of participants by age.

RESULTS AND DISCUSSION

Footprint data analysis

The results show that the prevalence of flatfoot is higher during the first decade of life and decreases after that (see Figure 2). This information will be useful for orthopedic technicians and parents who are worried about the health of their children. Moreover, health professionals such as orthopedists could use the information to detect if the development of the foot structure is normal according to the age of the patient.

Figure 2 describes the different types of flatfoot (left foot), being the flatfoot 3° where the contact surface is the highest. The prevalence of the different types of flat feet from Figure 2 shows that most of the participants have flatfoot 3° until 10 years of age. From that age, the medial arc begins to elevate and the contact surface decreases. The flatfoot never completely disappears, there was a relatively small percentage of prevalence 10-20 % for the three types of flatfoot between the ages of 32 and 55 years. Between the ages of 65 and 67 years, there is a small increment of the prevalence of flatfoot 1°.

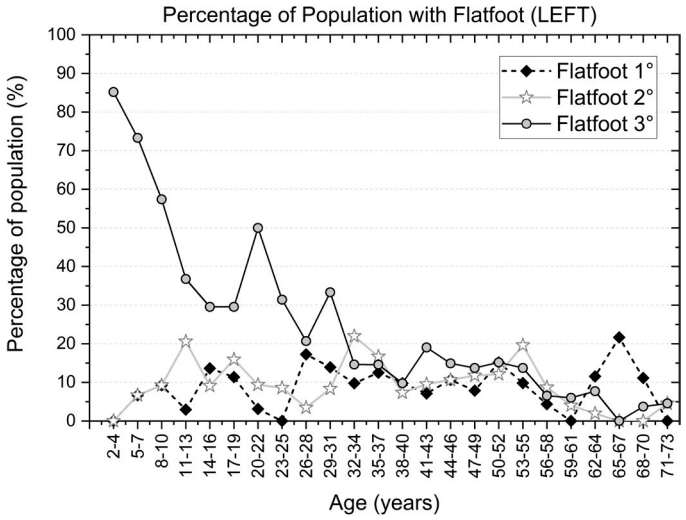

FIGURE 2. Prevalence of different types of flat feet in a Mexican population: Data from the left foot.

The CSI for the normal foot was considered between 0.25 and 0.45. A lower value of the CSI was considered as cavus foot, and when the contact surface of the medial region disappears the foot was categorized as extreme cavus (CSI = 0). Figure 3 presents the data distribution of the normal foot, cavus foot, and extreme cavus for all ages (left foot). From Figure 3, it can be seen that the normal foot begins with a low percentage of prevalence, and increases from 10 years of age. The cavus foot and extreme cavus stay most of the time below 10 % for all ages.

Similarly, the analysis of the morphology of the soles of the feet in the right foot follows a comparable trend that the left foot. Figure 4 shows that the prevalence of flatfoot 3° stays high until 16 years, then it decreases until 19 years and stays close to 30 % until 40 years. This behavior is different from the left foot. Furthermore, flatfoot 1° and 2° stay most of the time below 20 % for all ages, as shown in Figure 4. The data from Figure 2 and 4 demonstrate that both feet (left and right feet) are not completely symmetrical.

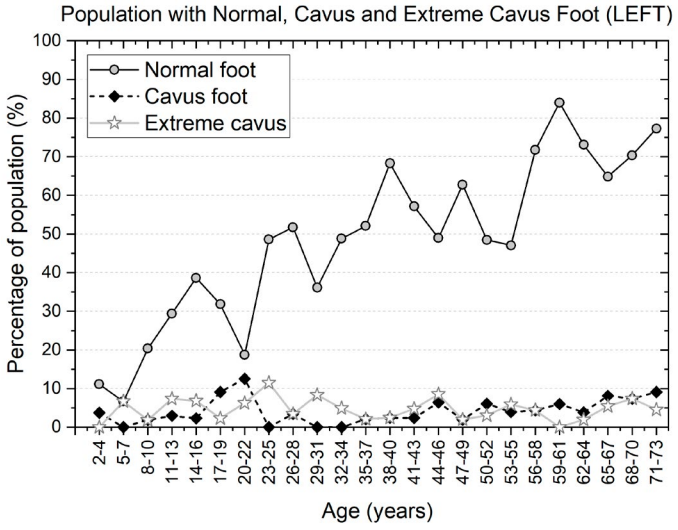

FIGURE 3. Prevalence of population with the normal foot, cavus foot, and extreme cavus: Data from the left foot.

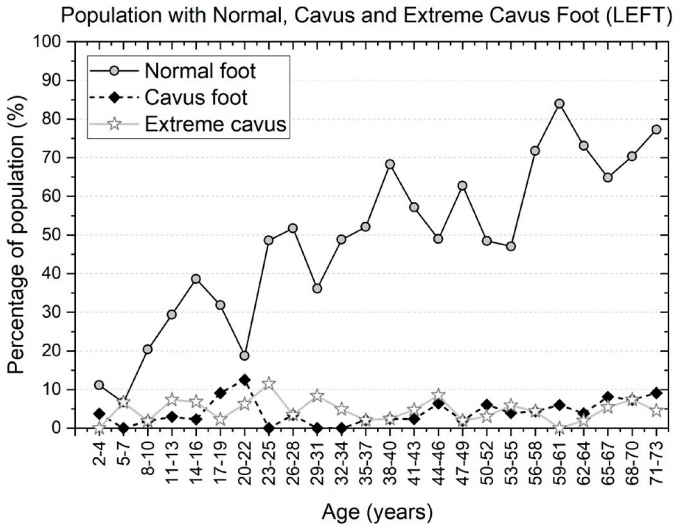

FIGURE 4. Prevalence of different types of flat feet in a Mexican population: Data from the right foot.

Figure 5 shows the prevalence of normal foot, cavus foot, and extreme cavus of the right foot. The normal foot stays less than 10 % when the participants are less than 10 years old and increases beyond 20 % when the participants are older than 11 years old, as shown in Figure 5. The prevalence of cavus foot and extreme cavus is most of the time less than 10 % for all ages.

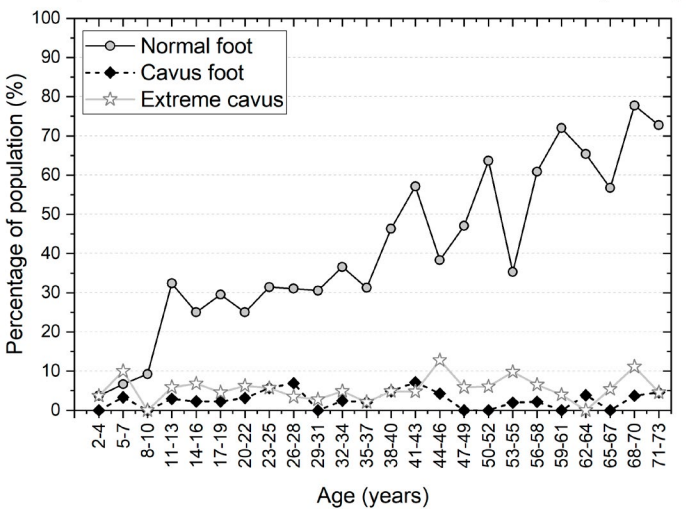

FIGURE 5. Prevalence of population with the normal foot, cavus foot, and extreme cavus: Data from the right foot.

Finally, in order to validate about the prevalence of the type of foot for people over 17 and under 73 years, a statistical analysis using a z-test for proportions was performed for the morphologies of cavus and flat feet, in the left foot. It was considered a confidence interval of 95 % and a p-value of 0.05. For cavus foot, it was observed that less than 17 % of the population have this morphology ($p = 0.018$). For flatfoot 1 and flatfoot 2, the p-values were 0.0168 and 0.0065, respectively, proving that the proportion of the population with these two morphologies is less than 16 %. For flatfoot 3 the proportion was less than 25 %, obtaining a p-value of 0.0079. For the right foot, it was performed the same statistical analysis, obtaining p-values less than 0.05 for the same percentages in the cavus foot and the three types of flatfoot.

From the results and at least for the Mexican population, the idea that at 3-5 years [5], 5-6 years [4], 10 years [2] [6] or 12-13 years [28] the vault of the feet would already be formed seems to be inaccurate. From the results found in the analysis, the maturation of the vault of the feet in a Mexican population seems to be beyond the first decade of life. Moreover, there is a health problem related to the morphology of the feet in the adult Mexican population that needs to be carefully studied. Further research needs to be done to study the effect of these musculoskeletal disorders on the gait biomechanics and how the quality of life of the Mexican population is affected. It has been found that the morphology of the soles of the feet could have an effect on the plantar pressure distribution and this could be a risk factor for producing musculoskeletal disorders [22]. Furthermore, it has been reported that the deformities of flatfoot and cavus foot could negatively influence productivity in adult life [29].

This information will be useful to clarify that the medial arc of the foot could have a delay, and for the Mexican population, the formation of the vault takes more time than the already reported by other authors [2] [4] [5] [6]. Therefore, parents should not be worried if children present flatfoot pathology at an early stage unless the pathology produces pain or discomfort. Moreover, it has been reported that there is no treatment, orthopedic device, external force, or insoles that help to form the medial arc [6] [28] [30].

It has been found that flatfoot is related to overweight and obesity [13] [15] [20]. Mexico has serious problems with overweight and obesity. According to the National Survey of Health and Nutrition (ENSANUT Spanish abbreviation, Guanajuato 2006-2018), it was established that overweight and obesity in boys and girls between 5 and 11 years old have increased from 27.8 % in 2006 to 45.1 % in 2018 in the state of Guanajuato. In adolescents, between 12 and 19 years old, overweight and obesity increased from 34 % in 2006 to 38.1 % in 2018. Although some studies have found that the prevalence of flatfoot is related to overweight or obesity [15] [20], other studies have found that body weight does

not affect plantar footprint alterations [10].

Although our results of the prevalence of cavus foot (less than 10 %) were not higher than the flatfoot in the young population, the values were similar to Aco Luna *et al.*, [10]. However, our values of the cavus foot were lower than the values found by Gonzalez *et al.*, [31] and Espinoza *et al.*, [32]. Although it was found that cavus foot is a pathology with low prevalence, some studies have developed personalized insoles for the treatment of cavus foot and comorbidities [33]. Contrary to our results, other authors have found a high prevalence in cavus foot (hollow foot) in children between 3 to 13 years [34]. It is difficult to compare our results with other studies because they used a different methodology and/or the anthropometric features of the population could be different.

The results of flatfoot (10-20 %) in the adult population agree with the results found by other researchers [21] [35] and disagrees with others [36]. Moreover, it has been found that the prevalence of flatfoot decreases as the child grows [3] [13] [37]. It is important to mention that the classification of the foot types could be influenced by the method employed (CSI, Arch Index, Staheli Arc Index, so on), therefore the comparison among studies should be carefully performed [38]. Although there are other methods to evaluate the footprint, the SCI is one of the most used methods to describe the type of feet. Furthermore, although there is a good correlation among them, it has been reported that the other methods can produce different outcomes with slightly less accuracy in some cases [23] [26] [39].

Although there are several studies related to the foot type [2] [3] [10] [14] [15] [20], to the author's knowledge, this is the first study developed in a Mexican population from 2 years to 73 years old. However, although this work is performed in a larger range of ages, the study is performed in a specific region of the country. Further studies should be performed in different regions of the country considering people of all ages.

One limitation of this study is that the analysis of the soles of the feet does not distinguish between flexible and rigid flatfoot. It is probable that the prevalence of flatfoot found in the first decade of life corresponds to flexible flatfoot as this type of foot disappears in adulthood. Moreover, most of the time the flexible flatfoot is asymptomatic and does not produce any pain. However, the prevalence of flatfoot that stays during adulthood could be the rigid type as this type of foot does not resolve with aging [4] [5] [12] [40] [41].

Another limitation of this study is that the results found cannot be generalized due to the sample population was from a limited region of the country. However, although there are some limitations of the study, the results clearly show the development and prevalence of the type of feet from the early stage to adulthood.

CONCLUSIONS

In conclusion, the analysis presented in this work shows that the formation of the medial arc could take more time than the reported by other authors. Moreover, it was found a relatively high prevalence of flatfoot in adult life should be studied. The cavus foot seems to be a pathology with low prevalence, lower than 10% for both feet, but it is something that should not be neglected.

Furthermore, as far as we know, this is the most completed study of the analysis of the morphology of the soles of the feet in a Mexican population from early stage to adulthood. This procedure to obtain the type of feet (flatfoot or cavus foot) is a secure method and does not represent a risk factor as they are not exposed to ionizing radiation, such as X-rays. The results found can be useful for orthopedists, physiotherapists, clinicians, and parents who are concerned about the foot health of their children.

AUTHOR CONTRIBUTIONS

J.A.R.F. designed and carried out experiments, performed statistical analyses and contributed to the

writing of the original draft. I.M.A. conceptualized the project, contributed to the writing of the original manuscript, performed data curation, organization and carried out research. M.L.R. participated in data curation, carried out formal analyses and validation, and reviewed the final version of the manuscript. L.A.O.L. provided resources, participated in the development of the methodology, and carried out experiments. S.L.O.V. carried out the formal analyses and contributed to the writing of the final version of the manuscript. A.V.L. contributed to the formal analyses, validation, and reviewed the final version of the manuscript.

ACKNOWLEDGEMENTS

The authors would like to thank the *Centro de Innovación Aplicada en Tecnologías Competitivas* and the *Consejo Nacional de Ciencia y Tecnología* for supporting the research.

CONFLICT OF INTEREST

The authors declare that they have no conflict of interest.

REFERENCES

[1] C. Álvarez Camarena and W. Palma Villegas, "Desarrollo y biomecánica del arco plantar", Ortho-tips, vol. 6, no. 4, pp. 215-222, 2010. [Online] Available: https://www.medigraphic.com/pdfs/orthotips/ot-2010/ot104c.pdf

[2] C. E. Fuentes-Venado, A. Ángeles-Ayala, M. S. Salcedo-Trejo, L. J. Sumano-Pérez, C. Y. Viveros-del Valle, E. O. Martínez-Herrera, M. G. Frías-de León, L. E. González-Gutiérrez, I. G. Monjaras-Bernal, and R. Pinto-Almazán, "Comparative assessment of flatfoot in preschool children," Bol. Med. Hosp. Infant. Mex., vol. 77, no. 6, pp. 312-319, Nov. 2020. doi: https://doi.org/10.24875/BMHIM.20000135

[3] A. Arizmendi Lira, E. Pastrana Huanaco, and B. Rodríguez Lara, "Prevalencia de pie plano en niños de Morelia," Rev. Mex. Pediatría, vol. 71, no. 2, pp. 66-69, Mar. 2004. [Online]. Available: https://www.medigraphic.com/pdfs/pediat/sp-2004/sp042c.pdf

[4] J. Mortazavi, R. Espandar, and T. Baghdadi, "Flatfoot in children: How to approach?," Iran. J. Pediatr., vol. 17, no. 2, pp. 163-170, 2007. [Online]. Available: https://www.researchgate.net/publication/26467530_Flatfoot_in_Children_How_to_Approach

[5] A. Atik and S. Ozyurek, "Flexible flatfoot," North. Clin. Istanbul, vol. 1, no. 1, pp. 57-64, 2014. doi:https://doi.org/10.14744/nci.2014.29292

[6] V. S. Mosca, "Flexible flatfoot in children and adolescents," J. Child. Orthop., vol. 4, no. 2, pp. 107-121, Apr. 2010. doi: https://doi.org/10.1007/s11832-010-0239-9

[7] H. Uden, R. Scharfbillig, and R. Causby, "The typically developing paediatric foot: How flat should it be? A systematic review," J. Foot Ankle Res., vol. 10, no. 37, pp. 1-17, Aug. 2017. doi: https://doi.org/10.1186/s13047-017-0218-1

[8] I. Miguel-Andrés, A. E. Rivera-Cisneros, J. J. Mayagoitia-Vázquez, S. L. Orozco-Villaseñor, and A. Rosas-Flores, "Índice de pie plano y zonas de mayor prevalencia de alteraciones músculo-esqueléticas en jóvenes deportistas," Fisioterapia, vol. 42, no. 1, pp. 17-23, Jan. 2020. doi: https://doi.org/10.1016/j.ft.2019.08.002

[9] L. Gómez Salazar, J. M. Franco Alvarez, J. J. Nathy Portilla, E. A. Valencia Esguerra, D. V. Vargas Bonilla, and L. Jiménez Hernández, "Características de la huella plantar en deportistas colombianos," Entramado, vol. 6, no. 2, pp. 158-167, Jul. 2010. [Online]. Available: https://www.redalyc.org/pdf/2654/265419645012.pdf

[10] J. A. Aco-Luna, F. Rodríguez-Jiménez, M. G. Guzmán-Coli, M. A. Enríquez-Guerra, and I. G. Chavarría-Bernardino, "Frequency of footprints alterations in school children from a Mexican community," Acta Ortop. Mex., vol. 33, no. 5, pp. 289-291, Sep. 2019. [Online]. Available: https://www.medigraphic.com/pdfs/ortope/or-2019/or195e.pdf

[11] L. Gómez, J. M. Franco, J. J. Nathy, E. Valencia, D. Vargas, and L. Jiménez, "Influencia del deporte en las características antropométricas de la huella plantar femenina," Rev. Educ. Física y Deport., vol. 28, no. 2, pp. 25-33, 2009. doi: https://doi.org/10.17533/udea.efyd.3061

[12] M. Bouchard and V. S. Mosca, "Flatfoot deformity in children and adolescents: Surgical indications and management," J. Am. Acad. Orthop. Surg., vol. 22, no. 10, pp. 623-632, Oct. 2014. doi: https://doi.org/10.5435/JAAOS-22-10-623

[13] K.-C. Chen, L.-C. Tung, C.-J. Yeh, J.-F. Yang, J.-F. Kuo, and C.-H. Wang, "Change in flatfoot of preschool-aged children: A 1-year follow-up study," Eur. J. Pediatr., vol. 172, no. 2, pp. 255-260, Feb. 2013. doi: https://doi.org/10.1007/s00431-012-1884-4

[14] G. Rivera-Saldívar, R. Torres-González, M. Franco-Valencia, R. Ríos-Monroy, F. Martínez-Ramírez, E. Pérez Hernández, and D. Duarte-Dagnino, "Factores de riesgo asociados a la conformación del arco longitudinal medial y del pie plano sintomático en una población escolar metropolitana en México," Acta Ortop. Mex., vol. 26, no. 2, pp. 85-90, 2012. [Online]. Available: https://www.scielo.org.mx/pdf/aom/v35n4/2306-4102-aom-35-04-317.pdf

[15] L. A. Valdez Jiménez, A. D. Saucedo Campos, J. R. Jiménez Flores, and S. Cristóbal Sigrist, "Pie plano flexible y su correlación con síndrome metabólico en niños y adolescentes," Rev. Mex. Ortop. Ped., vol. 18, no. 1, pp. 31-37, Jan. 2016. [Online]. Available: http://www.medigraphic.com/pdfs/opediatria/op-2016/op161f.pdf

[16] A. K. Reihaneh, A. Faranak, and G. Mostafa, "Prevalence of flat foot: comparison between male and female primary school students," Iran. Rehabil. J., vol. 11, no. 18, pp. 22-24, 2013. [Online]. Available: http://irj.uswr.ac.ir/article-1-300-en.pdf

[17] H. A. Miranda C., L. A. Flores Cu, S. Camacho López, H. Rostro González, and M. Cano Lara, "Interface for contour extraction and determination of morphologic parameters in digital images of footprints based on Hernandez-Corvo protocol," in VIII Lat. Am. Caribb. Conf. Eng. Technol., XLII Nat. Conf. Biomed. Eng. (IFMBE Proc.), Cancun, Mexico, 2020, pp. 367-376. doi: https://doi.org/10.1007/978-3-030-30648-9_48

[18] S. N. K. Kodithuwakku Arachchige, H. Chander, and A. Knight, "Flat feet: Biomechanical implications, assessment and management," Foot, vol. 38, no. 1. pp. 81-85, Mar-2019. doi: https://doi.org/10.1016/j.foot.2019.02.004

[19] S. L. Orozco-Villaseñor, J. J. Mayagoitia-Vázquez, I. Miguel-Andrés, K. D. De la Cruz-Alvarado, and R. Villanueva-Salas, "Factores de riesgo asociados a patologías musculoesqueléticas en deportistas con pie cavo anterior a través de estudios de baropodometría," Acta Ortop. Mex., vol. 35, no. 4, pp. 317-321, 2021. doi: https://doi.org/10.35366/103310

[20] H. I. Saldívar Cerón, A. Garmendia Ramírez, M. A. Rocha Acevedo, and P. Pérez Rodríguez, "Obesidad infantil: Factor de riesgo para desarrollar pie plano," Bol. Med. Hosp. Infant. Mex., vol. 72, no. 1, pp. 55-60, 2015. doi: https://doi.org/10.1016/j.bmhimx.2015.02.003

[21] A. G. Martínez Lozano, "Pie plano en la infancia y adolescencia. Conceptos actuales," Rev. Mex. Ortop. Ped., vol. 11, no. 1, pp. 5-13, Jan. 2009. [Online]. Available: https://www.medigraphic.com/pdfs/opediatria/op-2009/op091b.pdf

[22] I. Miguel-Andrés, J. J. Mayagoitia-Vázquez, S. L. Orozco-Villaseñor, M. León-Rodríguez, and D. Samayoa-Ochoa, "Efecto de la morfología de las plantas de los pies en la distribución de presión plantar en atletas jóvenes con diferentes tipos de pie," Fisioterapia, vol. 43, no. 1, pp. 30-37, Jan. 2021. doi: https://doi.org/10.1016/j.ft.2020.07.003

[23] A. N. Onodera, I. C. N. Sacco, E. H. Morioka, P. S. Souza, M. R. de Sá, and A. C. Amadio, "What is the best method for child longitudinal plantar arch assessment and when does arch maturation occur?," Foot, vol. 18, no. 3, pp. 142-149, Sept. 2008. doi: https://doi.org/10.1016/j.foot.2008.03.003

[24] L. A. Luengas C., M. F. Díaz H., and J. L. González M., "Determinación de tipo de pie mediante el procesamiento de imágenes," Ingenium Rev. Fac. Ing., vol. 17, no. 34, pp. 147-161, Nov. 2016. [Online]. Available: https://revistas.usb.edu.co/index.php/Ingenium/article/view/2744

[25] M. J. Muñoz-Neira, A. S. Martínez-Parra, C. G. Ruiz-Adarme, C. H. Triana-Castro, and J. L. Cornejo-Plata, "Diseño de un sistema de reconocimiento de patrones en imágenes termográficas y de huella plantar para la identificación de pie plano en niños con edades entre cinco y seis años," Rev. Cient., vol. 36, no. 3, pp. 313-324, Aug. 2019. doi: https://doi.org/10.14483/23448350.14345

[26] S. Pita-Fernández, C. González-Martín, T. Seoane-Pillado, B. López-Calviño, S. Pértega-Díaz, and V. Gil-Guillén, "Validity of footprint analysis to determine flatfoot using clinical diagnosis as the gold standard in a random sample aged 40 years and older," J. Epidemiol., vol. 25, no. 2, pp. 148-154, 2015. doi: https://doi.org/10.2188/jea.JE20140082

[27] K.-C. Chen, C.-J. Yeh, J.-F. Kuo, C.-L. Hsieh, S.-F. Yang, and C.-H. Wang, "Footprint analysis of flatfoot in preschool-aged children," Eur. J. Pediatr., vol. 170, no. 5, pp. 611-617, May 2011. doi: https://doi.org/10.1007/s00431-010-1330-4

[28] A. García-Rodríguez, F. Martín-Jiménez, M. Carnero-Varo, E. Gómez-Gracia, J. Gómez-Aracena, and J. Fernández-Crehuet, "Flexible flat feet in children: a real problem?," Pediatrics, vol. 103, no. 6, art. e84, Jun. 1999. doi: https://doi.org/10.1542/peds.103.6.e84

[29] G. Troiano, N. Nante, and G. L. Citarelli, "Pes planus and pes cavus in southern Italy: a 5 years study," Ann. Ist. Super. Sanità, vol. 53, no. 2, pp. 142-145, Apr. 2017. doi: https://doi.org/10.4415/ANN_17_02_10

[30] D. Whitford and A. Esterman, "A Randomized Controlled Trial of Two Types of In-Shoe Orthoses in Children with Flexible Excess Pronation of the Feet," Foot Ankle Int., vol. 28, no. 6, pp. 715-723, Jun. 2007. doi: https://doi.org/10.3113/FAI.2007.0715

[31] A. González de Aledo Linos, A. Rollán Rollán, C. Bonilla Miera, A. Montes Conde, M. C. Diego Santamaría, and M. Obeso García, "Resultados del screening con podoscopio en 948 ninos no seleccionados con especial referencia al pie cavo," An. Esp. Pediatr., vol. 45, no. 6, pp. 579-582, 1996. [Online]. Available: https://www.aeped.es/sites/default/files/anales/45-6-5.pdf

[32] O. Espinoza-Navarro, M. Olivares-Urquieta, P. Palacios-Navarrete, and N. Robles-Flores, "Prevalencia de Anomalías de Pie en Niños de Enseñanza Básica de Entre 6 a 12 Años, de Colegios de la Ciudad de Arica-Chile," Int. J. Morphol., vol. 31, no. 1, pp. 162-168, Mar. 2013. doi: https://doi.org/10.4067/s0717-95022013000100027

[33] P. Hernández-Gandarillas, S. L. Orozco-Villaseñor, J. de Jesús Mayagoitia-Vázquez, I. Miguel-Andrés, J. P. Herrera-Rangel, and K. D. de la Cruz-Alvarado, "Results of the Use of Personalized Insoles for the Treatment of Cavus Foot and Comorbidities," in VIII Lat. Am. Caribb. Conf. Eng. Technol., XLII Nat. Conf. Biomed. Eng. (IFMBE Proc.), Cancun, Mexico, 2020, pp. 921-932. doi: https://doi.org/10.1007/978-3-030-30648-9_119

[34] R. Woźniacka, A. Bac, S. Matusik, E. Szczygieł, and E. Ciszek, "Body weight and the medial longitudinal foot arch: High-arched foot, a hidden problem?," Eur. J. Pediatr., vol. 172, no. 5, pp. 683-691, May 2013. doi: https://doi.org/10.1007/s00431-013-1943-5

[35] S. Pita-Fernandez, C. Gonzalez-Martin, F. Alonso-Tejada, T. Sepane-Pillado, S. Pertega-Diaz, S. Perez-Garcia, R. Seijo-Bestilleiro, V. Balboa-Barreiro, "Flat foot in a random population and its impact on quality of life and functionality," J. Clin. Diagn. Res., vol. 11, no. 4, pp. 22-27, Feb. 2017. doi: https://doi.org/10.7860/JCDR/2017/24362.9697

[36] T. Bhoir, D. B. Anap, and A. Diwate, "Prevalence of flat foot among 18-25 years old physiotherapy students: Cross sectional study," Indian J. Basic Appl. Med. Res., vol. 3, no. 4, pp. 272-278, Sep. 2014. [Online]. Available: https://www.ijbamr.com/assets/images/issues/pdf/September%202014%20272-278.pdf.pdf

[37] E. Vergara Amador, R. F. Serrano Sánchez, J. R. Correa Posada, A. C. Molano, and O. A. Guevara, "Prevalence of flatfoot in school between 3 and 10 years. Study of two different populations geographically and socially," Colomb. Med., vol. 43, no. 2, pp. 141-146, Jun. 2012. doi: https://doi.org/10.25100/cm.v43i2.785

[38] M. E. Nikolaidou and K. D. Boudolos, "A footprint-based approach for the rational classification of foot types in young schoolchildren," Foot, vol. 16, no. 2, pp. 82-90, Jun. 2006. doi: https://doi.org/10.1016/j.foot.2006.02.001

[39] J. C. Zuil-Escobar, C. B. Martínez-Cepa, J. A. Martín-Urrialde, and A. Gómez-Conesa, "Medial longitudinal arch: Accuracy, reliability, and correlation between navicular drop test and footprint parameters," J. Manip. Physiol. Ther., vol. 41, no. 8, pp. 672-679, Oct. 2018. doi: https://doi.org/10.1016/j.jmpt.2018.04.001

[40] E. J. Harris, J. V. Vanore, J. L. Thomas, S. R. Kravitz, S. A. Mendelson, R. W. Mendicino, S H. Silvani, and S. C. Gassen, "Diagnosis and treatment of pediatric flatfoot," J. Foot Ankle Surg., vol. 43, no. 6, pp. 341-373, Nov. 2004. doi: https://doi.org/10.1053/j.jfas.2004.09.013

[41] F. Halabchi, R. Mazaheri, M. Mirshahi, and L. Abbasian, "Pediatric flexible flatfoot; clinical aspects and algorithmic approach," Ira. J. Pediatr., vol. 23, no. 3, pp. 247-60, Jun. 2013. [Online]. Available: https://www.ncbi.nlm.nih.gov/pmc/articles/PMC3684468/

RESEARCH ARTICLE

VOL. 44 | NO. 2 | **MAY - AUGUST 2023** | PP 16-26

Revista Mexicana de Ingeniería Biomédica

dx.doi.org/10.17488/RMIB.44.2.2

E-LOCATION ID: 1337

Electrochemical Studies of Magnesium Coated with Modified Chitosan and Electrosprayed as an Anticorrosive Protection Method in Bone Repair

Estudios Electroquímicos del Magnesio Recubierto con Quitosano Modificado y Electrorociado como Proceso de Protección Anticorrosiva en la Reparación de Hueso

José Luis Ramírez-Reyes[1], *Deni Esperanza Gaytán-Macías*[2], *Harlem Quintana-Camacho*[2], *Gonzalo Galicia Aguilar*[1] *Guillermina González Mancera*[3]

[1]Instituto de Ingeniería-Universidad Veracruzana, Veracruz - México

[2]Programa MIC-Instituto de Ingeniería-Universidad Veracruzana, Veracruz - México

[3]ULab-MEB-Facultad de Química-Universidad Nacional Autónoma de México - México

ABSTRACT

Magnesium (Mg) is essential for the metabolic reactions of the human body and is known for its biocompatibility, its mechanical and physical properties are similar to human bone, which is why it is considered to have high potential in *biomedical applications such as temporary and resorbable implants*. Through surface modifications, the high tendency to corrosion of Mg could be controlled, such as *biodegradable membranes* that prevent the passage of chloride ions present in the human organism. To prepare the membrane, solutions of chitosan modified with gelatin and/or glutaraldehyde are used and by means *of the electrospray method* applied to protect the Mg. To simulate body fluid conditions a Kokubo saline solution (BFK) was prepared. The study focuses on evaluating the corrosion rate of Mg with a coating made of a *chitosan electrosprayed membrane*, applying *electrochemical measurements of electrochemical impedance spectroscopy and linear polarization resistance*.

The key additive to improve the behavior of the membranes was observed with the use of gelatin, where the membrane with the best results lowing corrosion rates is the Mg CH+GE+GL system, which it was observed with very good physical integrity in the images of morphological analyzes of the surface after 30 days of exposure.

KEYWORDS: Bone Repair, chitosan modified, electrochemical techniques, electrosprayed coatings, magnesium

RESUMEN

El magnesio (Mg) es esencial para las reacciones metabólicas del cuerpo humano y es conocido por su biocompatibilidad, sus propiedades mecánicas y físicas son similares a las del hueso humano, por lo que se considera que tiene un alto potencial en *aplicaciones biomédicas como implantes temporales y reabsorbibles*. Mediante modificaciones superficiales se podría controlar la alta tendencia a la corrosión del Mg, como por ejemplo *membranas biodegradables* que impidan el paso de iones cloruro presentes en el organismo humano. Para preparar la membrana se utilizan soluciones de quitosano modificado con grenetina y/o glutaraldehído y mediante el *método de electrorociado* se aplican para proteger el Mg. Para simular las condiciones de los fluidos corporales se preparó una solución salina de Kokubo. El estudio se enfoca en evaluar la *velocidad de corrosión* del Mg con un recubrimiento hecho de una *membrana electrorociada con quitosano, aplicando técnicas electroquímicas de espectroscopia de impedancia electroquímica y resistencia de polarización lineal*. El aditivo clave para mejorar el comportamiento de las membranas se observó con el uso de gelatina, donde la membrana con mejores resultados bajando los índices de corrosión es el sistema Mg CH+GR+GL, el cual se observó con muy buena integridad física en las imágenes de análisis morfológicos de la superficie después de 30 días de exposición.

PALABRAS CLAVE: Magnesio, quitosano modificado, recubrimientos electro-rociados, reparación de hueso, técnicas electroquímicas

Corresponding author

TO: **José Luis Ramírez-Reyes**

INSTITUTION: **Instituto de Ingeniería-Universidad Veracruzana**

ADDRESS: **SS Juan Pablo II, s/n, Zona Universitaria, Veracruz, Ver. Mex. C. P. 94294**

CORREO ELECTRÓNICO: **luiramirez@uv.mx**

Received:

2 February 2023

Accepted:

18 May 2023

INTRODUCTION

Magnesium is an essential element for metabolic reactions in the human body and is known for its good biocompatibility, good mechanical properties (very close to human bone) and is considered a biodegradable material with potential in biomedical applications in the case of osteosynthesis, which is a process of intervention of fractures or fissures [1][2]. Its high electrochemical activity makes surface modification necessary in order to reduce corrosion rates. Thereby prolong its necessary mechanical properties throughout the recovery time of the bone tissue. Current investigations have focused on addressing this problem by implementing different strategies so that the rate of degradation of magnesium can be controlled within the physiological environment. Some of these are the use of magnesium alloys or protective techniques such as superficial modification treatments and protective recoveries [3]. However, in the surface modification of Mg, the required time for degradation depends on the targeted application, for instance in the design of coatings for tailor degradation is the unknown between the number of degradation test in the lab with the behavior of the coating in test in-vivo [4].

The main reactions reported for the Magnesium corrosion process are [5][6];

$$Mg \rightarrow Mg^{n+} + ne^- \text{ (Anodic reacción)} \quad (1)$$

$$2H_2O + 2e^- \rightarrow H_2 + 2OH^- \quad (2)$$

(Cathodic reaction at acidic pH)

$$2H_2O + O_2 + 4e^- \rightarrow 4OH^- \quad (3)$$

(Cathodic reaction at neutral or alkaline pH)

$$Mg^{n+} + nOH^- \rightarrow Mg(OH)_n \quad (4)$$

(Global reaction products)

Chitosan membranes (CH) have excellent properties, such as antimicrobial activity, biocompatibility, good bio adhesiveness, it is non-toxic, it optimizes wound healing, bone formation, as well as a vehicle and/or drug releaser, and they are very efficient in guided bone regeneration [7][8]. Biodegradability is a property sought in these materials, however, pure chitosan has low mechanical properties due to its brittleness, it is soluble only in acidic media, and it loses its antibacterial activity at pH > 6.5.

To overcome these drawbacks, the most efficient method is to mix it with other polymers to provide it with fluidity such as gelatin which, in addition to fulfilling its function as an additive, enhances the antimicrobial property of chitosan in the form of a flexible film [9][10][11][12][13].

There are many ways to produce these membranes; one example is to produce them using the electrospinning technique as electrospray, which generates micro-thin films with properties such as microporosity, large surface area, and biodegradable. Also, can be obtained by this technique as nanoparticles from a polymer in solution with a conductive solvent [14] [15] [16].

The first appearance of this technique was reported by Nollet from the 17th century, when he observed that *"a person, electrified by connection to a high-voltage generator, would not bleed normally if cut; the blood would come out of the wound in the form of drops"*. After that, Rayleigh defined a limit on the charge carried by a drop in 1882, Zeleny reported various modes of operation of electrospray during 1914, and Taylor determined the shape of the cone formed by the fluid at the capillary tip in an electric field in 1964. Widespread use of electrospray began after Dole introduced it as a method of generating gas-phase ions for mass spectrometry analysis in 1968 [17].

The present work focuses on evaluating the corrosion rate of structural Mg with a coating made of an electrosprayed chitosan membrane (CH) modified with gelatin (GE) and/or glutaraldehyde (GL). The electrochemical evaluation was carried out using the techniques of electrochemical impedance spectroscopy (EIS) and linear polarization resistance (LPR), applied

by means of a potentiostat to the Mg samples bare and coated with the membranes, to evaluate the process of degradation of the membrane and the anticorrosive protection to the Mg. Also, by means of surface modification treatment and evaluating in a Kokubo solution (BFK) at 37 °C body temperature. In addition to the challenges in this job, still hard research is being carried out for the control of biodegradation of Mg alloys, and for developing new type of surface modification approaches [4].

MATERIALS AND METHODS

Mg discs of 1 cm in diameter and 3 mm thick were used. They were roughened up to 600 grit sandpaper and ultrasonic washed together with chemical roughening with ethanol and acetic acid, as shown in Figure 1.

FIGURE 1. **Ultrasonic bath and morphological surface of washed Mg before the phosphate treatment.**

Kokubo Saline Solution (BFK)

All the used reactives were grade ACS and prepared for one L of solution following the methodology of Tadashi Kokubo [7] [18] [19] as shown in Table 1.

Order	Reactive	Quantity, g	Conc., mM
#1	NaCl	7.996	136.7
#2	$NaHCO_3$	0.350	4.16
#3	KCl	0.224	3
#4	$K_2HPO_4 \cdot 3H_2O$	0.1764	0.7737
#5	$MgCl_2 \cdot 6H_2O$	0.305	1.5
#6	1 kmol/m^3 HCl	40 cm^3	40
#7	$CaCl_2$	0.278	2.5
#8	Na_2SO_4	0.071	0.5
#9	$(CH_2OH)3CNH_2$	6.057	48.46
#10	1 kmol/m^3 HCl	pH Adjusting	

TABLE 1. **Chemical composition of the Kokubo solution (BFK) and the sequence order for the preparation.**

For the formation of the membrane, chitosan solutions were prepared at 1.5 % diluted concentration of a mixture of acetic acid and distilled water in a ratio of 9:1, mixing everything at a temperature of 60 ± 5 °C until dissolved. To compare with chitosan modified with gelatin and/or glutaraldehyde, it was carried out by adding 2 % gelatin in the solution together with chitosan, the modification with glutaraldehyde is done after the formation of the membrane, placing a drop of it on the coating, letting it absorb and evaporate.

The membranes were made with the Fluidnatek LE-100 used as electro spraying equipment, placing 3 ml of the chitosan solution in a syringe, as shown in Figure 2. The images show the membranes a) Chitosan, b) Chitosan modified with gelatin, c) Chitosan modified with glutaraldehyde and d) Chitosan modified with gelatin + glutaraldehyde. The Figure 3 show an image SEM with the dispersion of the microparticles contained in drops of chitosan at the contact with the Mg substrate. The processing parameters were as follows: applied voltage, −30 kV; feed solution flow rate, 0.3 ml/hr; distance between the nozzle and the substrate, 10 cm; deposit time, 30 min.

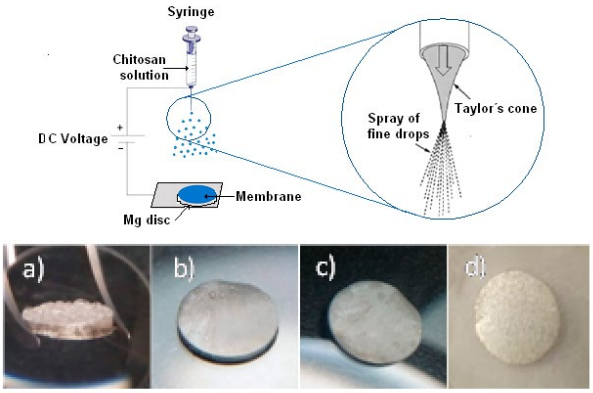

FIGURE 2. **Scheme of the spray process and samples with the sprayed membranes a) MgCH, b) MgCH+GE, c) MgCH+GL and d) MgCH+GE+GL over discs of Mg.**

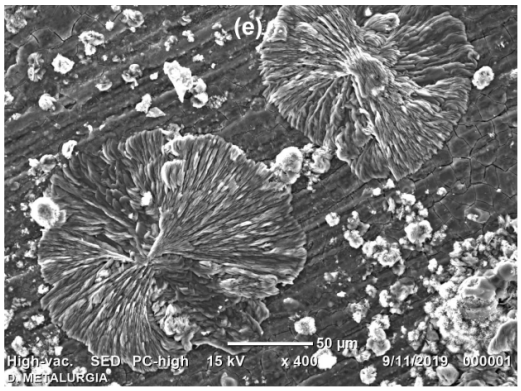

FIGURE 3. **Image SEM dispersion of the microparticles contained in drops of chitosan at Mg substrate.**

Once the samples with the membranes were ready, an electrochemical cell was prepared in a simulated Kokubo physiological body solution (BFK) and using a temperature of 37 °C as shown in the cell arrangement in Figure 4. The impedance spectroscopy technique (EIS) was carried out, using a frequency sweep from 10kHz to 0.01 Hz, with an amplitude of ± 10 mV peak-to-peak and 7 points per decade of frequency and the linear polarization resistance (LPR) where a bias of ± 20 mV/Ecorr was used. The corrosion potential (Ecorr), was monitored with respect to time. The electrochemical tests were carried out with a Bio-Logic brand potentiostat model SP-150, where the electrochemical monitoring was carried out from the first hour of immersion and subsequently measured every 24 hours for a period of 30 days.

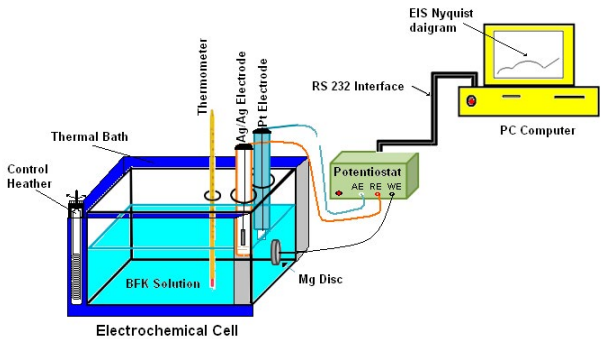

FIGURE 4. **Scheme and configuration of the electrochemical cell for the electrochemical evaluation.**

Some of the main chloride reactions expected in the Mg -BFK solution are described below;

$$Mg_{(s)} + 2H_2O_{(l)} \rightarrow Mg(OH)_{2(s)} + H_{2(g)} \quad (5)$$

$$2Mg_{(s)} + O_{2(g)} + 2H_2O_{(l)} \rightarrow 2Mg(OH)_{2(s)} \quad (6)$$

$$Mg(OH)_{2(s)} \rightarrow MgO_{(s)} + H_2O_{(l)} \quad (7)$$

$$MgO_{(s)} + H_2O_{(l)} \rightarrow Mg(OH)_{2(s)} \quad (8)$$

$$Mg(OH)_{2(s)} + 2NaCl_{(s)} \rightarrow MgCl_{2(s)} + 2NaOH_{(s)} \quad (9)$$

For the analysis of the surface morphology of the samples before and after exposure, a high-low vacuum scanning electron microscope, model SEM 6000 NEOSCOPE with a voltage of 150 keV, was used to perform the elemental chemical analysis of the membranes, the X-ray scattering technique known as EDS was used.

RESULTS AND DISCUSSION

The corrosion potential (Ecorr) and corrosion rates (CR) results are shown in Figure 5 and Figure 6 respectively, where we can see the same trend for bare Mg, Mg with chitosan membrane (Mg CH) and Mg with gelatin-modified chitosan (Mg CH+GE) and glutaraldehyde (Mg CH+GL), however, for Mg with the membrane modified with gelatin and glutaraldehyde (Mg CH+GE+GL) was observed that the Ecorr tends to rise more positive values, which implies an energy gain. This translates into thermodynamic stability for the reactivity of the species involved in the interface of the evaluated systems and the tendency of CR to decrease, implying that the metal-coating systems tend to improve the resistance against the corrosiveness of the environment.

Corrosion mechanism of Mg alloys in simulated body fluid always has been complicated because of many factors like the complex chemical composition

influence. However, the obtained CR values between 0.1 to 2 mm/y are in coincidence for in vitro conditions reported values [4].

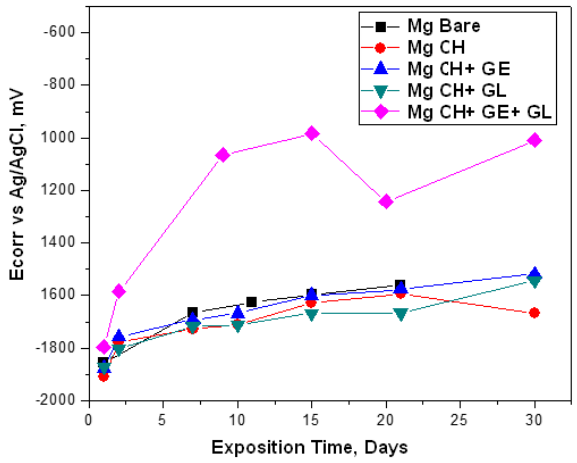

FIGURE 5. **Ecorr of bare and coated Mg at the immersion time measurements in the BFK solution at 37 ºC.**

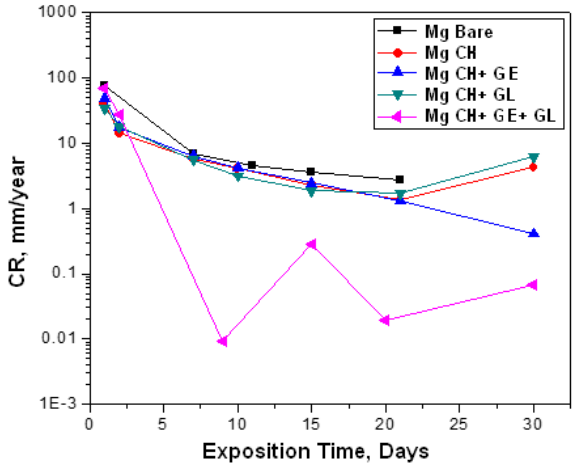

FIGURE 6. **Corrosion rate of Mg bare and coated with membranes in the BFK solution at 37 ºC.**

The Figure 7 is the Nyquist diagram of bare Mg and clearly shows the corrosion process suffered by magnesium with resistance up to 1.4 kΩ-cm2 before the presence of the coating. In the case of Mg coated with chitosan, we can see an increase in the corrosion resistance except for day 30, where it decreased due to the total degradation of the membrane and that exposed to the metal. For the chitosan membrane shown in the Nyquist of Figure 8, the resistance was increased by twice and no degradation is observed in the membrane.

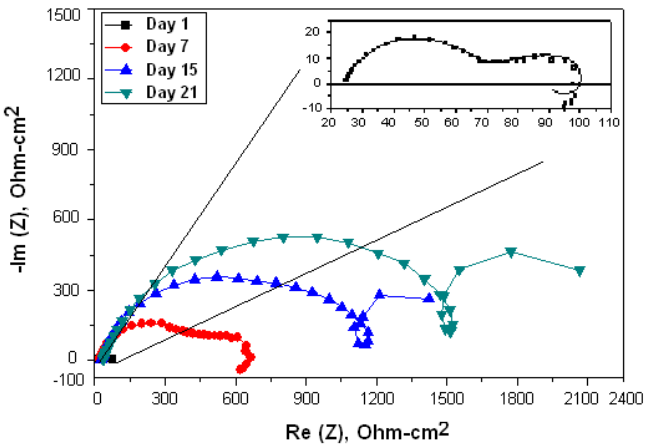

FIGURE 7. **Nyquist diagrams of the bare Mg in the BFK solution at 37 ºC the immersion time.**

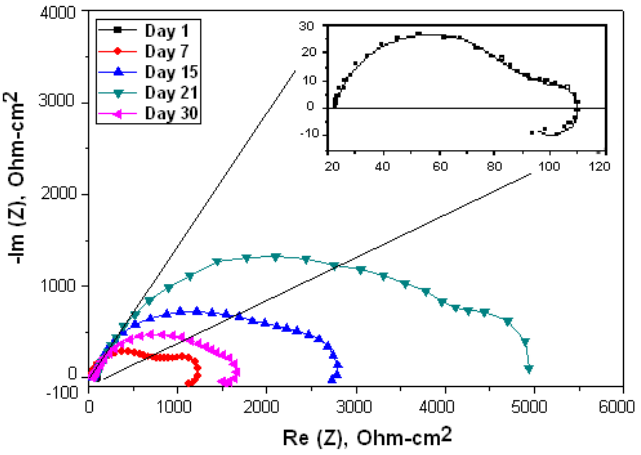

FIGURE 8. **Nyquist diagrams of the Mg coated with chitosan and immersed in BFK at 37ºC.**

For the gelatin-modified chitosan membrane shown in the Nyquist of Figure 9, the corrosion resistance was 3 times higher, and less degradation after 30 days as observed in the membrane. The Mg with chitosan modified with glutaraldehyde which is shown in the Nyquist of Figure 10 shows that the corrosion resistance is similar to the bare Mg and if a degradation of the membrane is observed on day 30.

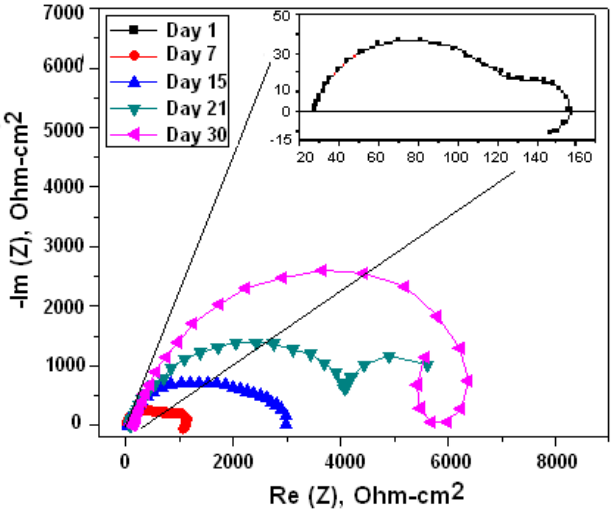

FIGURE 9. **Nyquist diagrams of the Mg coated with chitosan and modified with gelatin and immersed in BFK solution.**

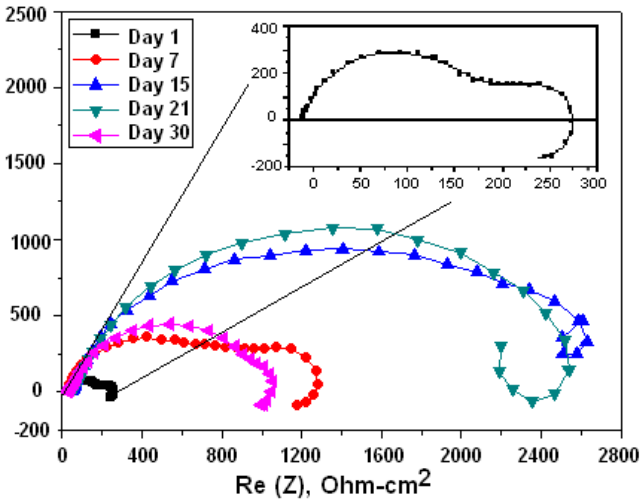

FIGURE 10. **Nyquist diagrams of the Mg coated with chitosan and modified with glutaraldehyde and immersed in BFK solution.**

The Nyquist diagram for the gelatin and glutaraldehyde modified chitosan coated Mg is shown in the Nyquist of Figure 11, it can be clearly seen that the corrosion resistance is extremely large compared to the other membranes, the corrosion process becomes slower and the membrane makes it difficult for chloride ions to reach Mg. In the Figure 12 the spectra obtained from Raman Spectroscopy of bare Mg, chitosan, and the different Mg+ membrane systems are shown, and observing the covering capacity of the additives CH, GE and GL over the Mg substrate. The diagram shows the peaks of 1050 cm-1 for Mg and 2885 cm-1 reported in the literature as characteristic of chitosan [20].

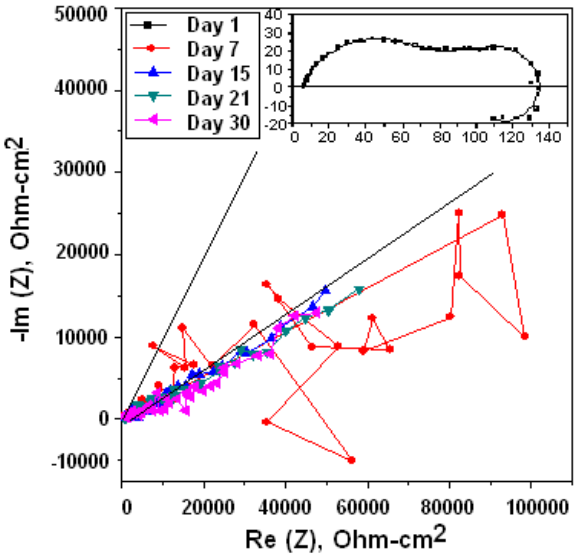

FIGURE 11. **Nyquist diagrams of the Mg coated with chitosan modified with gelatin plus glutaraldehyde and immersed in BFK.**

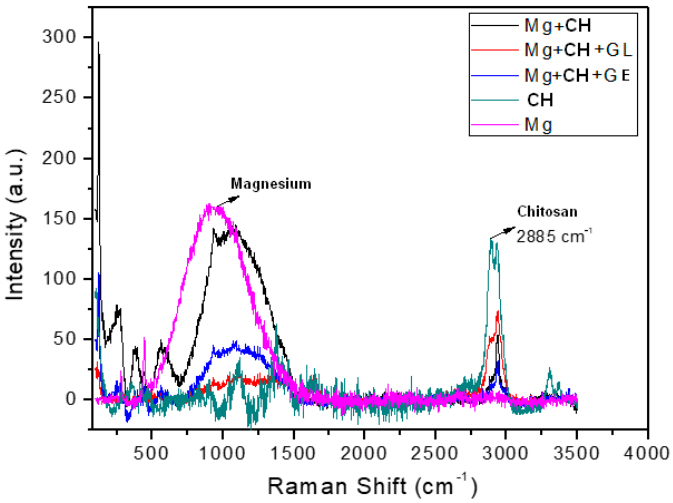

FIGURE 12. **Raman Spectroscopy response obtained from the bare and coated Mg with membranes of chitosan modified with gelatin and glutaraldehyde.**

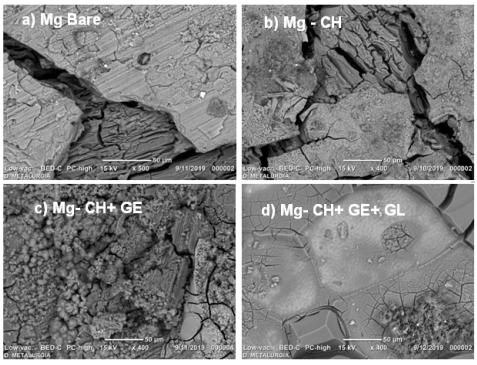

FIGURE 13. **SEM microscopy of samples after exposition to the BFK solution a) Bare Mg, b) Mg with chitosan, c) Mg with chitosan modified with gelatin and d) Mg with chitosan modified with grenetine plus glutaraldehyde.**

The Figure 13 show the SEM images of (a) corrosion products on the bare Mg, (b) coated Mg with chitosan, showing morphology with less corrosion than the bare Mg, (c) Mg coated with chitosan plus the gelatin, showing the dispersion of microspheres of the membrane, controlling the embrittlement of the coating and reducing the corrosion rate on the substrate and (d), the formed membrane practically intact, well formed and smooth, over the entire surface due to the cross-linking reaction produced by glutaraldehyde with chitosan, in addition to increasing mechanical resistance and flexibility given by the gelatin, showing the best anticorrosive effect over the Mg substrate.

Element	Mg without attack	Mg attacked	Mg-CH	Mg-CH+ GE	Mg-CH+ GE+ GL
C	25.17	27.05	31.03	44.52	43.8
O	1.6	36.08	42.2	30.55	32.2
Mg	73.23	32.2	12.1	4.9	5.3
Si		0.05	0.03	0.08	0.21
P		1.08	6.2	4.15	4.5
S		0.28	0.08	0.2	0.07
Cl		0.06	0.05	6.85	0.03
K		0.13	0.17		0.69
Na		0.28	0.87	0.26	0.97
Ca		1.98	6.1	5.7	11.8
Al		0.10	0.04	0.05	0.19
Total	100%	100%	100%	100%	100%

TABLE 2. **Elemental chemical composition detected in % mass by EDS on the surface of samples of coated Mg before and after the exposition to the BFK solution.**

Table 2 shows the results of the elemental chemical composition for the Mg samples and chitosan membranes, where it is observed that in the exposed Mg samples it registers the main elements (O, P and Ca) of the BFK solution, while the chitosan membranes raise the C, O, P and Ca content, lowering the detection of Mg due to the coating and the gelatin involves the presence of elements such as C, O, Cl, and Ca mainly, and when the coating system includes the glutaraldehyde the Si, Al and Ca increases such a bit, maybe due the trapping effect of such elements in the formed lattice. Then, as was observed in the EIS response, the best results were observed with the membrane made of CH+ GE+ GL.

In the literature there are many in-vitro studies that deal with a variety of topics, some evaluate and compare electrolytes, others evaluate the surface morphology of coatings such as chitosan [21]. others report the behavior of Mg alloys with other metals such as Zn, Ca, and others [4]. There are even several review-type papers on the applications of Mg and its alloys as a biomaterial [22], but in no work has the application of chitosan membranes modified with gelatin and glutaraldehyde been studied, and due to the results obtained, it is considered a contribution that deserves further studies with a view to its application at in-vivo conditions, even the membranes can also be used as a vehicle for the transport of drugs in post-operative treatments [23].

CONCLUSIONS

The membrane that degraded the least and had the best results with the lowest corrosion rates is that of the Mg-CH+GE+GL system and it is observed almost intact in the SEM results. The Raman information of the membranes, helped in the interpreting of the covering properties of the additives.

The corrosion protection also can be attributed to the synergistic effect of such additives; the gelatin serves

as a means for the chitosan to have greater resistance since it provides viscoelasticity, flexibility and mobility properties. Glutaraldehyde serves as a cross-linking agent between the chitosan polymer chains, creating greater cohesion in the membrane, improving its mechanical properties and its resistance to protect the Mg substrate against the corrosiveness of the medium.

With the results of the electrochemical evaluation, it was verified that the chitosan with the gelatin and glutaraldehyde acting independently, do not reach the anticorrosive protection properties and only by acting the whole system together is a synergistic effect achieved. The challenge in both strategies is to combine control of the corrosion behavior with the membrane biodegradation and desired biological performance for the in-vivo applications.

The electrospray process of the polymeric substances is another important factor due to the distribution and better coverage area provided by the microparticles that form the membrane. Also is recommended the chemical characterization of the membranes in the near future.

AKNOWLEGEMENTS

To the CONACYT for the scholarships for the Master in Corrosion Engineering students and their support in carrying out this research work.

CONFLICTS OF INTREST

The authors declare no conflict of interest.

AUTHOR CONTRIBUTIONS

D.E.G.M. conceptualized the project, participated in all the writing stages of the manuscript (preparation of the original draft, review and edition of the different versions and the final document), performed data curation, contributed to the research and oversaw the project. J.L.R.R. Designed and carried out experiments, performed statistical analyses, participated in all the writing stages of the manuscript, carried out analyses. H.Q.C. performed data curation, carried out and validated analyses, participated in the review of the final version of the manuscript. G.G.M. provided resources, designed and developed methodology and performed analyses SEM. G.G.A. carried out formal analyses, reviewed and edited the final version of the manuscript. All authors reviewed and approved the final version of the manuscript.

REFERENCES

[1] N. T. Kirkland, N. Birbilis, M. Staiger, "Assessing the corrosion of biodegradable magnesium implants: a critical review of current methodologies and their limitations," Acta Biomater., vol. 8, no. 3, pp. 925-936, Mar. 2012. doi: https://doi.org/10.1016/j.actbio.2011.11.014

[2] N. Ardila, Z. Ajji, M.-C. Heuzey, A. Ajji, "Chitosan electrospraying: Mapping of process stability and micro and nanoparticle formation," J. Aerosol Sci., vol. 126, pp. 85-98, Dec. 2018, doi: https://doi.org/10.1016/j.jaerosci.2018.08.010

[3] M. Carboneras Chamorro, C. Iglesias Urraca, E. Onofre Bustamante, M. A. Alobera Gracia, C. Clemente de Arriba, M.C. García Alonso, M. L. Escudero Rincón, "Materiales metálicos biodegradables en el campo biomédico," Acta Cienc. Tecnol., vol. 19, pp. 30-34, 2011. [Online]. Available: https://core.ac.uk/reader/36133460

[4] M. Esmaily, J.E. Svensson, S. Fajardo, N. Birbilis, G.S. Frankel, S. Virtanen, R. Arrabal, S. Thomas, L.G. Johans, "Fundamentals and advances in magnesiun alloy corrosion," Prog. Mater. Sci., vol. 89, pp. 92-193, Aug. 2017. doi: https://doi.org/10.1016/j.pmatsci.2017.04.011

[5] Y. Zheng, Magnesium Alloys as Degradable Biomaterials, 1st ed. Boca Ratón: CRC Press, 2019, pp. 600.

[6] Z. Song, G. Yu, Z. Xie, B. Hu, X. He, X. Zhang (2014). "Performance of composite coating on AZ31B magnesium alloy prepared by anodic polarization and electroless electrophoresis coating," Surf. Coat. Technol. vol. 242, pp. 83-91, Mar. 2014. doi: https://doi.org/10.1016/j.surfcoat.2014.01.022

[7] V. Valencia Goujon, "Estudio electroquímico de magnesio en medio fisiológico simulado (Kokubo) para su aplicación como biomaterial y uso de tratamientos de modificación superficial anticorrosivos," Bachelors dissertation, Univ. Nac. Aut. Mex., Mexico City, Mexico, 2013. [Online]. Available: https://repositorio.unam.mx/contenidos/353329

[8] A.S. Paredes, O.S. Orteg, A. González, L. Bustillos, "Análisis comparativo de la regeneración ósea obtenida con quitosano y plasma rico en fibrina," Acta Odontol. Venez., vol. 52, no. 2, Art. no. 2, 2014. [Online]. Available: https://www.actaodontologica.com/ediciones/2014/2/art-2

[9] C.A. Cárcamo Gatica, "Preparación de films de complejo polielectrolito quitosano-alginato y comparación de sus propiedades mecánicas y biológicas con films de quitosan," Bachelors dissertation, Univ. Chile, Santiago, Chile, 2005. [Online]. Available: https://repositorio.uchile.cl/handle/2250/105463

[10] A.E. Mochalova, L.V. Nikishchenkova, N.N. Smirnova, L.A. Smirnova, "Thermodynamic properties of chitosan-based hydrogels in the range 0-350 K," Polym. Sci. Ser. B, vol. 49, pp. 42-46, Apr. 2007. doi: https://doi.org/10.1134/S1560090407010101

[11] Y. Liu, S. Wang, W. Lan, "Fabrication of antibacterial chitosan-PVA blended film using electrospray technique for food packaging applications," Int. J. Biol. Macromol., vol. 107, no. Pt A, pp. 848-854, Feb. 2018. doi: https://doi.org/10.1016/j.ijbiomac.2017.09.044

[12] N.T.-P. Nguyen, L.V.-H. Nguyen, N.T. Thanh, V.V. Toi, T. Ngoc Quyen, P.A. Tran, H.-M. David Wang, T.-H. Nguyen, "Stabilization of silver nanoparticles in chitosan and gelatin hydrogel and its applications," Mater. Lett., vol. 248, pp. 241-245, Aug. 2019. doi: https://doi.org/10.1016/j.matlet.2019.03.103

[13] H. Quintana-Camacho, J.L. Ramírez-Reyes, A.L. Medina-Almazán, N. García-Navarro, G. Galicia-Aguilar, "Investigation of the corrosion behavior of phophate coating magnesium in a kokubo solution," Int. J. Electrochem. Sci., vol. 13, pp. 6072-6082, 2018. doi: https://doi.org/10.20964/2018.06.53

[14] J.A.S. Moreno, A.C. Mendes, K. Stephansen, C. Engwer, F.M. Goycoolea, A. Boisen, L.H. Nielsen, I.S. Chronakis, "Development of electrosprayed mucoadhesive chitosan microparticles," Carbohydr. Polym., vol. 190, pp. 240-247, Jun. 2018. doi: https://doi.org/10.1016/j.carbpol.2018.02.062

[15] R.M.D. Soares, N.M. Siqueira, M.P. Prabhakaram, S. Ramakrishna, "Electrospinning and electrospray of bio-based and natural polymers for biomaterials development," Mater. Sci. Eng. C., vol. 92, pp. 969-982, Nov. 2018. doi: https://doi.org/10.1016/j.msec.2018.08.004

[16] A. Jaworek, A.T. Sobczyk, A. Krupa, "Electrospray application to powder production and surface coating," J. Aerosol Sci., vol. 125, pp. 57-92, Nov. 2018. doi: https://doi.org/10.1016/j.jaerosci.2018.04.006

[17] S. Kavadiya, P. Biswas, "Electrospray deposition of biomolecules: Applications, challenges, and recommendations," J. Aerosol Sci., vol. 125, pp. 182-207, Nov. 2018. doi: https://doi.org/10.1016/j.jaerosci.2018.04.009

[18] T. Kokubo, "Bioactive glass ceramics: properties and applications," Biomaterials, vol. 12, no. 2, pp. 155-163, Mar. 1991. doi: https://doi.org/10.1016/0142-9612(91)90194-F

[19] J.Y. Wong, J.D. Bronzino, D.R. Peterson, Biomaterials: Principles and Practices, 1st Ed. Boca Ratón: CRC Press, 2012, pp. 288.

[20] A. Zaja c, J. Hanuza, M. Wandas, L. Dymińska, "Determination of N-acetylation degree in chitosan using Raman spectroscopy," Spectrochim. Acta A Mol. Biomol. Spectrosc., vol. 134, pp. 114-120, Jan. 2015. doi: https://doi.org/10.1016/j.saa.2014.06.071

[21] G.A.S. Kazi, T. Yamanaka, Y. Osamu, "Chitosan coating an efficient approach to improve the substrate surface for in vitro cultura System," J. Electrochem. Soc., vol. 166, no. 9, pp. B3025- B3030, 2019. doi: http://dx.doi.org/10.1149/2.0051909jes

[22] S. Sobieszcyk, A. Zieliński, "Coatings in Arthoplastiy: Review Paper," Adv. Mater. Sci., vol. 8, no. 4, Dec. 2008. [Online]. Available https://www.proquest.com/openview/e71b8f58cff352959f14f9b5dc1f-870d/1?pq-origsite=gscholar&cbl=2016339

[23] B. Pérez-Artacho, E. Sáez-Fernández, G.I. Martínez-Soler, V. Gallardo Lara, J.L. Arias Mediano, "Polímeros biodegradables en el transporte selectivo de moléculas antitumorales," ARS Pharm. vol. 51, s. 3, pp. 171-176, 2010. [Online]. Available: http://hdl.handle.net/10481/26416

RESEARCH ARTICLE

VOL. 44 | NO. 2 | **MAY - AUGUST 2023** | PP 27- 37

Revista Mexicana de Ingeniería Biomédica

dx.doi.org/10.17488/RMIB.44.2.3

E-LOCATION ID: 1334

Feasibility in the use of the UV-Visible region for the characterization of glucose in deionized water using Arduino 1

Viabilidad en el uso de la región UV-Visible para la caracterización de glucosa en agua desionizada mediante Arduino 1

Virginia Sanchez-Monroy[1], *Luis Enrique Barros-Martinez*[2], *Alejandro Hidalgo-Pedraza*[2], *Braulio Adriel Mendoza-Munguia*[2], *Miguel Sanchez-Brito*[2].

[1] Escuela Superior de Medicina, Instituto Politécnico Nacional, CDMX - México

[2]Escuela Superior de Cómputo, Instituto Politécnico Nacional, CDMX - México

ABSTRACT

With an estimated approximately 2 million deaths per year, diabetes is one of the top 5 deadliest noncommunicable diseases globally. Although this disease is not fatal, the degradation of the patient's health due to a bad plan to control their glucose levels can have a fatal outcome. In order to lay the foundations for the development of a device that allows estimating glucose levels in some body fluid, we present the results obtained not only for the estimation of glucose in deionized water, but also describe the development and configuration of the created device. After analyzing 50 signals obtained from 5 different glucose concentrations, the feasibility of using the developed device for the analysis is evident, since, considering the K-Nearest Neighbors (KNN) algorithm, all the signals were associated correctly to the glucose group to which they belong.

KEYWORDS: Deionized water, glucose concentration, UV-visible, Arduino, K-Nearest Neighbor

RESUMEN

Con un estimado de aproximadamente 2 millones de muertes por año, la diabetes es una de las 5 enfermedades no transmisibles más mortales a nivel mundial. Aunque esta enfermedad no es mortal, el deterioro de la salud del paciente por un mal plan para controlar sus niveles de glucosa puede tener un desenlace fatal. Con el fin de sentar las bases para el desarrollo de un dispositivo que permita estimar los niveles de glucosa en algún fluido corporal, presentamos los resultados obtenidos no solo para la estimación de glucosa en agua desionizada, sino que también describimos el desarrollo y configuración del dispositivo creado. Luego de analizar 50 señales obtenidos a partir de 5 concentraciones de glucosa diferentes, se evidencia la factibilidad de utilizar el dispositivo desarrollado para el análisis, ya que, considerando el algoritmo K-Nearest Neighbors (KNN), todas las señales se asociaron correctamente al grupo de glucosa al que pertenecen.

PALABRAS CLAVE: Agua desionizada, concentraciones de glucosa, UV-visible, Arduino, K-Nearest Neighbor

Corresponding author

TO: **Miguel Sanchez-Brito**

INSTITUTION: **Instituto Politécnico Nacional, Escuela Superior de Cómputo - México**

ADDRESS: **ESCOM IPN, Unidad Profesional Adolfo López Mateos, Av. Juan de Dios Bátiz, Nueva Industrial Vallejo, Gustavo A. Madero, 07320 Ciudad de México, CDMX**

CORREO ELECTRÓNICO: **msanchezbr@ipn.mx**

Received:

11 January 2023

Accepted:

24 May 2023

INTRODUCTION

Considering data exposed by the World Health Organization (WHO), noncommunicable diseases (NCDs) are the cause of approximately 41 million deaths worldwide [1]. In that same study, the WHO points to cardiovascular diseases, cancer, chronic respiratory diseases, and diabetes as the main NCDs. Attributable to diabetes, only in the year 2019, close to 2 million deaths were registered, in addition, in a similar research, with the objective of evaluating the behavior of the diagnosis of this disease, it was found that in the period between 2000 and 2019, the diagnosis rate of this disease had an increase of 3 % with an upward trend, suggesting that for later years more people may develop this condition, likely increasing the mortality rate [2]. The most common conditions that affect people with diabetes and ultimately lead to death are blindness, kidney failure, heart attack, stroke, and lower extremity injuries leading to amputations, however, as suggested by the WHO and the American Diabetes Association (ADA), the probability of developing these health conditions can be reduced by adopting a healthy diet, a correct physical exercise plan and, mainly, a continuous monitoring of glucose levels [2][3].

Despite the fact that there are endless strategies to monitor glucose levels in the human body, the mortality rates suggest that they are not used properly. In work such as those carried out by [4][5][6], the main difficulties of inadequate monitoring are indicated and in Table 1, we present them briefly.

In order to propose friendlier strategies for the interpretation of results and reduce the inconvenience derived from blood extraction or the need to use accessories (such as test strips), research papers such as those compiled in [7], have been proposed. In such studies, many techniques based on the analysis of non-invasively extracted biofluids to estimate the glucose level are proposed, likewise, it is possible to appreciate that the techniques that have allowed to obtain the best results are those based on spectroscopy: Fourier transform infrared (FTIR), Raman and ultraviolet-visible (UV-Vis) principally [8][9][10][11][12][13][14].

TABLE 1. Main factors that affect the self-monitoring of glucose levels in diabetic patients.

Measurement errors	
Humans	Incorrect use of blood glucose meters, incorrect execution of coding, inappropriate storage and use of test strips, inappropriate education of patients and diabetes equipment, etc.
Inherent in the device	Accuracy, ease of use.
Inherent in test strips	Lot to lot variations, vial to vial variations, strip to strip variations.
Environmental	Temperature, humidity, altitude, electromagnetic radiation. These uncontrolled factors can affect the strips.
Physiological	Perfusion of peripheral blood, hematocrit, triglycerides, uric acid.
Medication	Ascorbic acid, paracetamol, dopamine.

Through the interaction of a certain biological sample with different frequencies of the electromagnetic spectrum, spectroscopy allows knowing the molecular composition of the studied sample. These interactions cause the chemical bonds that make up the sample to vibrate. Such vibrations are recorded in a two-dimensional matrix called a spectrum. It is through the study of these spectra that it has been possible to propose solutions for the characterization of different

populations of patient groups. Despite the great advantage achieved with the papers presented by [7], the cost of the equipment required (spectrometers) to perform glucose estimation is unaffordable for the majority of the population.

In order to develop a reliable and accessible device for the population, which allows them to monitor their glucose levels in a non-invasive and friendly way, the possibility of developing a device that through the bombardment of electromagnetic frequencies achievable with a low-cost commercial LED and associated with the UV-Vis spectrum, is studied, in the first instance, to characterize the glucose levels in solutions prepared in deionized water to later think about analyzing a more complex biofluid such as blood or saliva. The feasibility of using electromagnetic frequencies contemplated by the UV-Vis region, to characterize samples of different nature from their glucose concentration, has been exposed in the investigations of [15][16][17][18].

The device developed and evaluated in this document, focuses on the analysis of the light level emitted and received by an LED with emission of electromagnetic frequencies considered in the UV-Vis, punctually, the range analyzed covers frequencies between (397-402 nm). Through the modification of the duty cycle (D) of the output port number 3 Pulse Width Modulation (PWM) of the Arduino 1 board, it was possible to simulate 255 different voltage values between 0 and 5 volts (output voltage for Arduino pins) with which the LED was turned on at different intensities. In front of the LED, the PT1302B/C2 phototransistor was placed in order to capture the level of light coming, mainly from the LED.

After analyzing 50 spectra of deionized water with 5 different glucose concentrations, it is concluded that the evaluated device could be used to characterize samples with different concentrations of the same molecule, since the 50 signals were correctly identified.

MATERIALS AND METHODS

This section is addressed in 3 different subsections to give details of the 3 main areas involved in the project: electronics, software development and data analysis through machine learning.

Device development

As a central unit for obtaining the UV-Vis spectrum, it was carried out using an Arduino 1 board. The process starts when the user presses the micro switch. Using the PWM pin (pin number 3), from the Arduino development board 1, we modulate the light intensity of the UV5TZ-400-15 LED, which has a viewing angle of up to 15° [19, p. 400-15]. This modulation was achieved by simulating the output voltage (Vef) of the pin, to perform this task, the duty cycle (D) of the pin was modified for the same period of time, consider the following example, for a time period of 5 seconds, if the LED stays on for 1 second D would be equivalent to 20% and considering that the Arduino output pins allow to obtain 5 volts, the Vef would correspond to 1 volt (this is 20% of 5 volts), the above would turn on the LED with a certain brightness. The PWM modules allow, through the *analogWrite*(AW) instruction, to write values between 0 and 8 bits, that is, values between 0 and 255, for this, it is necessary to provide the function as the first argument the output pin followed of the duty cycle to be simulated: *analogWrite*(OutputPIN, D). The LED anode was connected in series with a 330 Ohm (Ω) resistor to the PWM pin of the Arduino, while the cathode was connected to ground.

To capture the light transmitted through the sample and convert it to voltage, we use the reverse-biased phototransistor PT1302B/C2 [20]. The cathode of the PT1302B/C2 was connected in series with a 20 Kilo Ohms (KΩ) resistor and to the 5 volt output of the Arduino while the anode was connected to an analog pin 2 (A2) on the board to record the voltage received from the UV5TZ-400-15 LED via the Arduino *analogRead*

instruction. On the display, the user D and the value received by the phototransistor will be presented.

Using deionized water and 99.5 % D-glucose, solutions with 500 mg/dL, 250 mg/dL, 100 mg/dL, and 50 mg/dL were prepared. Of each solution, 10 microliters (μl) were deposited on a 1 millimeter (mm) thick microscope slide by pipetting and allowed to dry at room temperature. From each sample with the 4 solutions prepared with different glucose concentrations, 10 spectra were captured. In addition, 10 spectra of the empty slide were captured. To ensure that the slide was always placed in the correct position to be irradiated, an alligator clip was soldered to a servomotor with a rotation angle of 0° to 90°, thus, after calibrating the LED and the phototransistor, the servomotor would place Always in the same orientation the slide. Figure 1 shows the electronic diagram of the connections mentioned.

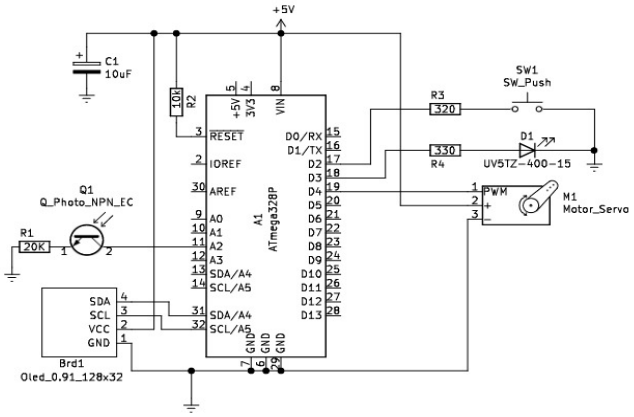

FIGURE 1. **Device electronic diagram.**

Software for data acquisition

The operation described at the end of the previous subsection allows the device to radiate a sample, however, it is necessary to capture and save this information to be able to analyze it later. To achieve the above, it is necessary to develop a computer program that allows, through the Universal Serial Bus (USB) input of the Arduino, to link the device developed with a computer to safeguard the information obtained from the radiation of each sample.

To enable communication between Arduino and a computer, it is necessary to include the data to be transferred in the *Serial.println(data)* function, and previously, define the baud rate for communication in the *setup()* section using the *Serial.begin(9600)*; instruction. In this way, Arduino will have the possibility of sharing all the values that are included in one or more instructions *Serial.println(data)*.

To record the data in the computer, it is necessary to develop a program that allows analyzing the USB connections of the computer to detect the one that matches the Arduino board, to later establish communication with the board using the baud rates defined in Arduino. It is worth mentioning that a usual value for the baud rate is 9600, the value adopted in this work, although this value may vary.

Once the Arduino radiation process is finished, the software will save a *.txt* file on the computer with records of both the value of D and the voltage received by the transistor.

Data analysis

After radiating the sample with the values of 255 Vef (because it is only possible to write 8-bit values with a PWM pin), and after capturing the values of the light transmitted through the sample, the resulting vector was normalized using Equation 1.

$$Normalized\ Value = \frac{real\ value\ captured}{maximum\ captured\ value} \quad (1)$$

To verify the feasibility of the team and the proposed strategy, the k-nearest neighbors (KNN) strategy was used with different values of k and a similarity metric based on the Euclidean distance (D.E.) [21], Equation 2.

$$D.E. = \sqrt{(x_{i+1} - x_i)^2 + (y_{i+1} - y_i)^2} \quad (2)$$

For our case, from Equation 2, X represents the indices of the vector that is analyzed (the variations of D, that is, values from 0 to 255) while Y, the values recorded by the phototransistor and stored in the Arduino 1 board.

The KNN strategy assigns the membership or class to an unknown vector based on the class to which the k closest vectors belong. For this, it is necessary to define a method to calculate the distance of the vector under study with respect to all the others, the Euclidean distance in our case. In this sense, KNN requires that the signals belonging to the same family have a subregion where they have a very similar altitude (or with a minimum standard deviation), since otherwise errors in the associations would be frequent [22][23][24][25]. In order to evaluate all the signal through the KNN strategy, the leave-one-out-cross validation (LOOCV) strategy was followed. According to LOOCV, a signal from the database is separated in order to be compared against the rest and, based on some similarity metric, assign a membership to one of the available classes. This process is carried out with each of the registered samples [22].

The flow diagram for the radiation of a sample is presented below in Figure 2.

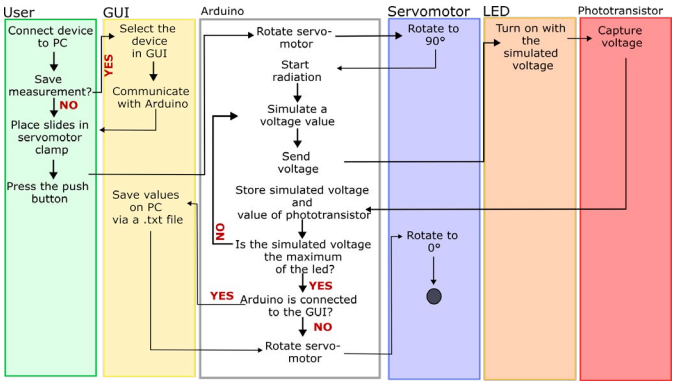

FIGURE 2. **Process diagram for the use of the proposed device.**

The research hypothesis is that there must be a linear correlation between the light level emitted and received, unless something hinders its free transit. Between the LED and the transistor, the glass slide with 10 microliters of one of the prepared solutions will be located. After finishing the radiation process for one sample, the slide was cleaned with isopropyl alcohol in order to receive the next sample of the same concentration as the previous one. The described process was repeated until 10 measurements of each concentration were formed, therefore, since there were 5 different glucose concentrations, there was finally a database of 50 measurements. In the measurements of each glucose concentration, a particular behavior was sought that would allow them to be differentiated from the measurements of the other concentrations.

RESULTS AND DISCUSSION

Figure 3 shows the developed device, where the graphical user interface (GUI) developed to establish the communication process in a friendly way is presented.

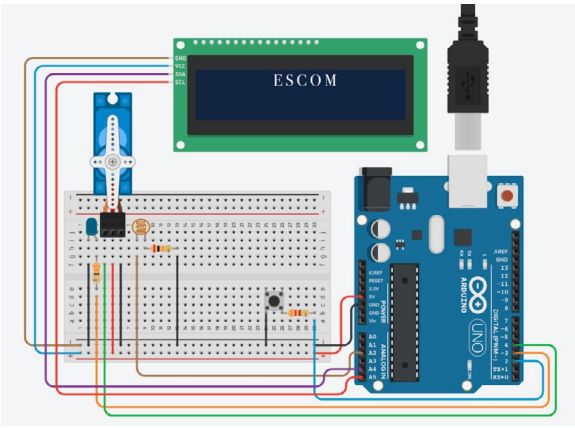

FIGURE 3. **Developed device.**

To guarantee that the samples were irradiated in the correct place, the slide was placed in a clamp welded to a servomotor, thus always placing the sample to be analyzed in the same position. Once the 10 signals of each concentration were captured, including the empty slide, the formula of Equation 1 to normalize them between 0 and 1. Figure 4 shows the comparison of the mean signal calculated for each of the concentrations prepared.

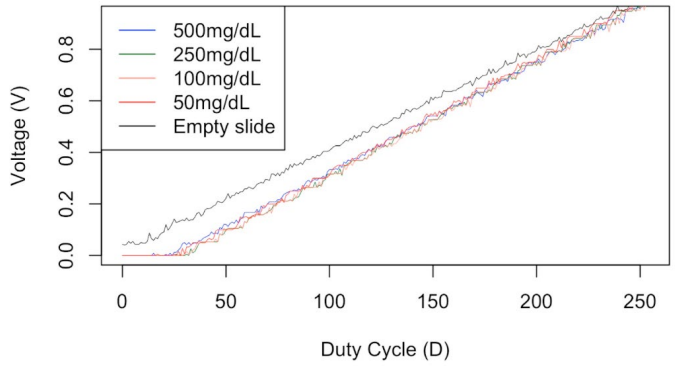

FIGURE 4. Comparison of averages of the different glucose concentrations evaluated.

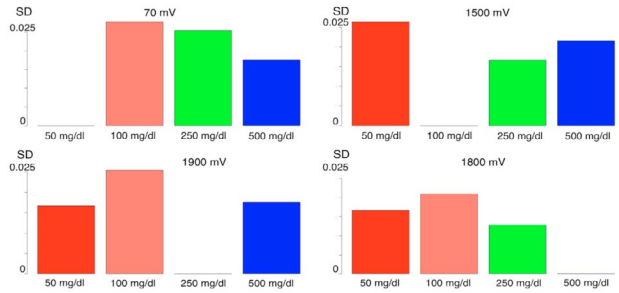

FIGURE 5. Behavior of the standard deviations for the different glucose concentrations, considering different simulated voltages.

Following the guidelines of the KNN algorithm and the LOOCV segmentation, 4 different evaluations were carried out considering different values for K. The results are presented in Table 2.

TABLE 2. KNN algorithm performance considering different values of K.

KNN performance		
K value	Misclassified signal	Accuracy percentage
2	2	96
3	0	100
4	0	100
5	1	98

To validate the results shown in Table 2, we calculated the standard deviation of the signals considering the 255 possible values for D. In accordance with [26], the standard deviation (SD) is defined as the concentration with respect to the arithmetic mean of a set of values, this implies that, with a certain value of D, the signal of the same population has a standard deviation close to 0. Figure 5 shows the standard deviations behavior of the mV received when the sample interacts with a certain simulated voltage (70, 1500, 1900 and 1800 mV).

Thanks to Figure 5 it is possible to validate the results presented in Table 2 considering the following:

- The LOOCV strategy consists of randomly separating a signal from a database, omitting the fact that the group to which it belongs is known in order to assign it a membership through some mathematical model.

- The KNN strategy compares a new measurement against properly categorized measurements from a database based on Euclidean distance. In this way, the new signal will adopt the membership of the K closest values in the measurements registered in the database.

- The standard deviation (SD) is a measure of dispersion from the mean of a population. A standard deviation equal to 0 means that the mean of a population is exactly equal to a value of the new signal to be classified, which means that this new signal has exactly the same height (or mV received in our case) as the signal of a population.

Considering the previous points and the results presented in Table 3, it is possible to infer that there are points in which the measurements of the different

populations have exactly the same height between them and considering the results of the same table for the misclassified signal, it is It is possible to say that these signals belong to the same population. Through the modification of values for D in the PWM Arduino PIN, it is possible to obtain SD close to 0 at different points of the signal for the different glucose concentrations. Such regions are presented in Table 3. The D values indicated in Table 3 do not mean that there is no overlap in the values of the voltage received from the different glucose concentrations, but rather that with such a D value, a SD equal to 0 was obtained for a given glucose concentration.

TABLE 3. Key D values to characterize the different concentrations of glucose.

Key D values		
Glucose (mg/dL)	D Value (%)	Received millivolts. (mV)
50	35, 36, 37, 48, 49, 51, 58, 71, 84, 96, 97, 98, 99, 108, 109, 110, 148, 240 and 252.	100,100,100,200,200, 200,300,400,500,600, 600,600,600,700, 700,700,1100 1900 and 2000
100	78, 88, 104, 140, 154, 179, 188, 212, 214, 215 and 224.	400, 500, 600, 900, 1000,1200, 1300, 1500,1500,1500 and 1600
250	100, 236 and 244.	600, 1700 and 1900
500	32, 34, 64, 122, 123, 132, 133, 157, 160, 178, 180, 181, 190, 192, 193 and 204.	100,100,400,1000, 1000,1100,1100, 1300,1400,1600, 1600,1600,1700, 1700,1700 and1800

Table 3 expresses that, for example, when the 10 samples of glucose concentrations were irradiated at 250 md/dl, generating the simulated voltages corresponding to the modification of the duty cycle (D) of the Arduino PWM PIN with values of 100, 236 and 244, and after normalizing the signals, we always obtained voltages of 600, 1700 and 1900 mV.

Different spectroscopy strategies, including UV-Vis, have proven to be useful for the characterization of different glucose concentrations, analyzing samples with a molecular composition even higher than that exposed in the present work [8][9][10][11][12][13][14][15][16][17][18], for this, they use spectrometers capable of regulating the different ranges of the frequencies of the electromagnetic spectrum.

Although the investigations focused on quantifying glucose levels in more complex samples (in terms of molecular composition) than those studied in this work report accuracy percentages higher than 90 % thanks mainly to a linear behavior of the UV-Vis spectrum [15][16][17][18], the models reported by the authors require all the measurements obtained by the spectrometer used in their research, which cover frequency ranges between 250 nm and up to 900 nm.

The results obtained in the present work coincide with the aforementioned authors, evidencing the feasibility of using low frequencies of UV-Vis spectroscopy to quantify glucose concentrations; however, a couple of points to highlight is that in this research it is carried out considering 6 frequencies (out of 397 at 402 nm), in addition to not requiring mixing the samples with gold or silver nanoparticles or with more complex molecular solutions such as those of the authors of [15][16][17] [18], as in related works.

Being emitted by a low-cost LED, the frequencies considered in this work open the possibility of developing a device that allows the identification of different levels of concentrations of deionized water

with glucose. However, based on the results obtained through the K-NN exercise, it is difficult to think about obtaining a specific punctual result, since with different values of K the percentage of accuracy was reduced.

CONCLUSIONS

In the present work, we propose a novel technique that, considering the results obtained, allows us to correctly identify the concentrations of glucose mixed in deionized water.

Through the modulation of the output voltage of a PWM pin of the Arduino 1 board, we regulate the light intensity produced by the UV5TZ-400-15 LED. The light intensity emitted by the LED was recovered using the PT1302B/C2 phototransistor. By working with 8 bits, it was possible to produce 255 variations of the output voltage for the LED, each sample analyzed was subjected to these 255 luminous variations, thus obtaining a vector of 255 elements (millivolts). After subjecting 50 samples of deionized water with 5 different concentrations of glucose (10 for each concentration) to the light radiation process produced by the LED and using the KNN algorithm, it was possible to find that when hit by a specific light intensity, the samples with the same glucose concentration presented similar behaviors, this is, whenever they were irradiated at a certain luminosity out of the 255 possible, the 10 different samples with the same glucose concentration allowed the photodiode to always capture the same number of millivolts. For each glucose concentration, the above behavior was observed with different light intensities, however, between the different concentrations of gloss, the light intensities that produced this effect were never the same (Table 3). This was what allowed KNN to correctly identify all 50 samples.

Despite the fact that works such as those presented by [8][9][10][11][12][13][14][15][16][17][18], have proposed techniques to characterize more complex samples (with more additional molecules to water and glucose) based on their glucose level using UV-Vis spectroscopy. There are several significant differences between these works and the one presented in this article. Probably the most important is the strategy used, while in spectroscopy the frequencies of the emitting sources are modulated, in the present work we simulate different voltages with which the LED turns on at a certain brightness, however, the frequency with which the Arduino PWM PIN works remains constant. Additionally, in the works [8][9][10][11][12][13][14][15][16][17][18], the authors need to use nanoparticles to highlight the effects of glucose in the samples analyzed while in the present work the samples are studied without any additional component, although this can be attributed to the fact that in their studies the authors studied samples with additional molecules to water and glucose, which interfere with their measurements. Finally, there is the field of the quality of the materials, while the authors of the related works use spectrometers, the device elaborated in the present work, considers commercial materials.

The purpose of this research work is to develop a device that allows to reliably estimate glucose levels in samples with a large number of molecules such as saliva, therefore, despite the fact that the results obtained are encouraging, it is necessary to experiment with sample more complex, for this purpose it is proposed to gradually add more components to the concentrations and repeat the exercises carried out here.

AUTHOR CONTRIBUTIONS

V.S.M. performed data curation, developed the methodology, carried out formal analyses and research, contributed to the research and oversaw the project, validated analyses, participated in the review, editing and the different writing stages of the manuscript. A.H.P. performed data curation, carried out formal analyses, participated in the use of specialized software, validated analyses, participated in the

review, editing and the different writing stages of the manuscript. L.E.B.M. performed data curation, carried out formal analyses, participated in the use of specialized software, validated analyses, participated in the review, editing and the different writing stages of the manuscript. M.S.B. conceptualized the project, performed data curation, developed the methodology, carried out formal analyses and research, contributed to the research and oversaw the project, validated analyses, participated in the review, editing and the different writing stages of the manuscript. All authors reviewed and approved the final version of the manuscript.

REFERENCES

[1] World Health Organization (WHO), Non communicable diseases (2022). Available: https://www.who.int/news-room/fact-sheets/detail/noncommunicable-diseases (accessed Oct. 03, 2022).

[2] World Health Organization (WHO), Diabetes (2022). Available: https://www.who.int/es/news-room/fact-sheets/detail/diabetes (accessed Oct. 03, 2022).

[3] American Diabetes Association (ADA), Diabetes Symptoms, Causes, & Treatment (2023). Available: https://diabetes.org/diabetes (accessed Oct. 03, 2022).

[4] M. Erbach, G. Freckmann, R. Hinzmann, B. Kulzer, R. Ziegler, L. Heinemann and O. Schnell, "Interferences and Limitations in Blood Glucose Self-Testing: An Overview of the Current Knowledge," J. Diabetes Sci. Technol., vol. 10, no. 5, pp. 1161-1168, Sep. 2016, doi: https://doi.org/10.1177/1932296816641433

[5] M. Franciosi, G. Lucisano, F. Pellegrini, A. Cantarello, A. Consoli, L. Cucco, R. Ghidelli, G. Sartore, L. Sciangula and A. Nicolucci, "ROSES: role of self-monitoring of blood glucose and intensive education in patients with Type 2 diabetes not receiving insulin. A pilot randomized clinical trial," Diabet. Med., vol. 28, no. 7, pp. 789-796, 2011, doi: https://doi.org/10.1111/j.1464-5491.2011.03268.x

[6] O. Schnell, H. Alawi, T. Battelino, A. Ceriello, P. Diem, A.-M. Felton, W. Grzeszczak, K. Harno, P. Kempler, I. Satman, B. Vergès, "Self-Monitoring of Blood Glucose in Type 2 Diabetes: Recent Studies," J. Diabetes Sci. Technol., vol. 7, no. 2, pp. 478-488, Mar. 2013, doi: https://doi.org/10.1177/193229681300700225

[7] A. S. Bolla and R. Priefer, "Blood glucose monitoring- an overview of current and future non-invasive devices," Diabetes Metab. Syndr. Clin. Res. Rev., vol. 14, no. 5, pp. 739-751, Sep. 2020, doi: https://doi.org/10.1177/193229681300700225

[8] C. Srichan, W. Srichan, P. Danvirutai, C. Ritsongmuang, A. Sharma, and S. Anutrakulchai, "Non-invasively accuracy enhanced blood glucose sensor using shallow dense neural networks with NIR monitoring and medical features," Sci. Rep., vol. 12, no. 1, art. 1769, Feb. 2022, doi: https://doi.org/10.1038/s41598-022-05570-8

[9] X. Yang, T. Fang, Y Li, L. Guo, F. Li, F. Huang, and L. Li, "Pre-diabetes diagnosis based on ATR-FTIR spectroscopy combined with CART and XGBoots," Optik, vol. 180, pp. 189-198, Feb. 2019, doi: https://doi.org/10.1016/j.ijleo.2018.11.059

[10] E. Guevara, J. C. Torres-Galván, M. G. Ramírez-Elías, C. Luevano-Contreras, and F. J. González, "Use of Raman spectroscopy to screen diabetes mellitus with machine learning tools," Biomed. Opt. Express, vol. 9, no. 10, pp. 4998-5010, Oct. 2018, doi: https://doi.org/10.1364/BOE.9.004998

[11] B. M. Chege, Z. Birech, P. W. Mwangi, and F. O. Bukachi, "Utility of Raman spectroscopy in diabetes detection based on biomarker Raman bands and in antidiabetic efficacy studies of herbal extract Rotheca myricoides Hochst," J. Raman Spectrosc., vol. 50, no. 10, pp. 1358-1366, 2019, doi: https://doi.org/10.1002/jrs.5619

[12] S. K. Benson, K. M. Boyce, R. M. Bunker, et al., "Multinuclear NMR and UV-Vis spectroscopy of site directed mutants of the diabetes drug target protein mitoNEET suggest that folding is intimately coupled to iron-sulfur cluster formation," Inorg. Chem. Commun., vol. 63, pp. 86-92, Jan. 2016, doi: https://doi.org/10.1016/j.inoche.2015.11.022

[13] J. Torres-Gamez, J. A. Rodriguez, M. E. Paez-Hernandez, and C. A. Galan-Vidal, "Application of Multivariate Statistical Analysis to Simultaneous Spectrophotometric Enzymatic Determination of Glucose and Cholesterol in Serum Samples," Int. J. Anal. Chem., vol. 2019, art. 7532687, Jan. 2019, doi: https://doi.org/10.1155/2019/7532687

[14] S. Shokouhi, M. R. Sohrabi, and S. Mofavvaz, "Comparison between UV/Vis spectrophotometry based on intelligent systems and HPLC methods for simultaneous determination of anti-diabetic drugs in binary mixture," Optik, vol. 206, art. 164304, Mar. 2020, doi: https://doi.org/10.1016/j.ijleo.2020.164304

[15] N. D. Nguyen, T. V. Nguyen, A. D. Chu, H. V. Tran, L. T. Tran, and C. D. Huynh, "A label-free colorimetric sensor based on silver nanoparticles directed to hydrogen peroxide and glucose," Arab. J. Chem., vol. 11, no. 7, pp. 1134-1143, Nov. 2018, doi: https://doi.org/10.1016/j.arabjc.2017.12.035

[16] X. Luo, J. Xia, X. Jiang, M. Yang, and S. Liu, "Cellulose-Based Strips Designed Based on a Sensitive Enzyme Colorimetric Assay for the Low Concentration of Glucose Detection," Anal. Chem., vol. 91, no. 24, pp. 15461-15468, Dec. 2019, doi: https://doi.org/10.1021/acs.analchem.9b03180

[17] S. Jiang, Y. Zhang, Y. Yang, Y. Huang, G. Ma, Y. Luo, P. Huang, and J. Lin, "Glucose Oxidase-Instructed Fluorescence Amplification Strategy for Intracellular Glucose Detection," ACS Appl. Mater. Interfaces, vol. 11, no. 11, pp. 10554-10558, Mar. 2019, doi: https://doi.org/10.1021/acsami.9b00010

[18] M. Bartosiak, J. Giersz, and K. Jankowski, "Analytical monitoring of selenium nanoparticles green synthesis using photochemical vapor generation coupled with MIP-OES and UV-Vis spectrophotometry," Microchem. J., vol. 145, pp. 1169-1175, Mar. 2019, doi: https://doi.org/10.1016/j.microc.2018.12.024

[19] Digi-Key Electronics. "UV5TZ-400-15". Digi-Key Electronics. Available: https://www.digikey.com/es/products/detail/bivar-inc/UV5TZ-400-15/3095679 (accessed Oct. 15, 2022).

[20] Everlight. "PT1302B-C2 Datasheet - 5mm Phototransistor". Everlight. Available: http://www.datasheet.es/PDF/796537/PT1302B-C2-pdf.html (accessed Dec. 18, 2022).

[21] L. Liberti, and C. Cavor, *Euclidean Distance Geometry: An Introduction*, Durham, USA: Springer, 2010, pp. 133. [Online]. Available:https://doi.org/10.1007/978-3-319-60792-4 (accessed Nov. 21, 2022).

[22] A. Géron, *Hands-On Machine Learning with Scikit-Learn, Keras, and TensorFlow: Concepts, Tools, and Techniques to Build Intelligent Systems*. Canada: O'Reilly Media, Inc., 2019, pp. 856.

[23] Q. Chen, H. Lin, and J. Zhao, *Advanced Nondestructive Detection Technologies in Food*, Singapure: Springer, 2021, pp. 333. [Online]. Available: https://doi.org/10.1007/978-981-16-3360-7 (accessed Nov. 21, 2022).

[24] J. Workman, *The Concise Handbook of Analytical Spectroscopy*, USA: World Scientific, 2016, pp. 1828. [Online]. Available: https://doi.org/10.1142/8800 (accessed Nov. 21, 2022).

[25] R. White, *Chromatography/Fourier Transform Infrared Spectroscopy and Its Applications,* Boca Raton, USA: CRP Press, 1989, pp. 344. [Online]. Available: https://doi.org/10.1201/9781003066323 (accessed Nov. 21, 2022).

[26] E. B. Mode, *Elementos de probabilidad y estadística,* Barcelona, Spain: Editorial Reverté, 2021, pp. 380.

REVIEW ARTICLE

VOL. 44 | NO. 2 | **MAY - AUGUST 2023** | PP 38-51

Revista Mexicana de Ingeniería Biomédica

dx.doi.org/10.17488/RMIB.44.2.4

E-LOCATION ID: 1347

Mucoadhesive polymeric systems for vaginal drug delivery: a systemic review

Sistemas poliméricos mucoadhesivos para la liberación vaginal de fármacos: revisión sistemática

Maryel Hernández-González[1], *Claudia Rodríguez-González*[1], *Miguel Domínguez-Acosta*[1], *Juan Hernández-Paz*[1] *Imelda Olivas-Armendáriz*[1]

[1]Instituto de Ingeniería y Tecnología, Universidad Autónoma de Ciudad Juárez, Ciudad Juárez - México

ABSTRACT

Intravaginal drug administration has many advantages in comparison to other delivery routes: its local and systemic effect, lower dosages, and easiness of administration. Furthermore, makes it a reliable and comfortable way of therapy. This route can be used to prevent and treat a wide range of conditions including, sexually transmitted infections (STIs), hormonal treatment, birth control, and cancer treatment. The dosage forms may vary from ovules, tablets, rings, gels, creams, films and many more; lately adding the mucoadhesiveness to the characteristics to reduce the waste of active molecules. This review focuses on the way mucoadhesive polymeric systems have been applied in vaginal delivery. This review presents a bibliographical compilation of results from various investigations published in scientific databases: Science Direct, SciELO, and PubMed Central. Results compiled demonstrate that the intravaginal drug administration can be an alternative form of medication for women with more stable and prolonged results than traditional routes requiring lower doses and avoiding the first-pass effect.

KEYWORDS: Mucoadhesive polymeric systems, vaginal drug delivery, treatment

RESUMEN

La administración de fármacos por vía intravaginal cuenta con múltiples ventajas a comparación de otras rutas, puede lograr un efecto tanto local como sistémico, las dosis requeridas son menores, facilidad de administración entre otras, hacen que esta forma de administración sea confiable y cómoda. Esta vía de administración puede ser empleada para prevenir y tratar diferentes trastornos, como enfermedades de transmisión sexual, desordenes hormonales, anticonceptivos y tratamiento contra el cáncer. La presentación de las dosis puede variar, desde óvulos, tabletas, anillos, geles, cremas, películas entre otros, agregando a esta, en los últimos tiempos, la característica de mucoadhesividad para reducir el desecho de moléculas activas. Este trabajo se enfoca en las aplicaciones que han tenido los sistemas poliméricos mucoadhesivos en la vía intravaginal. La bibliografía recolectada se obtuvo de bases de datos como *Science direct*, SciELO, y PubMed Central. Los resultados obtenidos demuestran que la administración de fármacos por vía intravaginal puede ser una forma alternativa para medicación en mujeres, con resultados más estables y prolongados que otras rutas, requiriendo menores dosis y evitando el efecto de primer paso.

PALABRAS CLAVE: Sistemas poliméricos mucoadhesivos, liberación vaginal de fármacos, tratamiento

Corresponding author

TO: Imelda Olivas-Armendáriz

INSTITUTION: Instituto de Ingeniería y Tecnología-Universidad Autónoma de Ciudad Juárez

ADDRESS: Av. Plutarco Elías Calles #1210 Fovissste Chamizal Ciudad Juárez, Chih., Méx. C.P. 32310

CORREO ELECTRÓNICO: iolivas@uacj.mx

Received:

17 March 2023

Accepted:

29 May 2023

INTRODUCTION

The modern history of intravaginal drug administration began around 1918, when Dr. David I. Macht published his research called "On the Absorption of Drugs and Poisons Through the Vagina" in which through this route morphine, atropine and other drugs, like contraceptives, were provided to female patients that were unable to take their medications orally due to vomiting or any other stomach-related illnesses [1][2][3]. This was followed by the research "Absorption from the Vagina" done by Robinson in 1925, in which he focused on the absorption of different molecules such as insulin, potassium iodide, sodium salicylate and others, obtaining that not all molecules were absorbed, such as methylene blue [2]. These are not the first attempts to provide treatment vaginally. Before common era (BCE), the internal part of female reproductive system was already used to apply remedies passed from generation to generation without really knowing where it all began. The first ever record found dates back to 1850 BCE in ancient Egypt, showing that gynecology is an important part of our medicine with more than 4,000 years of practice [3].

The female genital track provides local effect on what was considered "woman affairs" using products such as douches, tampons, suppositories, "uterine wafers", among others, to administer natural or more sophisticated remedies [1][4]. Back in common era, since the pioneering work done by Dr. Macht and Robinson, multiple products have been synthesized to carry different types of drugs with the purpose of treating multiple diseases from chronical, infectious, and even hormonal imbalances which can be attended with local and systemic effects through this route using ovules, creams, gels, rings, films, tablets, nanoparticles, and the like [5][6][7] (Figure 1).

Even though gynecology is an ancient medical practice, the use of this route for drug administration has slowly but steadily developed fighting against stereotypes and taboos that have interfered with its growth, but science has made its way through, and the technique has become for some ailments even more reliable than oral and intramuscular route [7]. The local and systemic effect achievable with vaginal drug delivery systems has many advantages and can be used for many purposes. It does not require a first pass effect and does not involve the circulatory system for local effects [8]. It can carry drugs to prevent and treat different illnesses even during pregnancy and lactation and can interact with mucus and skin [9][10]. That is why every day more groups are focusing their research on active molecules that can be administered through the vagina [11][12][13][14][15].

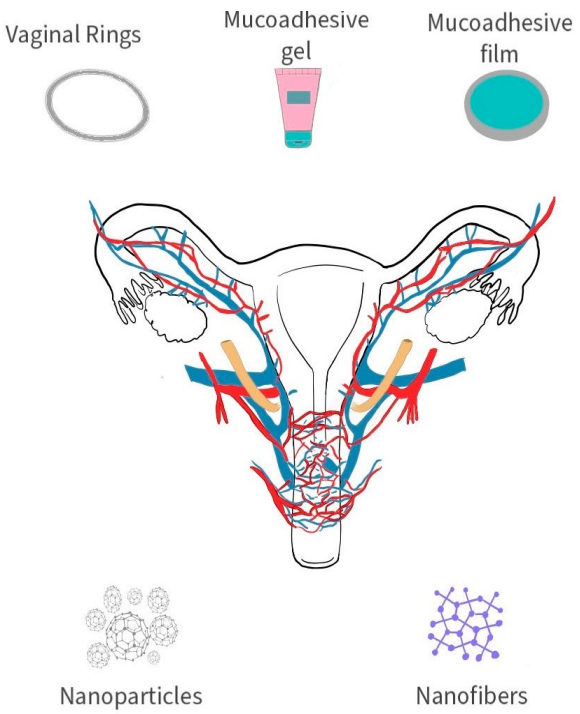

FIGURE 1. **Vaginal drug delivery systems (VDDS)**

Many biomaterials can be used to administer drugs through different routes but for the intravaginal administration specifically, polymers are preferred. Their mechanical properties, biocompatibility and overall performance has made them the number one choice for this application. Hydroxypropyl methylcellulose (HPMC) [11] Chitosan [12], sodium alginate [12], Carbopol [13], Polyethylene glycol (PEG) [11] and different types of gums [14] are only some of the

more commonly used polymers that can be synthetized in forms of tablets, gels, rings, nano structures, films, patches, and so on (Figure 1). Furthermore, polymers also have the ability of fixing with the mucosa layer, becoming bioadhesive thus gaining various advantages like reduction in doses and in frequency of application due to increased residence time, also a prolonged and controlled release, higher bioavailability with lower concentration of bioactive molecules, no first-pass metabolism, specific targeting, and lower or non-enzymatic degradation [15].

MATERIALS AND METHODS

The present investigation was performed based on an extensive bibliographical review, consulting the Science Direct, SciELO, and PubMed Central databases, with a search strategy designed to obtain publications related to vaginal mucoadhesive drug delivery systems. The inclusion and exclusion criteria used in the bibliographic search are found in Table 1. Results included 76 articles, all in English, in which mucoadhesive drug delivery systems were made with biodegradable polymeric matrices.

TABLE 1. Inclusion and exclusion criteria used in the bibliographic review.

Inclusion criteria	Exclusion criteria
Publications between the years 2004 – 2022.	Publications prior to 2004, except for transcendental references that are an inherent part of the history of these devices.
English language publications.	Publications in a language other than English
Publications in vaginal drug delivery adhesive systems.	Publications related to drug delivery systems of other organs and tissues.

RESULTS AND DISCUSSION

Mucoadhesive systems to delivery drugs

The cervix is covered by a semipermeable mucus which is mostly mucin. This makes a protector barrier and becomes an obstacle for the absorption of drugs within the medium (Figure 2). In the last decade, systems for intravaginal applications have been made with different mucoadhesive polymers such as PEG 400, HPMC, Chitosan, Carbopol, and the like to promote the absorption of the drugs liberated in the vagina [16] [1]. These systems present advantages over conventional treatments by having big contact surfaces allowing a deeper mucus penetration and avoiding as much waste as possible. This leads to a better absorption that can be as slow or fast as wanted depending on the materials used; also, allows to a better penetration of the metabolic and physiological barriers leading to bigger biodisposition of the drugs and lower risk of unwanted side effects [1][2].

In the synthesis of controlled release systems, many different polymers have been used both natural and synthetic because it has been seen that the adhesion between mucus and materials occur because hydrogen links are formed. Hydrophobic interactions can also happen or electrostatic, even macromolecule entanglements. This can produce mucoadhesion because the contact between the mucus and the system allows the humectation and expansion of the material leading to diffusion of the carrier lessening the chances of interactions between the drugs and mucus [16].

Choosing the right polymer depends mostly on the application, the mucoadhesiveness that is needed, the release time and the drug that is going to carry. As an example, HPMC and PEG 400 helps penetrate the mucus barrier and allows the release closer to the tissue. This system has characteristics such as biocompatibility, biodegradation and does not produce an immune response. It also allows hydrogen links to

form which facilitate the interaction with the mucus barrier; through FTIR analysis, it was shown that hydrogen bonds and Van Der Waals forces are present [1][2][15][16].

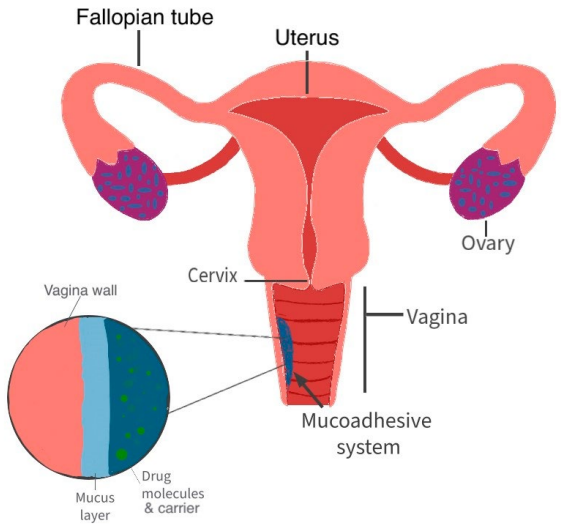

FIGURE 2. Mucoadhesive system in contact with the vaginal wall.

Mucoadhesive systems to delivery anesthetics

From our current time, the first medical report of vaginal administration of drugs was done by Dr. Macht in 1918. In it, he developed research and provided pain medication called morphine to female patients that couldn't take it orally. In his methodology he introduced a pill that was first synthetized to be taken orally and administered through the vaginal canal and waited for the signs of the medication to take effect [3][6]. At this time oral purpose pills were not administered through this female cavity, but several presentations to provide drug delivery intravaginally had been developed from diaphragms, capsules, creams, ovules, suppositories, etc. Today drug administration focuses on bioadhesive forms that produce less leakage such as films [11], soft gel capsules [17], rings [18], hydrogels [19], foams [20], and others [3][6][21]. Since Macht's study several trials [16][22][23] [24] have been made to provide pain medication from different sources to women with or without capacity to take the active molecules through other rout. from ketorolac to morphine. Compounds are used in these studies to alleviate the pain these people are suffering due to different causes, either chronic or acute, from surgeries, diseases, or hormonal imbalances [25][26][27].

In 2011, Perioli and their team tried alleviating the pain from a group of women using Benzydamine, which is a Non-Steroidal Anti-Inflammatory Drug also known as NSAID, that reduces pain and inflammation and can be contained in different presentations including mucoadhesive systems. In this work they synthesized vaginal tablets using polymers such as HPMC and/or Carbopol with prolonged release periods of over 40 hours obtaining promising results, especially on the release and residence time of the drugs [28].

Sometime later in 2017, Sanz *et al.* utilized Doxepin (which is a drug typically used to treat depressive disorders and other mental disorders, but it has shown good reactions when used in the treatment of pain) to relieve pain after a gynecological surgery using a mucoadhesive system for the delivery with orafix as the bioadhesive platform, menthol and transcutol [29]. Another example of VDDS is the work published by Pinheiro de Queiroz *et al.*, which administered 5 % lidocaine for the treatment of localized pain after a cesarean and obtained results even after 36 h. That's why it was considered ideal for drug delivery for long periods of time [30].

Viral infections such as Human Papilloma Virus (HPV) can be manifested through painful symptoms, erosions, ulcers, and scars are usually part of these processes [31]. To treat these infections, antivirals are accompanied by anti-inflammatory and analgesic drugs (Table 2), like Ketorolac. This compound has properties like opioids and can be used to treat from moderate to severe pain, but with no addictiveness potential or sedative properties. It has a similar yet less intense effect to morphine but without the side effects [32].

For all these characteristics El Moussaoui S. and her

work group used a mucoadhesive Alginate-based hydrogel, using sodium alginate to deliver ketorolac vaginally to treat Condyloma acuminata, a disease caused by HPV. In this study they concluded that up to 73 % of the ketorolac was released in the first 6 h after administered, a faster permeation compared to through human skin and higher retention time up to 24 h [16]. Another drug often used in vaginal administration is diazepam, this molecule part of the benzodiazepines is often administered through suppositories and have the capacity of relaxing the pelvic floor and relieve pelvic pain locally because it controls the painful spasms and stiffness that causes them [23][33].

TABLE 2. Materials, presentation, and drugs to pain medicine.

Presentation	Materials	Drug	Effect	Reference
Vaginal tablet	HPMC, Carbopol	Benzydamine	NSAID	[9]
Gel	Orafix, menthol and transcutol	Doxepin	Pain relief	[10]
Patch	NE	Lidocaine	Anesthetic	[11]
Hydrogel	sodium alginate	ketorolac	NSAID	[12]

To treat Sexually Transmitted Infections

According to the World Health Organization (WHO) 2021, more than 1 million people acquire STIs daily. Also 500 million have a genital infection with herpes simplex. There are more than 30 different parasites, viruses, and bacteria that cause these infections; 8 of those being most common, 4 curable: syphilis, gonorrhea, chlamydia and trichomoniasis, and 4 incurables: Hepatitis B, Herpes simplex (HSV), Human Immunodeficiency Virus (HIV), HPV [34].

Candidiasis is the second most common vaginal infection worldwide with 1.4 million cases every year only in the US. It is considered one of the main causes of inflammation of the vagina, also known as vaginitis. Several approaches have been tested in order to treat and prevent this yeast infection (Table 3).

Vaginal drug administration is not the exception, vaginal films made of polymers such as HPMC, Chitosan, and such have been developed to administer the necessary drugs to eradicate this fungus [35][36]. Worldwide many research groups work to provide options for better treatment of STIs. In 2021, one group worked with a mucoadhesive films to deliver tioconazole to treat vaginal candidiasis [35]. In 2017 another one prefers to treat the fungus infection by administering probiotics [13] while in 2014 another group administered clotrimazole through a hydroxypropyl cellulose mucoadhesive film [36] and in 2014 another research group used a chitosan bioadhesive gel to administer econazole nitrate and miconazole nitrate [37]. Hombach on the other hand, opted for delivering Nystatin and compared the advantages between mucoadhesive gels and mucoadhesive tablets made out of Polyacrylic Acid (PAA) obtaining good results on both, depending on how the release wanted to be. For example, if it needs a prolonged release time, the tablet would be a better option, but if the rheology needs to be more stable, then gel is the option. Gel interacted better with water, but the interaction of the PAA and nystatin seem better on the tablet, therefore, both presentations are good realizing this drug [38]. In general, all research cited showed promising results due to the high levels of absorption of the active molecule compared to the oral alternatives. The residence time of all applications were less than 20 minutes with no secondary effects reported caused by the carrier materials.

Candidiasis and many other infections can be a consequence of a weaker immune system resulting in one of the most feared diseases, HIV/ acquired immunodeficiency syndrome (AIDS). According to WHO, HIV continues to be a public health issue with an estimated 37.7 million people living with the disease. It is mostly acquired through body fluids from infected people, especially from high-risk sexual behavior [39]. In order to treat this STI, several polymeric systems have been created, such as Enggi *et al.*, who developed

a mucoadhesive gel to administer with cabotegravir, registering great permeation results and residence time lapse. Better than the regular oral and injection route, making it a possible future replacement. Cazorla-Luna and his team preferred a bilayer film made of ethylcellulose and other biopolymers, obtaining good mechanical properties and adherence to the vaginal mucosa with presence of the drug even after a week allowing a biweekly administration [40][41]. Nematpour *et al*. administered clotrimazole using nanofibers of polyvinyl alcohol (PVA) and sodium alginate (SA) obtained from electrospinning generating properties suitable for a drug delivery system [42]. Stella Dolci and her team used the advantages of vaginal films, gelatin and polymers to deliver econazole. In both of their studies (2018 and 2020), they obtained good results improving in 2020 the release time frame with Gelucire, a combination of glycerides that can also work as crosslinker [43][44].

For microbial infections, several approaches have been made, but attacking directly and with a prolonged drug release has demonstrated better results for antimicrobial activity. Similarly Lupo reported using metronidazole with a chitosan mucoadhesive system, as well as Sousa who bet for a chitosan-based system to treat common vulvovaginal infections like trichomoniasis, candidiasis and bacterial vaginosis with a Drug Delivery System mucoadhesive to increase the retention time of the drug [45][46]. Campaña-Seoane M. and her team studied the pharmacokinetics and residence time of vaginal mucoadhesive silicone emulsions with ciprofloxacin, which is an effective antibiotic often used to treat STIs, showing that even after 24 hours of administration the system still had a significant concentration of the drug making possible its future in vivo trials with bigger species [47]. In 2019 Jalil and their team synthetized vaginal films made of gellan gum and a combination of other polymers, named by this team AMENA, to administer metronidazole, concluding that the film has all the properties needed to perform as an antimicrobial system [12]. Herpes viruses have infected approximately 4 billion people globally with either HSV-2 or HSV-1 or both. This virus can be transmitted very easily and be present even without symptoms, therefore, many people have been infected and don't even know [48]. In order to fight this unwanted disease Ijaz M. and collaborators developed a mucoadhesive delivery system for Acyclovir using thiolate polymers showing good results for the vaginal mucoadhesion on porcine vaginal adhesion [49]. Edisson-Mauricio and collaborators worked on a polymeric film made of HPMC and polymethacrylate Eudragit S100 for the release of acyclovir to protect against herpes [50]. As for Ramyadevi *et al*., the mucoadhesive gel and nanoparticles with acyclovir allowed them to reduce the normal dosage ten times, showing promising results for further applications [51].

To prevent Sexually Transmitted Infections

As previously stated, according to WHO some STIs are incurable, therefore, their prevention is a key element of selfcare. VPH, Hepatitis B and HIV are a few of the most feared STIs because once infected there's no cure, only treatment to lessen the symptoms. In the case of VPH and Hepatitis B, several injections have been released to the market to prevent the spreading of these infections and teenagers are immunized before they are sexually active, thus preventing future infections [34][52]. Throughout history different active molecules have been administered using the most common medication routes, like oral, parental and intravenous to prevent and/or treat STIs, specifically HIV, with good results. Unfortunately, continued administration can affect different organs like the liver and gastrointestinal system due to the toxic nature of the molecules. Therefore, other approaches must be studied to provide these patients with a more effective treatment to better their life expectancy and general health. Also, to try to lessen the number of new cases by preventing the spreading with more information sites and providing the convenient drugs to community

sectors at risk. For women, the intravaginal route is a promising way to prevent, treat and alleviate local and systemic infections that threatens their wellbeing [6][53].

TABLE 3. Diseases (STIs) treated with mucoadhesive delivery systems.

Disease	Materials	Active molecule	Reference
Candidiasis	Chitosan/HPMC	Tioconazole	[13]
	Na-CMC, Carbopol, Chitosan	Probiotics	[14]
	HPMC, sodium alginate	Clotrimazole	[15]
	PVA-SA		[16]
	Chitosan	Econazole nitrate, miconazole nitrate	[17]
	Gelatin	Econazole nitrate	[18], [19]
	Poly acrylic acid	Nystatin	[20]
HIV/AIDS	HPMC, Carbomer, PEG400	cabotegravir	[21]
	HPMC, chitosan, guar gum and Eudragit	Tenofovir	[22]
	Gums and Eudragit L100		[23]
	Ethylcellulose and Xanthan gum		[24]
Microbial infections	chitosan	Metronidazole	[25]
	Gellan gum, AMENA		[26]
	Silicon	Ciprofloxacin	[27]
Herpes	β-CD-CHO	Acyclovir	[28]
	HPMC and polymethacrylate Eudragit S100		[29]
	polyvinyl pyrrolidone–Eudragit		[51]

HIV is one of the most feared diseases worldwide, existing since late 1800s in Africa, but truly being acknowledged in mid-1970s when it came to America. According to the Centers for Disease Control and Prevention (CDC) [54] it is considered one of the biggest epidemics and one of the most dangerous viruses that attacks the body's immune system and if not treated can lead to AIDS. In order to prevent the transmission of this vicious virus, barrier methods are required. Specifically male condoms, but it still represents a risk, therefore, new methods have been developed in order to try to reduce new infections. Notario-Perez's and his team worked with mucoadhesive vaginal tables made of HPMC, Chitosan, guar gum and Eudragit to prevent sexual transmission of HIV releasing tenofovir [55]; and later on, switch from using a vaginal table to a vaginal film based on HPMC administrating the same drug [56]. Martins-Illana and her team used several types of gums and Eudragit L100 to administer Tenofovir to prevent the transmission of this virus [14]. The same drug that Cazorla R. and his team administered through a bilayer film based on biopolymers such as ethylcellulose and xanthan gum, which is a natural polymer that can be plasticized with glycerol. Some of the obtained results showed a longer release period than expected, approximately 15 days with zero toxicity and optimal mechanical conditions [41].

Hormonal treatment and birth control

From the start of human history vaginal related medical assistance has evolved. Contraception, abortion and pregnancy practices were the gynecologic beginnings of women sexual care. Even the Egyptians (1850 BCE) considered the vaginal route one of the five routes of drug administration, but religion beliefs and "good morals" have gotten in the way of its development. The importance of women's sexuality wasn't considered until 1885 CE, when the first contraceptive drug was commercialized, based on quinine [20]. Nowadays women health care, specifically sex related, is looked after and freely spoken opening the possibility of vaginal drug administration [5][57].

Several infections within the pelvic area related to hormones have been treated using the vaginal route, from endometriosis, problems related with menopause, to abortions. All can be handled with medication administered intravaginally [58]. Several presentations have been used in order to carry these drugs and mucoadhesive polymeric systems are not the exception as shown in Table 4 [51][55].

For endometriosis several approaches have been

applied throughout the years. Surgical to hormonal treatments are administered to reduce the symptoms of this chronic disease that affects roughly 190 million women in the reproductive age worldwide. Hormones like progestogen and estrogen or combinations of both are used to treat the pain and/or infertility associated with this disease [59]. Normally, oral route is the approach used to administer these drugs, but recently vaginal methods are being used to reduce the side effects associated with taking hormones. Vercellini *et al.* compared a combination of progestogen and estrogen carried by a vaginal ring and a patch obtaining better results with the vaginal mucoadhesive ring because the mucoadhesive system showed a longer residence time and a steadier release pattern [27].

Menopause is a natural process that all females go through, where hormones are involved. It marks the end of the menstrual cycles and finishes the carrying capacity of new life for women meaning big changes in the life of the person going through it. This stage of life has big repercussions physically and mentally speaking, thus in order to lessen the symptoms present within this process, several drugs have been developed, from natural hormones to processed molecules with different forms of administration including oral and injections. In 1988 Carlstrom and collaborators suggested the vaginal administration of follicle-stimulating hormones, globulin, estradiol and progesterone. In this study they used a mucoadhesive gel inserted intravaginally with a special applicator, obtaining higher concentration levels of the hormones on the blood system even though a lower dosage than normal was administered. In addition to reporting a lower liver and kidney activity than when oral administration was used. In this study in general, the new intravaginal administration of hormones was an "overall success" [60]. Later, Ballagh reported the use of a vaginal ring made of medroxyprogesterone acetate for hormone delivery for contraception and menopause purposes. It contained progestin, progesterone, etonogestrel, levongestrel/ norgestrel, megestrol, nestorone, norgestrien, and in general estrogen and progestin combinations. The hormone release rate was higher in the first 48 hours, but effects could be seen even after a week of the administration proving to be a great alternative to oral administration [18]. On the other hand, are the traditional remedies, many communities have used Curcuma comosa and its extracts to treat hormonal imbalances because it contains phytoestrogens. Estrogen replacement therapy can help the cognitive decline women experiment postmenopausal, that is the reason Tunpanich P. and team synthesized a system made of polycarbophil (PCP), HPMC and silica, for Curcuma comosa controlled release [17] [61].

TABLE 4. Mucoadhesive drug delivery systems for Hormonal treatment and birth control.

Presentation	Materials	Drug	Reference
Mucoadhesive ring	NE	Progestogen and estrogen	[30]
Gel	NE	globulin, estradiol, and progesterone	[31]
Ring	medroxyprogesterone acetate	progestin, progesterone, etonogestrel, levonorgestrel/ norgestrel, megestrol, nestorone, norgestrien estrogen, and progestin combinations	[32]
Bio adhesive tablet	HPMC, Carbopol 934 and PEG 6000	Salbutamol	[8]

Preterm labor is one of the major causes of infant illnesses and deaths around the world. It can affect the new life and the mother's health, hence, should be avoided as much as possible and treated with caution. Salbutamol is a drug used to arrest preterm labor, usually administered intravenously, but Abu El-Enin and his team showed that it can also be administered using a vaginal bioadhesive tablet made of HPMC, Carbopol 934 and PEG 6000 obtaining higher concentrations within time than the leader drug

Ventolin [8]. Another example and application of this administration route is shown in El-Refaey's work, published in 1994, were they administered a combination of oral mifepristone and intravaginal misoprostol for an early induction of abortion; showing good results with fewer side effects compared to other techniques [26]. This last example is also a great concern in the overall public health, because many women suffer from bad practices due to the illegalness of abortion, thus early alternatives that care for the health of patients are very important [6].

Mucoadhesive systems used for Cancer treatment

Women's reproductive system, as the rest of the body, is capable of growing cancer cells and tumors. When it happens, it is called gynecologic cancer; it can affect the cervix, ovaries, uterus, vagina, vulva, and even the fallopian tubes (Figure 3). According to the CDC this is one of the main causes of women deaths around the globe [62]. In any cancer treatment the whole body is attacked with drugs to try to kill as many cancer cells as possible, but in the process many healthy cells are destroyed, since most active molecules used for chemotherapy are highly toxic. Therefore, localized systems are required to minimize the side effects, result of the shatter cells [63] [64] [65].

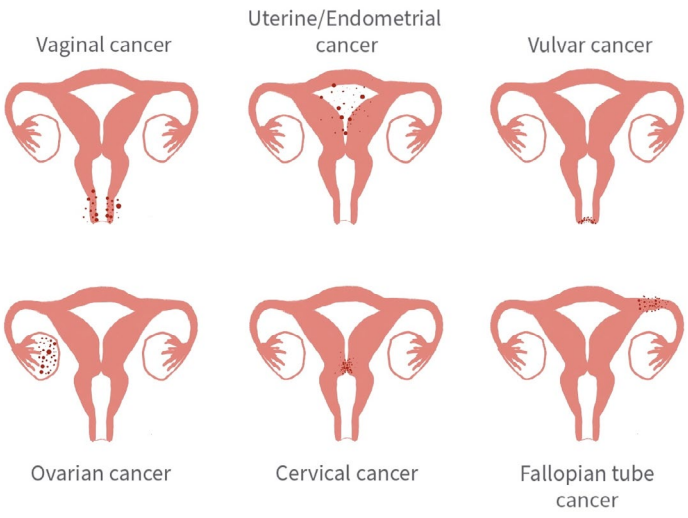

FIGURE 3. **Types of gynecological cancer.**

In an effort to apply the active molecules as close to the tumor as possible, many research groups have used the vaginal route to treat gynecologic cancers (Table 5). Zong *et al.* showed in their study, that carrying cisplatin through a polymeric film and gel can help to shrink tumors considerably. They obtained better residence results with the HPMC film than the HPMC gel because it was more mucoadhesive and it had less leakage [66]. Cisplatin, since its discovery in 1972, has been one of the most used anticancer drugs for its mechanism capable of taking the cells to apoptosis [67]. That is the reason Mohammad Reza *et al.*, delivered this molecule using PAA hydrogels, reducing the regular doses of cisplatin but maintaining the efficiency [68]. Later on, Aggarwal's team developed poly-caprolactone and chitosan nanofibers to vehicle cisplatin to treat cervical cancer. Because poly-caprolactone has an adhesive nature, the studies showed that it can transport and stay in the cervix for an extended period with high bioavailability [69].

Another group working on treating cancer is Meyskens F. L. *et al.*, with a retinol like molecule vehicle with a collagen sponge, which changed daily and helped reduce the tumor size, but had high toxic levels [22][24]. Woolfson D. and team preferred a bio adhesive cervical patch of Carbopol and glycerin to deliver 5-Fluorouracil directly to cervical tissue with sufficient drug release to obtain a good clinical effect [70][71].

Mucins are highly glycosylated proteins used for protection and control of the local molecular microenvironment of organs and tumors during cancer process and metastasis. Because of this, they can be used as markers in cancer as a therapeutic target [72]. Chunyan Li *et al.* worked on a mucoadhesive phenylboronic acid-rich nanoparticles to vehicle and release a mucin-responsive drug to treat cervical carcinoma, with release up to 72 h. [73]. Similarly, Liqian Ci synthetized a system amino-functionalized hydrogel with Poloxamer 407 and acetate gossypol (AG) to carry different drugs showing mucin sensitivity. This is why

it is considered an important biomarker for tumor targeting, because it covers most tumors; that is one of the many reasons Liqian's work is considered ideal to be used on chemotherapy [74].

As for natural medicine, curcumin is in the spotlight for its anti-cancer effects. That is why Damiani and his team decided to deliver it through a mucoadhesive polymeric liquid made of polyethyleneimine (FPC) and chitosan, showing that the system has an affinity for Hela cells [75]. Berginc and team opted for mucoadhesive liposomes coated with chitosan and Carbopol to deliver curcumin. In their study they compared liposomes coated and not coated, evaluating the tissue retention and permeability and obtaining a better residence time, release and mucoadhesion with the coated group [76].

TABLE 5. Mucoadhesive drug delivery systems for cancer treatment.

Presentation	Materials	Drug	Reference
Film	HPMC	Cisplatin	[33]
Hydrogel			
	PAA		[34]
Nanofibers	poly-caprolactone and chitosan		[35]
Sponge	Collagen	Retinol	[36]
Cervical patch	Carbopol / glycerin	5-Fluorouracil	[37], [38]
Mucoadhesive nanoparticles	phenylboronic acid	Mucin responsive drugs	[39]
Hydrogel	Poloxamer 407 and acetate gossypol (AG)		[40]
Mucoadhesive polymeric liquid	polyethyleneimine (FPC) and chitosan	Curcumin	[41]

CONCLUSIONS

Presently, intravaginal delivery systems are a more common way to administer drugs. Its growth has been slow but steady, showing satisfactory results locally and around the system. This form of administration has broken stereotypes and taboos about women's health and care, and even though their existence is long before current era, it has flourished in the last decades. On the other hand, mucoadhesive systems have evolved throughout the years alongside this administration route, covering the necessity of long release periods. Due to their capacity of working for many hours, days and even weeks, reducing the loss of active molecules through discharge and delivering drugs for several purposes from STDs to hormonal and cancer treatments with overall good results. These mechanisms allow lower dosages with steadier residence times and permit the avoidance of the first pass effect. Mucoadhesive VDDS are mostly manufactured with biocompatible and bioinert polymers to ensure a secure interaction with the active molecules and the mucus layer. This allows the penetration of the molecules into the vagina wall thus enhancing drug absorption.

Ethical statement

The author(s) declared no potential conflicts of interest with respect to the research, authorship, and/or publication of this article.

AUTHOR CONTRIBUTIONS

M.E.H.G. performed formal analyses and research, participated in the writing of the first stages of the manuscript. C.A.R.G. conceptualized the project, performed methodology and oversaw the project. M.D.A. participated in the review and editing of the different stages of the manuscript. J.F.H.P. conceptualized the project, performed methodology and oversaw the project. I.O.A. carried out formal analyses, oversaw the project, participated in the review and editing of the different stages of the manuscript. All authors reviewed and approved the final version of the manuscript.

REFERENCES

[1] D. I. Macht, "On the absorption of drugs and poisons through the vagina," J. Pharmacol. Exp. Ther., vol. 10, no. 7, pp. 509-522, Jan. 1918. [Online]. Available: https://jpet.aspetjournals.org/content/10/7/509

[2] G. D. Robinson, "Absorption from the human vagina," BJOG, vol. 32, no. 3, pp. 496-504, Sep. 1927,doi: https://doi.org/10.1111/j.1471-0528.1925.tb06358.x

[3] J. M. Stevens, "Gynaecology from ancient Egypt: The papyrus kahun: A translation of the oldest treatise on gynaocology bas survived from tha ancient world", Med. J. Aust., vol. 2, no. 25-26, pp. 949-952, Dec. 1975, doi: https://doi.org/10.5694/j.1326-5377.1975.tb106465.x

[4] J. das Neves, F. Notario-Pérez, B. Sarmento, "Women-specific routes of administration for drugs: A critical overview," Adv. Drug. Deliv. Rev., vol. 176, art. no. 113865, Sep. 2021, doi: https://doi.org/10.1016/j.addr.2021.113865

[5] N. Dobaria, R. Mashru, N. H. Vadia, "Vaginal drug delivery systems: A Review of Current Status," East Cent. Afr. J. Pharm. Sci., vol. 10, no. 1, pp. 3-13, 2007, doi: https://doi.org/10.4314/ecajps.v10i1.9754

[6] N. J. Alexander, E. Baker, M. Kaptein, U. Karck, L. Miller, E. Zampaglione, "Why consider vaginal drug administration?," Fertil Steril, vol. 82, no. 1, pp. 1-12, Jul. 2004, doi: https://doi.org/10.1016/j.fertnstert.2004.01.025

[7] A. Hussain, F. Ahsan, "The vagina as a route for systemic drug delivery," J. Control. Release, vol. 103, no. 2, pp. 301-313, Mar. 2005, doi: https://doi.org/10.1016/j.jconrel.2004.11.034

[8] A. S. M. Abu El- Enin, A. M. Elbakry, R. El Hosary, M. A. Fouad Lotfy, and R. Yahia, "Formulation, development, in vivo pharmacokinetics and pharmacological efficacy evaluation of novel vaginal bioadhesive sustained core-in-cup salbutamol sulphate tablets for preterm labor," J. Drug Deliv. Sci. Technol., vol. 60, Art. no. 102076, Dec. 2020, doi: https://doi.org/10.1016/j.jddst.2020.102076

[9] J. W. Yoo, K. Dharmala, C. H. Lee, "The physicodynamic properties of mucoadhesive polymeric films developed as female controlled drug delivery system," Int. J. Pharm., vol. 309, no. 1-2, pp. 139-145, Feb. 2006, doi: https://doi.org/10.1016/j.ijpharm.2005.11.020

[10] A. Jalil, M. H. Asim, N. N. Le, F. Laffleur, B. Matuszczak, M. Tribus, A. Bernkop-Schnürch, "S-protected gellan gum: Decisive approach towards mucoadhesive antimicrobial vaginal films," Int. J. Biol. Macromol., vol. 130, pp. 148-157, Feb. 2019, doi: https://doi.org/10.1016/j.ijbiomac.2019.02.092

[11] M. T. Sánchez, M. A. Ruiz, H. Castán, M. E. Morales, "A novel double-layer mucoadhesive tablet containing probiotic strain for vaginal administration: Design, development and technological evaluation," Eur. J. Pharm. Sci., vol. 112, pp. 63-70, Jan. 2018, doi: https://doi.org/10.1016/j.ejps.2017.11.006

[12] A. Martín-Illana, R. Cazorla-Luna, F. Notario-Pérez, L. M. Bedoya, J. Rubio, A. Tamayo, R. Ruiz-Caro, M. D. Veiga, "Smart vaginal bilayer films of Tenofovir based on Eudragit® L100/natural polymer for the prevention of the sexual transmission of HIV," Int. J. Pharm., vol. 602, Jun. 2021, doi: https://doi.org/10.1016/j.ijpharm.2021.120665

[13] L. Kumar, S. Verma, B. Vaidya, V. Gupta, "Bioadhesive Polymers for Targeted Drug Delivery," in Nanotechnology-Based Approaches for Targeting and Delivery of Drugs and Genes, V. Mishra, P. Kesharwani, M. C. I. Mohd Amin, A. Iyer, Ed., London, United Kingdom: Academic Press, 2017, ch. 10, pp. 322-362. [Online]. Available: https://doi.org/10.1016/B978-0-12-809717-5.00012-9

[14] S. El Moussaoui, F. Fernández-Campos, C. Alonso, D. Limón, L. Halbaut, M. L. Garduño-Ramirez, A. C. Calpena, M. Mallandrich, "Topical mucoadhesive alginate-based hydrogel loading ketorolac for pain management after pharmacotherapy, ablation, or surgical removal in condyloma acuminata," Gels, vol. 7, no. 1, art. no. 8, Jan. 2021, doi: https://doi.org/10.3390/gels7010008

[15] C. Karavasili, G. K. Eleftheriadis, C. Gioumouxouzis, E. G. Andriotis, D. G. Fatouros, "Mucosal drug delivery and 3D printing technologies: A focus on special patient populations," Adv. Drug Deliv. Rev., vol. 176, art. no. 113858, Sep. 2021. doi: https://doi.org/10.1016/j.addr.2021.113858

[16] B. Valamla, P. Thakor, R. Phuse, M. Dalvi, P. Kharat, A. Kumar, D. Panwar, S. B. Singh, P. Giorgia, N. K. Mehra, "Engineering drug delivery systems to overcome the vaginal mucosal barrier: Current understanding and research agenda of mucoadhesive formulations of vaginal delivery," J. Drug Deliv. Sci. Technol., vol. 70, art. no. 103162, Apr. 2022, doi: https://doi.org/10.1016/j.jddst.2022.103162

[17] P. Tunpanich, E. Limpongsa, T. Pongjanyakul, B. Sripanidkulchai, N. Jaipakdee, "Mucoadhesive sustained-release tablets for vaginal delivery of Curcuma comosa extracts: Preparation and characterization," J. Drug. Deliv. Sci. Technol., vol. 51, pp. 559-568, Jun. 2019, doi: https://doi.org/10.1016/j.jddst.2019.03.030

[18] S. A. Ballagh, "Vaginal ring hormone delivery systems in contraception and menopause," Clin. Obstet. Gynecol., vol. 44, no. 1, pp. 106-113, Mar. 2001, doi: https://doi.org/10.1097/00003081-200103000-00014

[19] L. Ci, Z. Huang, Y. Liu, Z. Liu, G. Wei, W. Lu, "Amino-functionalized poloxamer 407 with both mucoadhesive and thermosensitive properties: preparation, characterization and application in a vaginal drug delivery system," Acta. Pharm. Sin. B., vol. 7, no. 5, pp. 593-602, Sep. 2017, doi: https://doi.org/10.1016/j.apsb.2017.03.002

[20] I. Löwy, "'Sexual chemistry' before the Pill: Science, industry and chemical contraceptives, 1920-1960," Br. J. Hist. Sci., vol. 44, no. 2, pp. 245-274, Jun. 2011, doi: https://doi.org/10.1017/s0007087410000762

[21] R. Palmeira-de-Oliveira, A. S. Oliveira, J. Rolo, M. Tomás, A. Palmeira-de-Oliveira, S. Simões, J. Martínez-de-Oliveira, "Women's preferences and acceptance for different drug delivery routes and products," Adv. Drug. Deliv. Rev., vol. 182, art. no. 114133, Mar. 2022, doi: https://doi.org/10.1016/j.addr.2022.114133

[22] F. L. Meyskens, V. Graham, M. Chvapil, R. T. Dorr, D. S. Alberts, E. A. Surwit, "A phase I trial of β-all-trans-retinoic acid delivered via a collagen sponge and a cervical cap for mild or moderate intraepithelial cervical neoplasia," J. Natl. Cancer Inst., vol. 71, no. 5, pp. 921-925, Nov. 1983, doi: https://doi.org/10.1093/jnci/71.5.921

[23] S. F. Lai, M. T. Lam, H. W. R. Li, E. H. Y. Nga, "A randomized double-blinded non-inferiority trial comparing fentanyl and midazolam with pethidine and diazepam for pain relief during oocyte retrieval," Reprod. Biomed. Online, vol. 40, no. 5, pp. 653-660, May. 2020, doi: https://doi.org/10.1016/j.rbmo.2020.01.021

[24] V. Graham, E. S. Surwit, S. Weiner, F. L. Meyskens, "Phase II trial of β-all-trans-retinoic acid for cervical intraepithelial neoplasia delivered via a collagen sponge and cervical cap," West. J. Med., vol. 145, no. 2, pp. 192-195, Aug.1986. [Online]. Available: https://www.ncbi.nlm.nih.gov/pmc/articles/PMC1306873/

[25] T. Issat, J. Beta, M. A. Nowicka, T. Maciejewski, A. J. Jakimiuk, "A Randomized, Single Blind, Placebo-Controlled Trial for the Pain Reduction During the Outpatient Hysteroscopy After Ketoprofen or Intravaginal Misoprostol," J. Minim. Invasive Gynecol., vol. 21, no. 5, pp. 921-927, 2014, doi: https://doi.org/10.1016/j.jmig.2014.04.006

[26] H. El-Refaey, A. Templeton, "Early induction of abortion by a combination of oral mifepristone and misoprostol administered by the vaginal route," Contraception, vol. 49, no. 2, pp. 111-114, Feb. 1994, doi: https://doi.org/10.1016/0010-7824(94)90085-X

[27] P. Vercellini, G. Barbara, E. Somigliana, S. Bianchi, A. Abbiati, L. Fedele, "Comparison of contraceptive ring and patch for the treatment of symptomatic endometriosis," Fertil Steril., vol. 93, no. 7, pp. 2150-2161, May. 2010, doi: https://doi.org/10.1016/j.fertnstert.2009.01.071

[28] L. Perioli, V. Ambrogi, C. Pagano, E. Massetti, C. Rossi, "New solid mucoadhesive systems for benzydamine vaginal administration," Colloids Surf. B, vol. 84, no. 2, pp. 413-420, Jun. 2011, doi: https://doi.org/10.1016/j.colsurfb.2011.01.035

[29] R. Sanz, B. Clares, M. Mallandrich, J. Suñer-Carbó, M. J. Montes, A. C. Calpena, "Development of a mucoadhesive delivery system for control release of doxepin with application in vaginal pain relief associated with gynecological surgery," Int. J. Pharm., vol. 535, no. 1-2, pp. 393-401, Jan. 2018, doi: https://doi.org/10.1016/j.ijpharm.2017.11.027

[30] V. K. P. de Queiroz, A. M. da Nóbrega Marinho, G. A. M. de Barros, "Analgesic effects of a 5% lidocaine patch after cesarean section: A randomized placebo-controlled double-blind clinical trial," J. Clin. Anesth., vol. 73, art. no. 110328, Oct. 2021, doi: https://doi.org/10.1016/j.jclinane.2021.110328

[31] Organización Mundial de la Salud (OMS), "Cáncer cervicouterino," WHO. https://www.who.int/es/news-room/fact-sheets/detail/human-papillomavirus-(hpv)-and-cervical-cancer (accessed 2022).

[32] Drugbank Online, "Ketorolac," Drugbank Online. https://go.drugbank.com/drugs/DB00465 (accessed Apr. 11, 2021).

[33] A. M. Larish, R. R. Dickson, R. A. Kudgus, R. M. McGovern, J. M. Reid, W. M. Hooten, W. T. Nicholson, L. E. Vaughan, T. L. Burnett, S. K. Laughlin-Tommaso, S. S. Faubion, I. C. Green, "Vaginal Diazepam for Nonrelaxing Pelvic Floor Dysfunction: The Pharmacokinetic Profile," J. Sex. Med., vol. 16, no. 6, pp. 763-766, Jun. 2019, doi: https://doi.org/10.1016/j.jsxm.2019.03.003

[34] World Health Organization (WHO), "Sexually transmitted infections (STIs)," WHO. https://www.who.int/news-room/fact-sheets/detail/sexually-transmitted-infections-(stis) (accessed 2022).

[35] N. L. Calvo, G. Tejada, L. A. Svetaz, A. D. Quiroga, V. A. Alvarez, M. C. Lamas, D. Leonardi, "Development and optimization of a new tioconazole vaginal mucoadhesive film using an experimental design strategy. Physicochemical and biological characterization," J. Pharm. Biomed. Anal., vol. 205, art. no. 114303, Oct. 2021, doi: https://doi.org/10.1016/j.jpba.2021.114303

[36] R. Mishra, P. Joshi, T. Mehta, "Formulation, development and characterization of mucoadhesive film for treatment of vaginal candidiasis," Int. J. Pharm. Investig., vol. 6, no. 1, p. 47-55, 2016. [Online]. Available: https://www.ncbi.nlm.nih.gov/pmc/articles/PMC4787062/

[37] Z. A. Şenyiğit, S. Y. Karavana, B. Eraç, Ö. Gürsel, M. H. Limoncu, E. Baloğlu, "Evaluation of chitosan based vaginal bioadhesive gel formulations for antifungal drugs," Acta Pharm., vol. 64, no. 2, pp. 139-156, Jun. 2014, doi: https://doi.org/10.2478/acph-2014-0013

[38] P. Bassi, G. Kaur, "Bioadhesive vaginal drug delivery of nystatin using a derivatized polymer: Development and characterization," Eur. J. Pharm. Biopharm., vol. 96, pp. 173-184, Oct. 2015, doi: https://doi.org/10.1016/j.ejpb.2015.07.018

[39] World Health Organization (WHO), "HIV/AIDS," WHO. https://www.who.int/news-room/fact-sheets/detail/hiv-aids (accessed Oct. 20, 2021).

[40] C. K. Enggi, H. T. Isa, S. Sulistiawati, K. A. R. Ardika, S. Wijaya, R. M. Asri, S. A. Mardikasari, R. F. Donnelly, A. D. Permana, "Development of thermosensitive and mucoadhesive gels of cabotegravir for enhanced permeation and retention profiles in vaginal tissue: A proof of concept study," Int. J. Pharm., vol. 609, art. no. 121182, Nov. 2021, doi: https://doi.org/10.1016/j.ijpharm.2021.121182

[41] R. Cazorla-Luna, F. Notario-Pérez, A. Martín-Illana, L. M. Bedoya, A. Tamayo, J. Rubio, R. Ruiz-Caro, M. D. Veiga, "Development and in Vitro/ Ex Vivo Characterization of Vaginal Mucoadhesive Bilayer Films Based on Ethylcellulose and Biopolymers for Vaginal Sustained Release of Tenofovir," Biomacromolecules, vol. 21, no. 6, pp. 2309-2319, Apr. 2020, doi: https://doi.org/10.1021/acs.biomac.0c00249

[42] N. Nematpour, P. Moradipour, M. M. Zangeneh, E. Arkan, M. Abdoli, L. Behbood, "The application of nanomaterial science in the formulation a novel antibiotic: Assessment of the antifungal properties of mucoadhesive clotrimazole loaded nanofiber versus vaginal films," Mater. Sci. Eng. C Mater. Biol. Appl., vol. 110, art. no. 110635, May 2020, doi: https://doi.org/10.1016/j.msec.2020.110635

[43] L. S. Dolci, A. Liguori, S. Panzavolta, A. Miserocchi, N. Passerini, M. Gherardi, V. Colombo, A. Bigi, B. Albertini, "Non-equilibrium atmospheric pressure plasma as innovative method to crosslink and enhance mucoadhesion of econazole-loaded gelatin films for buccal drug delivery," Colloids Surf. B, vol. 163, pp. 73-82, Mar. 2018, doi: https://doi.org/10.1016/j.colsurfb.2017.12.030

[44] L. S. Dolci, B. Albertini, M. F. di Filippo, F. Bonvicini, N. Passerini, S. Panzavolta, "Development and in vitro evaluation of mucoadhesive gelatin films for the vaginal delivery of econazole," Int. J. Pharm., vol. 591, art. no. 119979, Dec. 2020, doi: https://doi.org/10.1016/j.ijpharm.2020.119979

[45] N. Lupo, B. Fodor, I. Muhammad, M. Yaqoob, B. Matuszczak, A. Bernkop-Schnürch, "Entirely S-protected chitosan: A promising mucoadhesive excipient for metronidazole vaginal tablets," Acta Biomater., vol. 64, pp. 106-115, Dec. 2017, doi: https://doi.org/10.1016/j.actbio.2017.10.014

[46] V. H. S. Araujo, M. P. C. de Souza, G. C. Carvalho, J. L. Duarte, M. Chorilli, "Chitosan-based systems aimed at local application for vaginal infections," Carbohydr. Polym., vol. 261, art. no 117919, Mar. 2021, doi: https://doi.org/10.1016/j.carbpol.2021.117919

[47] M. Campaña-Seoane, A. Pérez-Gago, G. Vázquez, N. Conde, P. González, A. Martinez, X. Martínez, L. García Varela, M. Herranz, P. Aguiar, A. Fernández-Ferreiro, R. Laguna, F. J. Otero-Espinar, "Vaginal residence and pharmacokinetic preclinical study of topical vaginal mucoadhesive W/S emulsions containing ciprofloxacin," Int. J. Pharm., vol. 554, pp. 276-283, Jan. 2019, doi: https://doi.org/10.1016/j.ijpharm.2018.11.022

[48] World Health Organization (WHO), "Herpes simplex virus," WHO. https://www.who.int/news-room/fact-sheets/detail/herpes-simplex-virus (accessed 2022).

[49] M. Ijaz, J. A. Griessinger, A. Mahmood, F. Laffleur, A. Bernkop-Schnürch, "Thiolated Cyclodextrin: Development of a Mucoadhesive Vaginal Delivery System for Acyclovir," J. Pharm. Sci., vol. 105, no. 5, pp. 1714-1720, May 2016, doi: https://doi.org/10.1016/j.xphs.2016.03.009

[50] E.-M. Pacheco-Quito, L.-M. Bedoya, J. Rubio, A. Tamayo, R. Ruiz-Caro, M.-D. Veiga, "Layer-by-layer vaginal films for acyclovir controlled release to prevent genital herpes," Int. J. Pharm., vol. 627, art. no. 122239, Nov. 2022, doi: https://doi.org/10.1016/j.ijpharm.2022.122239

[51] D. Ramyadevi, K. S. Rajan, B. N. Vedhahari, K. Ruckmani, N. Subramanian, "Heterogeneous polymer composite nanoparticles loaded in situ gel for controlled release intra-vaginal therapy of genital herpes," Colloids Surf. B, vol. 146, pp. 260-270, Oct. 2016, doi: https://doi.org/10.1016/j.colsurfb.2016.06.022

[52] Centers for Disease Control and Prevention (CDC), "Sexually Transmitted Diseases (STDs), Prevention," Sexually Transmitted Diseases (STDs), Prevention. https://www.cdc.gov/std/prevention/default.htm (accessed 2022).

[53] S. Gupta, R. Gabrani, J. Ali, S. Dang, "Exploring Novel Approaches to Vaginal Drug Delivery," Recent Pat. Drug. Deliv. Formul., vol. 5, no. 2, pp. 82-94, May 2011, doi: https://doi.org/10.2174/187221111795471418

[54] Centers for Disease Control and Prevention (CDC), "HIV," HIV Basics. https://www.cdc.gov/hiv/basics/whatishiv.html (accessed 2022).

[55] F. Notario-Pérez, R. Cazorla-Luna, A. Martín-Illana, R. Ruiz-Caro, A. Tamayo, J. Rubio, M. D. Veiga, "Optimization of tenofovir release from mucoadhesive vaginal tablets by polymer combination to prevent sexual transmission of HIV," Carbohydr. Polym., vol. 179, pp. 305-316, Jan. 2018, doi: https://doi.org/10.1016/j.carbpol.2017.10.001

[56] F. Notario-Pérez, A. Martín-Illana, R. Cazorla-Luna, R. Ruiz-Caro, L. M. Bedoya, J. Peña, M. D. Veiga, "Development of mucoadhesive vaginal films based on HPMC and zein as novel formulations to prevent sexual transmission of HIV," Int. J. Pharm., vol. 570, art. no. 118643, Oct. 2019, doi: https://doi.org/10.1016/j.ijpharm.2019.118643

[57] C. K. Sahoo, P. Kumar Nayak, D. K. Sarangi, T. K. Sahoo, "Intra Vaginal Drug Delivery System: An Overview," Am. J. Adv. Drug. Deliv., vol. 1, no. 1, pp. 43-55, Apr. 2013, [Online]. Available: https://www.primescholars.com/articles/intra-vaginal-drug-delivery-systeman-overview.pdf

[58] A. Hussain, F. Ahsan, "The vagina as a route for systemic drug delivery," J. Control Release, vol. 103, no. 2, pp. 301-313, Mar. 2005, doi: https://doi.org/10.1016/j.jconrel.2004.11.034

[59] World Health Organization (WHO), "Endometriosis," WHO. https://www.who.int/news-room/fact-sheets/detail/endometriosis (accessed Oct. 20, 2021).

[60] K. Carlström, H. Pschera, N. O. Lunell, "Serum levels of oestrogens, progesterone, follicle-stimulating hormone and sex-hormone-binding globulin during simultaneous vaginal administration of 17β-oestradiol and progesterone in the pre- and post-menopause," Maturitas, vol. 10, no. 4, pp. 307-316, Dec. 1988, doi: https://doi.org/10.1016/0378-5122(88)90066-7

[61] J. Su, K. Sripanidkulchai, J. M. Wyss, B. Sripanidkulchai, "Curcuma comosa improves learning and memory function on ovariectomized rats in a long-term Morris water maze test," J. Ethnopharmacol., vol. 130, no. 1, pp. 70-75, Jul. 2010, doi: https://doi.org/10.1016/j.jep.2010.04.012

[62] Centers for Disease Control and Prevention (CDC), "Gynecologic Cancers," Gynecologic Cancers. https://www.cdc.gov/cancer/gynecologic/index.htm (accessed 2022).

[63] M. Crespo, "Cyclometallated platinum(IV) compounds as promising antitumour agents," J. Organomet. Chem., vol. 879, pp. 15-26, Jan. 2019, doi: https://doi.org/10.1016/j.jorganchem.2018.10.008

[64] Organización Panamericana de la Salud (OPS), "Cáncer cervicouterino," OPS. https://www.paho.org/es/temas/cancer-cervicouterino (accessed 2022).

[65] S. Mukherjee, "The Emperor of all Maladies". New York: Scribner Book Company, 2010, pp. 592.

[66] S. Zong, X. Wang, Y. Yang, W. Wu, H. Li, Y. Ma, W. Lin, T. Sun, Y. Huang, Z. Xie, Y. Yue, S. Liu, X. Jing, "The use of cisplatin-loaded mucoadhesive nanofibers for local chemotherapy of cervical cancers in mice," Eur. J. Pharm. Biopharm., vol. 93, pp. 127-135, Apr. 2015, doi: https://doi.org/10.1016/j.ejpb.2015.03.029

[67] S. Ahmad, "Kinetic aspects of platinum anticancer agents," Polyhedron, vol. 138, pp. 109-124, Dec. 2017, doi: https://doi.org/10.1016/j.poly.2017.09.016

[68] M. R. Vakili, W. Mohammed-Saeid, A. Aljasser, J. Hopwood-Raja, B. Ahvazi, Y. Hrynets, M. Betti, A. Lavasanifar, "Development of mucoadhesive hydrogels based on polyacrylic acid grafted cellulose nanocrystals for local cisplatin delivery," Carbohydr. Polym., vol. 255, art. no. 117332, Mar. 2021, doi: https://doi.org/10.1016/j.carbpol.2020.117332

[69] U. Aggarwal, A. K. Goyal, G. Rath, "Development and characterization of the cisplatin loaded nanofibers for the treatment of cervical cancer," Mater. Sci. Eng. C Mater. Biol. Appl., vol. 75, pp. 125-132, Jun. 2017, doi: https://doi.org/10.1016/j.msec.2017.02.013

[70] D. A. Woolfson, D. F. McCafferty, P. A. McCarron, J. H. Price, "Liquid Scintillation Spectrometry of 5-Fluorouracil in Cervical Tissue Folloing in Vitro Surface Application of a Bioadhesive Cervical Patch," Pharm. Res., vol. 11, no. 9, pp. 1315-1319, Sep. 1994, doi: https://doi.org/10.1023/a:1018950613353

[71] A. D. Woolfson, D. F. McCafferty, P. A. McCarron, J. H. Price, "A bioadhesive patch cervical drug delivery system for the administration of 5-fluorouracil to cervical tissue," J. Control. Release, vol. 35, no. 1, pp. 49-58, Jul. 1995, doi: https://doi.org/10.1016/0168-3659(95)00018-4

[72] M. A. Hollingsworth, B. J. Swanson, "Mucins in cancer: Protection and control of the cell surface," Nat. Rev. Cancer, vol. 4, no. 1, pp. 45-60, Jan. 2004, doi: https://doi.org/10.1038/nrc1251

[73] C. Li, Z. Liu, X. Yan, W. Lu, Y. Liu, "Mucin-controlled drug release from mucoadhesive phenylboronic acid-rich nanoparticles," Int. J. Pharm., vol. 479, no. 1, pp. 261-264, Feb. 2015, doi: https://doi.org/10.1016/j.ijpharm.2014.12.011

[74] L. Ci, Z. Huang, Y. Liu, Z. Liu, G. Wei, W. Lu, "Amino-functionalized poloxamer 407 with both mucoadhesive and thermosensitive properties: preparation, characterization and application in a vaginal drug delivery system," Acta Pharm. Sin. B, vol. 7, no. 5, pp. 593-602, Sep. 2017, doi: https://doi.org/10.1016/j.apsb.2017.03.002

[75] F. D. Victorelli, G. M. F. Calixto, K. C. dos Santos, H. H. Buzzá, M. Chorilli, "Curcumin-loaded Polyethyleneimine and chitosan polymer-based Mucoadhesive liquid crystalline systems as a potential platform in the treatment of cervical Cancer," J. Mol. Liq., vol. 325, art. no. 115080, Mar. 2021, doi: https://doi.org/10.1016/j.molliq.2020.115080

[76] K. Berginc, S. Suljaković, N. Škalko-Basnet, A. Kristl, "Mucoadhesive liposomes as new formulation for vaginal delivery of curcumin," Eur. J. Pharm. Biopharm., vol. 87, no. 1, pp. 40-46, Feb. 2014, doi: https://doi.org/10.1016/j.ejpb.2014.02.006

ARTÍCULO DE REVISIÓN

VOL. 44 | NO. 2 | **MAY - AUGUST 2023** | PP 52-73

Revista Mexicana de Ingeniería Biomédica

dx.doi.org/10.17488/RMIB.44.2.5

E-LOCATION ID: 1345

Técnicas de Neuroimagenología en la Cuantificación de la Neuroplasticidad en Pacientes con Enfermedad Vascular Cerebral

Neuroimaging Techniques for Neuroplasticity Quantification in Stroke Patients

Martín Emiliano Rodríguez-García[1], *Norma Marín-Arriaga*[2], *Silvia Gabriela Macías-Arriaga*[2] *Bernardo Salazar-Cárdenas*[2] *Tania Ramírez-Rodríguez*[2], *Víctor Hugo Aparicio-Jiménez*[2], *Raquel Valdés-Cristerna*[1] *Jessica Cantillo-Negrete*[3]

[1] Departamento de Ingeniería Eléctrica, Universidad Autónoma Metropolitana, Ciudad de México - México

[2] Servicio de Resonancia Magnética, Instituto Nacional de Rehabilitación Luis Guillermo Ibarra Ibarra, Ciudad de México - México

[3] División de Investigación en Neurociencias Clínica, Instituto Nacional de Rehabilitación Luis Guillermo Ibarra Ibarra, Ciudad de México - México

RESUMEN

Las técnicas de neuroimagenología otorgan información relevante del estado funcional y anatómico del cerebro humano. Esta información es particularmente importante cuando existe una lesión cerebral causada por alguna patología, tal como la enfermedad vascular cerebral (EVC). En pacientes afectados por esta enfermedad, se ha determinado que la neuroplasticidad es el mecanismo principal de recuperación de la función motora perdida. Debido a la alta prevalencia de la EVC a nivel mundial y especialmente en países en vías de desarrollo, es necesario continuar investigando los mecanismos de recuperación involucrados en esta patología. La resonancia magnética funcional (RMF) y la imagenología por tensor de difusión (ITD) son dos de las técnicas de neuroimagenología más utilizadas con este fin. La RMF permite analizar la actividad neuronal generada al ejecutar tareas de movimiento, mientras que la ITD proporciona información estructural de la anatomía cerebral. En esta revisión narrativa, se presentan diversos estudios que han utilizado estas técnicas de neuroimagenología en la cuantificación de los cambios de neuroplasticidad en pacientes con EVC tras participar en algún programa de neurorrehabilitación. Comprender mejor estos cambios de neuroplasticidad permitiría diseñar esquemas de rehabilitación que proporcionen un mayor beneficio a los pacientes con EVC.

PALABRAS CLAVE: enfermedad vascular cerebral, imagenología por tensor de difusión, neuroimagenología, neuroplasticidad, resonancia magnética funcional

ABSTRACT

Neuroimaging techniques provide relevant information of the functional and anatomical status of the human brain. This information is of particular importance when a pathology, like stroke, produces a brain injury. In stroke patients, it has been determined that neuroplasticity is the primary recovery mechanism of the lost motor function. Due to worldwide high prevalence, especially in developing countries, it is necessary to continue the research of the recovery mechanisms involved in this pathology. To this end, functional magnetic resonance imaging (fMRI) and diffusion tensor imaging (DTI) are two of the most used neuroimaging techniques. In stroke patients, fMRI allows the analysis of the neural activity produced by the execution of motor tasks, whereas DTI provides structural information of the brain anatomy. In this narrative review, multiple studies that employ these neuroimaging techniques for quantification of neuroplasticity changes in stroke patients after undergoing a neurorehabilitation program are presented. Better understanding of these neuroplasticity changes would allow researchers to design and provide more beneficial rehabilitation schemes to stroke patients.

KEYWORDS: diffusion tensor imaging, functional magnetic resonance imaging, neuroimaging, neuroplasticity, stroke

Corresponding author

TO: **Jessica Cantillo-Negrete**

INSTITUTION: **Instituto Nacional de Rehabilitación Luis Guillermo Ibarra Ibarra, División de Investigación en Neurociencias Clínica, Ciudad de México - México**

ADDRESS: **Calzada México-Xochimilco 289, Col. Arenal de Guadalupe, Tlalpan, 14389, Ciudad de México, México.**

EMAIL: **jcantillo@inr.gob.mx**

Received:

11 March 2023

Accepted:

6 July 2023

INTRODUCCIÓN

La enfermedad vascular cerebral (EVC) se encuentra entre las primeras causas de discapacidad en adultos a nivel mundial [1]. Además, la demanda por servicios de rehabilitación posterior a una EVC está aumentando [1]. Sin embargo, recientemente se ha reportado que países en vías de desarrollo, como México, muestran una falta de progreso en el tratamiento de esta enfermedad en los últimos años [2]. Esto se refleja en métricas como la mortalidad y la prevalencia de la EVC, las cuales se han mantenido constantes desde hace 15 años en lugar de mostrar una tendencia en decremento [1][2]. En la actualidad, se cuenta con más información acerca de las causas que producen una EVC, como un coágulo en un vaso sanguíneo o la ruptura de éste, que acerca de los factores que promueven la recuperación funcional de los pacientes [3]. Comprender los procesos fisiológicos que se encuentran detrás del proceso de recuperación tras una EVC es de gran importancia, ya que esto permitiría desarrollar nuevos y mejores procedimientos de neurorrehabilitación.

La consecuencia con mayor impacto de la EVC es la pérdida de la función motora, conocida como hemiparesia [4]. Las deficiencias funcionales motoras que presentan los pacientes con EVC pueden ser tratadas con terapia física o con terapias experimentales como aquellas que utilizan un sistema de interfaz cerebro-computadora (ICC) [5][6]. No obstante, el grado de efectividad de la terapia es diferente entre pacientes debido a distintos factores que afectan el proceso de rehabilitación, tales como la extensión y ubicación de la EVC, y el grado de discapacidad motora inicial [5][6]. Por lo tanto, resultaría benéfico entender de mejor manera cómo ocurre la recuperación funcional y qué factores la afectan a favor o en contra.

La recuperación de los pacientes posterior a la EVC, en términos de la función cerebral y la conectividad, se ha atribuido principalmente al mecanismo de neuroplasticidad [7][8]. La neuroplasticidad se define como la habilidad del sistema nervioso a responder a estímulos intrínsecos o extrínsecos al reorganizar su estructura, función y sus conexiones [9]. Estos cambios están asociados con el desarrollo y el aprendizaje [10][11][12]. Además, ocurren a lo largo de la vida y pueden incrementar posterior a una lesión o afección [13][14].

Los cambios en neuroplasticidad pueden observarse en varios niveles, tales como cambios celulares o sinápticos, cambios en la función y estructura de regiones cerebrales, y cambios de comportamiento como adaptabilidad o el mejorar alguna habilidad [15][16]. Estos cambios pueden mantenerse a largo plazo mediante dos mecanismos. El primero, es la potenciación a largo plazo (PLP), que involucra un refuerzo constante en las sinapsis que produce un incremento de larga duración en la transmisión de señales entre neuronas [17][18]. Y, el segundo, es la depresión a largo plazo (DLP), que produce un efecto opuesto a la PLP en la excitabilidad de la sinapsis [19]. Ambos mecanismos juegan roles importantes en la modulación bidireccional a largo plazo de las conexiones neuronales, la cual es la base biológica del aprendizaje y la memoria [20]. Por otra parte, se han definido mecanismos de neuroplasticidad estructurales involucrados en la recuperación motora de pacientes con EVC, como un aumento en la proliferación axonal, ramificación de dendritas, sinaptogénesis, neurogénesis y gliogénesis [21][22][23].

Estudiar los efectos funcionales o estructurales que producen los mecanismos de neuroplasticidad en pacientes con EVC podría esclarecer el proceso de recuperación motora en esta población. Por esto, se han propuesto distintos métodos que ofrecen una gran variedad de información acerca de los mecanismos patológicos y de recuperación producidos tras una EVC [24][25]. Entre estos métodos se encuentran las técnicas de neuroimagenología, las cuales tienen la habilidad de mostrar los procesos neuronales encargados de la recuperación funcional en pacientes de manera no invasiva [26].

La resonancia magnética funcional (RMF) es una de

estas técnicas que se ha utilizado ampliamente para conocer aquellos mecanismos neuronales responsables de la reorganización cerebral después de una EVC [3]. La RMF se basa en las propiedades magnéticas de la oxihemoglobina y de la desoxihemoglobina para detectar cambios locales en el flujo cerebral debido a la actividad neuronal en esa zona [27]. Debido a la alta demanda de oxígeno de las neuronas activas, el flujo sanguíneo de la región se incrementa por medio de un acoplamiento neurovascular [28]. Este incremento local de oxígeno en sangre permite, cuando el paciente ejecuta una tarea, localizar y cuantificar la respuesta de la actividad neuronal a dicha tarea. Además, la RMF es una técnica que no utiliza radiación ionizante o rastreadores químicos, por lo que es ideal para estudios clínicos de patologías neurovasculares como la EVC [29].

La RMF se ha empleado en varios estudios con pacientes con EVC cuya función motora de extremidad superior está afectada. En estos trabajos se ha reportado que la actividad cerebral está alterada tanto en el hemisferio lesionado (ipsilesional) como en el no afectado (contralesional) [30][31][32]. Por ejemplo, en pacientes con discapacidades motrices iniciales más severas, es más probable que ocurra un reclutamiento importante del hemisferio contralesional y una atenuación en la actividad del hemisferio ipsilesional [33][34]. Por otra parte, una mejor recuperación motora de los pacientes ha sido asociada a una reconfiguración lateralizada hacia el hemisferio ipsilesional de la red de conectividad neuronal, lo que asemeja el comportamiento observado en sujetos sanos [35][36].

Asimismo, estudiar la estructura de comunicación en el cerebro también resulta de gran importancia para entender la función cerebral y, por lo tanto, su recuperación. El cerebro humano contiene un gran número de neuronas que se comunican entre ellas por medio de axones, formando así redes complejas de neuronas. La imagenología por tensor de difusión (ITD) es una técnica de neuroimagenología no invasiva por resonancia magnética de difusión que puede medir la organización axonal macroscópica en tejidos del sistema nervioso [37]. Una EVC puede afectar directamente tractos de materia blanca y causar una degeneración *Walleriana*, la cual consiste en la desmielinización y degeneración distal de axones afectados [38].

En distintos estudios se ha observado que métricas obtenidas a partir de la ITD, referentes a la integridad de la materia blanca, pueden servir como biomarcadores de recuperación o respuesta a programas de rehabilitación para extremidad superior [39][40][41]. La mayoría de los estudios de ITD se enfocan al análisis del tracto corticoespinal (TCE) debido a su importancia en la ejecución motora, en la recuperación funcional y a que frecuentemente se ve afectado por lesiones causadas por una EVC [39][42]. Además, se han reportado asociaciones entre métricas de la ITD y la recuperación motora de extremidad superior en pacientes con EVC en algunos meta-análisis [43][44].

La información obtenida de RMF o ITD puede proporcionar una medición cuantitativa de la neuroplasticidad de pacientes con EVC, quienes pueden presentar cambios en ambos hemisferios cerebrales tras un programa de neurorrehabilitación [7]. Una forma de cuantificar estas diferencias inter-hemisféricas, las cuales se presentan a lo largo del programa de terapia proporcionado, es mediante índices de asimetría. Estos índices permiten interpretar la diferencia de una métrica definida en ambos hemisferios [45]. Por ejemplo, si I y C representan una métrica en el hemisferio ipsilesional y contralesional, respectivamente, se puede calcular un índice de asimetría de dicha métrica mediante I/C o mediante $(I-C)/(I+C)$ [45]. Sin embargo, uno de los aspectos importantes en el cálculo de los índices de asimetría es la métrica a utilizar [46]. En RMF, comúnmente se utiliza como métrica el número de vóxeles que muestren actividad neuronal significativa dado un umbral estadístico [46][47][48]. En cambio, en la ITD se han utilizado métricas de difusión para el cálculo de índices de asimetría [39][49].

Las técnicas de RMF y de ITD representan, respectivamente, métodos no invasivos de neuroimagenología funcional y estructural que otorgan información relevante acerca del estado y la evolución de pacientes con EVC. Además, éstas permiten analizar cambios en neuroplasticidad como la reorganización neuronal y la formación de nuevas conexiones en compensación por el daño causado por la lesión cerebral [7]. El objetivo de esta revisión narrativa es presentar las bases del funcionamiento de la RMF y de la ITD, así como estudios que utilizan estas técnicas para estimar neuroplasticidad en pacientes con EVC y, finalmente, ilustrar cómo se cuantifican los cambios asociados a la rehabilitación motora para la extremidad superior con ambas técnicas de neuroimagenología. Esto permitirá sintetizar los avances en el campo y establecer la utilidad de la RMF y la ITD en la cuantificación de la neuroplasticidad en pacientes con EVC tras recibir programas de terapia para extremidad superior.

MATERIALES Y MÉTODOS

Se realizó una revisión de la literatura para identificar trabajos donde se utilizó la RMF, la ITD o ambas, como herramientas para la cuantificación de neuroplasticidad en pacientes con EVC tras recibir un programa de neurorrehabilitación para extremidad superior. Los artículos incluidos en esta revisión narrativa fueron publicados previo a enero de 2023 y cumplieron los siguientes criterios: 1) publicados en revistas revisadas por pares; 2) publicados en inglés; 3) estudios en pacientes con EVC; 4) estudios que proporcionaron programas de neurorrehabilitación motora para extremidad superior; 5) que hayan realizado estudios de neuroimagenología a los pacientes, ya sea RMF, ITD o ambas, en distintos momentos del programa de neurorrehabilitación proporcionado; y 6) que hayan estimado cuantitativamente la neuroplasticidad de los pacientes con EVC debida al programa de neurorrehabilitación usando los estudios de neuroimagen. La búsqueda de trabajos se realizó en PubMed y Google Scholar, utilizando los siguientes términos y/o combinaciones de estos: *analysis, bci, diffusion tensor imaging, dti, functional magnetic resonance imaging, fmri, hemiparesis, neuroimaging, neuroplasticity, neurorehabilitation, principles, rehabilitation, stroke, upper-extremity.*

RESULTADOS Y DISCUSIÓN

Resonancia magnética funcional

En esta sección se abordan las bases del funcionamiento de la RMF, seguidas por métodos de análisis de lateralidad de las activaciones neuronales y, finalmente, se discuten los trabajos encontrados en la literatura que cuantifican la neuroplasticidad con esta técnica. En total, se incluyeron cinco trabajos en este apartado, los cuales se muestran en la Tabla 1.

La RMF es realizada comúnmente con la técnica dependiente del nivel de oxígeno en sangre, o *blood oxygen level-dependent* (BOLD), la cual aprovecha las diferentes propiedades magnéticas intrínsecas de la oxihemoglobina y la desoxihemoglobina [50][51]. Las sustancias diamagnéticas, como la oxihemoglobina, poseen electrones apareados en todos los subniveles de energía, lo que ocasiona que se produzca una magnetización extremadamente débil y en dirección opuesta (antiparalela) ante la presencia de un campo magnético externo [52]. Por otra parte, las sustancias paramagnéticas, como la desoxihemoglobina, contienen electrones de valencia no apareados, lo cual produce una magnetización importante en la misma dirección (paralela) que un campo magnético externo aplicado [52]. En particular, las propiedades paramagnéticas de la desoxihemoglobina en sangre causan un desfasamiento en los protones de los tejidos, lo que ocasiona una pérdida local de señal tanto en sangre como en tejidos cercanos [50][53]. Además, la afluencia de sangre oxigenada local es producto de un incremento neto en el balance de sangre arterial oxigenada y la sangre venosa desoxigenada [54][55]. Por lo tanto, la señal local de la RMF aumentará conforme la proporción local de oxi/desoxihemoglobina incremente, indicando así un aumento en la actividad neuronal en esa zona [27][56].

Otro aspecto importante para determinar las activaciones presentes en alguna región del cerebro es definir adecuadamente el diseño experimental de un estudio de RMF. Un diseño apropiado del estudio permite tener una potencia estadística adecuada en el experimento, *i.e.*, una mejor capacidad para detectar señales relevantes en un análisis grupal [57].

En la RMF basada en tareas, donde es de gran importancia la manera en que los estímulos son presentados como una función del tiempo, se pueden utilizar diseños en bloques o diseños relacionados a eventos [54][55]. Ejemplos de estos diseños, y la comparación visual entre ellos, se muestran en la Figura 1. El diseño en bloques (Figura 1a) es el más simple y consiste en presentar estímulos consecutivos como una serie de bloques, donde los estímulos de distintas condiciones se presentan en bloques alternados [55]. Estas condiciones alternantes pueden ser, por ejemplo, un bloque de reposo seguido por un bloque de alguna tarea motora o mental. La duración específica de cada bloque depende del tipo del estímulo, siendo el rango de 15 a 30 s el más común [55]. En un bloque en particular, la respuesta hemodinámica al consumo local de oxígeno se mantiene y no regresa al estado inicial hasta el final de dicho bloque. Asimismo, este diseño en bloques permite obtener una buena potencia estadística, amplitud de la señal y robustez en el estudio [54][55]. Por otra parte, en el diseño relacionado a eventos (Figura 1b), las tareas son presentadas en orden aleatorio, lo que permite observar cambios en la respuesta hemodinámica "momento a momento" [55]. Este tipo de diseño considera cada ejecución de la tarea como un evento individual, lo que se traduce a una menor potencia estadística [54][55].

TABLA 1. Resumen de los trabajos incluidos en esta revisión que utilizaron la RMF para cuantificar cambios de neuroplasticidad en pacientes con EVC tras recibir un programa de neurorrehabilitación para extremidad superior.

Trabajos	Número de pacientes con EVC	Tipo de terapia proporcionada	Índice utilizado	Resultados relacionados a neuroplasticidad
Caria *et al*. (2011) [58]	1	ICC	IL	Lateralización de las activaciones hacia las regiones motoras ipsilesionales posterior a la terapia ICC, especialmente en la región premotora dorsal y en el área motora suplementaria, de acuerdo con cambios en el IL.
Young *et al*. (2015) [59]	16	ICC	IL	Correlación del IL con el número de sesiones de terapia proporcionadas, lo que indica un mayor reclutamiento contralesional a mayor número de sesiones de terapia proporcionadas. El IL se calculó en las cortezas motora primaria y premotora, el tálamo y el cerebelo.
Ramos-Murguialday *et al*. (2019) [60]	28	ICC	IL	Cambios significativos en el IL lateralizados hacia el hemisferio ipsilesional en las cortezas motora, premotora y somatosensorial posterior a la terapia ICC. No se encontraron diferencias significativas entre el IL pre-terapia y el IL en la sesión de seguimiento.
Yuan *et al*. (2020) [61]	12	ICC	IL	Lateralización de las activaciones hacia las cortezas motora, premotora y somatosensorial ipsilesionales posterior a la terapia ICC de acuerdo con el IL.
Demers *et al*. (2022) [62]	13	TMIR	IL	Cambios significativos del IL post-terapia entre el grupo experimental (n = 7) y el control. El IL mostró una lateralización hacia el hemisferio ipsilesional en la corteza premotora dorsal en el grupo experimental.

*ICC: Interfaz cerebro computadora, IL: Índice de lateralidad, TMIR: terapia de movimiento inducido por restricción.

Sin embargo, el diseño relacionado a eventos ofrece una mayor flexibilidad y un análisis temporal más preciso de la actividad cerebral [54][55]. Además, es posible combinar los diseños en bloques con los relacionados a eventos en un diseño mixto. Esto proporciona información de activaciones funcionales tanto mantenidas como esporádicas y, además, ofrece simultáneamente las ventajas de los diseños en bloque y de los relacionados a eventos [54][63]. Sin embargo, el diseño mixto sufre de una peor estimación de la respuesta hemodinámica y una menor fortaleza estadística de la señal mantenida (*i.e.,* a lo largo del bloque) [63]. Además, requiere de más sujetos de estudio para detectar efectos estadísticamente significativos en la señal mantenida [54][63].

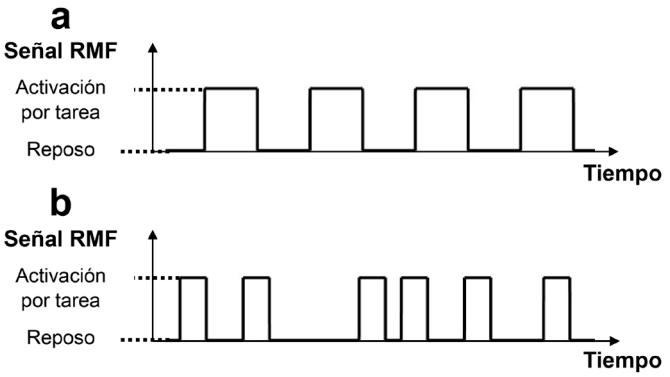

FIGURA 1. Ejemplos de diseños en la RMF basada en tareas. (a) Diseño en bloques. (b) Diseño relacionado a evento. Figura de elaboración propia.

En la RMF basada en tareas y, particularmente, en estudios con pacientes con EVC, el diseño en bloques es de los más utilizados debido a su sencillez y a la alta potencia estadística que puede proporcionar [64][65][66][67][68][69].

En los estudios de RMF con pacientes con EVC es común utilizar reposo y tareas motoras como condiciones en el diseño en bloques. Este diseño permite evaluar el estado físico y cognitivo de los pacientes al momento del estudio, así como observar cambios en la actividad cerebral al realizar tareas motoras [29]. Además, algunos estudios sugieren que la actividad neuronal observada mediante la técnica BOLD es importante para el pronóstico de la recuperación funcional motora de la extremidad superior de los pacientes. Por ejemplo, Lasek-Bal *et al.* realizaron un estudio de RMF a 13 pacientes con EVC de tipo isquémico en los primeros 4 días desde el inicio de la patología [70]. En su diseño en bloques, los pacientes realizaron un movimiento de pianista con la mano afectada. En este experimento, la señal BOLD mostró que la actividad neuronal producida al realizar la tarea motora se localiza principalmente en las regiones ipsilesionales de la corteza motora primaria, la corteza motora suplementaria y en la corteza premotora en pacientes con menor grado de discapacidad [70]. A su vez, se reportó una tendencia a una mayor recuperación motora de la extremidad superior si los pacientes mostraban activaciones en el área motora suplementaria ipsilesional [70].

Además de auxiliar en el pronóstico, la RMF también ha sido utilizada en estudios con pacientes con EVC para analizar cambios de neuroplasticidad tras recibir un programa de rehabilitación para extremidad superior. En la literatura se pueden encontrar principalmente ejemplos con terapias experimentales basadas en sistemas ICC (terapias ICC), tales como los artículos presentados en la Tabla 1 [58][59][60][61].

Las secuencias BOLD que se utilizaron en los programas de terapias siguen un diseño en bloques, en donde se alternan bloques de reposo con bloques de tareas motoras. Estas tareas incluyeron la ejecución e imaginación de flexión y extensión de los dedos de ambas manos [58][60], pulsar botones secuencialmente con los dedos de la mano afectada [59], y comprimir un tubo de plástico con los dedos índice, medio y pulgar de ambas manos [62]. Estos estudios muestran que los pacientes con EVC que reciben terapias de neurorrehabilitación alcanzan distintos grados de mejora en la función motora de extremidad superior. Además, se determinaron como factores que afectan en la recuperación el

tipo de paradigma ICC utilizado, el número de sesiones de terapia y la intensidad de éstas. Asimismo, señalan la relevancia de analizar los cambios en la lateralización de la activación neuronal como parte del proceso de neurorrehabilitación, particularmente cuando los pacientes intentan mover la extremidad superior afectada.

En la Figura 2 se muestra un ejemplo de cómo las activaciones significativas (p<0.05, corregida por *family-wise error* (FWE)) de un paciente con EVC pueden cambiar antes (2a) y después (2b) de recibir una terapia ICC para extremidad superior. Estos mapas de activaciones significativas fueron obtenidos tras el procesamiento de las correspondientes secuencias BOLD en la interfaz gráfica de usuario del software SPM12 [71], siguiendo la metodología ejemplo del análisis de primer nivel descrita en su manual de usuario, incluyendo el preprocesamiento espacial, la especificación del modelo y la inferencia [72]. En estas secuencias BOLD, el paciente intentó realizar flexión y extensión continua de los dedos de la mano afectada (izquierda). Esta tarea motora se alternó con reposo, siguiendo un diseño en bloques. Aquí, se observa que las activaciones neuronales significativas muestran una tendencia bilateral pre-terapia y que éstas cambian hacia una lateralización sobre el hemisferio ipsilesional post-terapia. Sin embargo, esta interpretación es subjetiva al basarse en un análisis visual de los resultados. Por lo tanto, utilizar una métrica que permita una evaluación cuantitativa de estos cambios de lateralización, producidos por mecanismos de neuroplasticidad, resultará de gran importancia para comprender y puntualizar los cambios clínicos producidos en pacientes con EVC tras recibir una terapia ICC, o una terapia convencional, para extremidad superior.

Una de las propuestas más utilizadas en la literatura para cuantificar las activaciones presentes en las secuencias BOLD es el índice de lateralidad (IL), como se resume en la Tabla 1. El IL es un índice de asimetría que permite la interpretación más directa de las asimetrías hemisféricas [45]. Además, el IL permite evaluar la dominancia hemisférica al realizar la tarea definida en la secuencia BOLD. Al ser un índice de asimetría, la ecuación para calcular el IL está dada por: $IL=(R-L)/(R+L)$, donde R y L representan una métrica en el hemisferio derecho e izquierdo, respectivamente [46][47][48].

En estudios con pacientes con EVC, esta fórmula puede adaptarse para comparar la misma métrica en el hemisferio ipsilesional *(I)* y contralesional *(C)* de la siguiente manera: $IL=(I-C)/(I+C)$ [61][73]. Esto permite mantener la información de la ubicación de la lesión en la comparación inter-hemisférica [61][73]. Como se mencionó anteriormente, la métrica utilizada es comúnmente la cantidad de vóxeles que muestran activaciones significativas, dado un umbral estadístico, en cada hemisferio cerebral tras comparar los bloques de tarea con los bloques de reposo de la secuencia BOLD realizada [58][59][61][67][73][74][75]. El número de vóxeles con activaciones significativas en cada hemisferio se cuantifica dentro de regiones de interés (RI) definidas con un atlas anatómico [61][67], con un estudio previo [59], o con una selección manual de estas regiones [58][74]. En la Figura 2c se presenta un ejemplo de un conjunto de RI que pueden ser utilizadas para el cálculo del IL. Las RI mostradas se encuentran descritas en el atlas anatómico AAL3 [76] incluido en el software SPM12 [71] e incluyen el opérculo rolándico, el área motora suplementaria, los giros pre- y post-centrales, el núcleo lenticular (putamen y globo pálido), el cerebelo y el tálamo.

La selección de la métrica a utilizar y la definición de las RI representan los puntos más importantes en el cálculo del IL [46][75]. Este índice puede tomar valores desde -1 hasta 1, correspondientes a una activación neuronal completamente lateralizada hacia el hemisferio contralesional o ipsilesional, respectivamente. Por otra parte, un valor de IL igual a 0 indicaría una distribución simétrica de las activaciones significativas entre ambos hemisferios. Además, algunos trabajos han definido un umbral para caracterizar el IL calculado:

un valor de $|IL|\leq 0.2$ indica actividad bilateral, mientras que un $IL>0.2$ o un $IL<-0.2$ representa actividad lateralizada hacia el hemisferio ipsilesional o contralesional, respectivamente [75][77]. Un ejemplo del uso e interpretación de este índice se encuentra en la Figura 2d. Aquí, se muestran los IL calculados en la plataforma MATLAB [78] mediante la fórmula aritmética mencionada anteriormente con las activaciones significativas de los hemisferios ipsilesional y contralesional presentadas en las Figuras 2a y 2b sobre el grupo ejemplo de RI de la Figura 2c. Las activaciones del cerebelo ipsilesional y contralesional fueron contabilizadas dentro de las activaciones del hemisferio opuesto debido a la decusación del tracto piramidal a nivel cerebelar [79].

Como se mencionó anteriormente, estas activaciones significativas son producidas en una secuencia BOLD cuando el paciente con EVC intenta flexionar y extender los dedos de la mano afectada (izquierda) previo (Figura 2a) y posterior (Figura 2b) a recibir una terapia ICC para extremidad superior. El aumento en el IL indica una lateralización de las activaciones neuronales hacia el hemisferio ipsilesional al finalizar el programa de terapia proporcionado. Esto refleja que las activaciones generadas post-terapia en el hemisferio ipsilesional del paciente al mover la mano afectada tienen una mayor semejanza con las activaciones contralaterales esperadas de un sujeto sano [35][36].

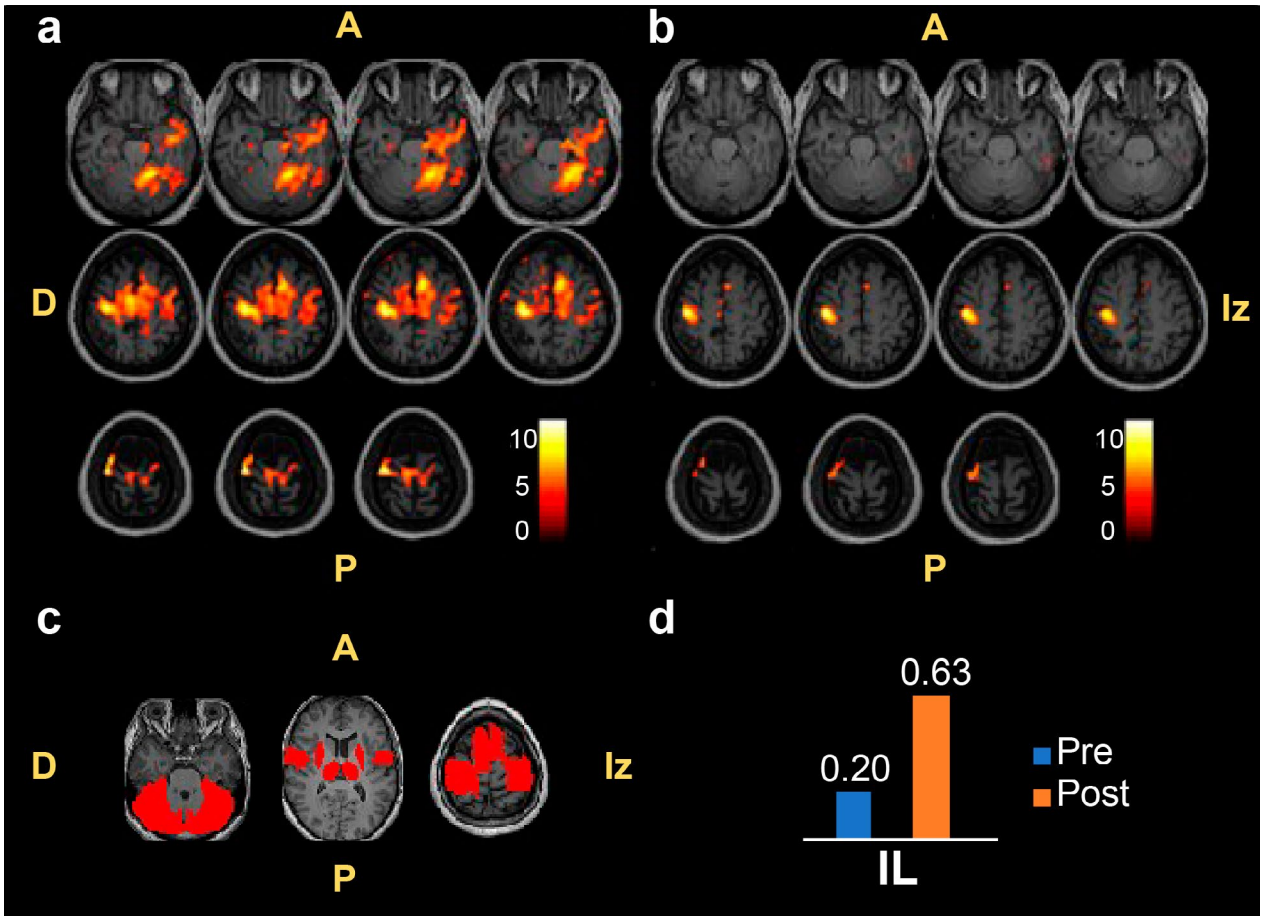

FIGURA 2. Imágenes por RMF de un paciente con EVC que recibió una terapia ICC para extremidad superior. La secuencia BOLD realizada involucra intención de movimiento de la mano afectada (izquierda). (a) Cortes axiales de activaciones significativas ($p<0.05$, FWE) sobre imágenes estructurales T1 pre-terapia. (b) Cortes axiales de activaciones significativas ($p<0.05$, FWE) sobre imágenes estructurales T1 post-terapia. (c) Vista axial de las RI ejemplo montadas sobre imágenes estructurales T1. (d) IL de las secuencias BOLD pre-terapia (azul) y post-terapia (anaranjado). Figura de elaboración propia. A: anterior, P: posterior, D: derecha, Iz: izquierda.

El IL ha sido utilizado en los estudios con pacientes con EVC para caracterizar la lateralidad de su actividad neuronal tras recibir algún programa de rehabilitación para extremidad superior. Por ejemplo, Demers *et al.* proporcionaron una terapia de movimiento inducido por restricción (TMIR) a 7 pacientes con EVC durante 2 semanas, donde observaron un aumento en el IL en la corteza premotora dorsal al finalizar el programa de terapias [62]. La tarea realizada por los pacientes durante la RMF consistía en sujetar repetitivamente un tubo de plástico con los dedos pulgar, índice y medio de su mano afectada [62]. Esta tarea se realizó en bloques, alternándose con una condición de reposo. El incremento en el IL indica una mayor lateralización de las activaciones neuronales hacia la corteza premotora dorsal ipsilesional en los pacientes tras recibir la TMIR [62].

Además, el IL también ha sido reportado en los estudios donde se proporcionan terapias ICC para extremidad superior a pacientes con EVC. Caria *et al.* reportaron un caso de estudio donde se emplearon 3 sesiones de RMF para observar cambios en la lateralización de la actividad neuronal al recibir dos tipos de terapia ICC [58]. Los autores indicaron que conforme avanzó el proceso de terapia, el IL calculado en cada estudio de RMF mostraba una lateralización cada vez más pronunciada hacia el hemisferio ipsilesional durante la flexión y extensión de los dedos de la mano afectada, especialmente en la región premotora dorsal y en el área motora suplementaria [58]. En un estudio posterior, Ramos-Murguialday *et al.* proporcionaron un programa de terapia ICC a 28 pacientes con EVC, donde encontraron un cambio significativo entre el IL calculado pre-terapia y el IL calculado al finalizar la terapia en las cortezas motora, premotora y somatosensorial, indicando un cambio en la activación hacia el hemisferio ipsilesional al flexionar y extender los dedos de la mano afectada [60].

Por otra parte, Young *et al.* reportaron un mayor reclutamiento del hemisferio contralesional al pulsar botones con la mano afectada en su grupo experimental (n=16) de pacientes con EVC tras recibir terapia ICC [59]. Este reclutamiento se encontró en la red motora contralesional, definida como el conjunto de las cortezas motora primaria y premotora, el tálamo y el cerebelo [59]. Esta actividad lateralizada hacia el hemisferio no afectado es atribuida por los autores a que la lesión por EVC de los pacientes incluidos en este estudio se encontraba principalmente a nivel cortical, afectando directamente la corteza motora ipsilesional [59]. Además, reportaron una correlación significativa entre el número de terapias proporcionadas a los pacientes con los cambios reflejados en el IL post-terapia con respecto al IL pre-terapia [59]. Esto indica que un mayor número de terapias recibidas por el paciente corresponden a un mayor reclutamiento de la red motora contralesional. En el trabajo de Yuan et al., se reportó que los pacientes con EVC (n=12) mostraron un cambio significativo en el IL entre la RMF pre-terapia con los estudios post-terapia y de seguimiento [61]. El IL calculado en las cortezas motora, premotora y somatosensorial en la sesión de pre-terapia indicó una activación bilateral cuando los pacientes imaginaban abrir y cerrar la mano afectada. Por otra parte, en las sesiones de post-terapia y seguimiento, este índice señaló un cambio en la lateralización de las activaciones neuronales hacia el hemisferio ipsilesional en las mismas regiones anatómicas al realizar la tarea motora [61].

Estos trabajos indican una lateralización de las activaciones neuronales post-terapia tanto al hemisferio ipsilesional como al contralesional. Una posible explicación de esta diferencia son los criterios de inclusión o exclusión definidos en cada uno de los trabajos. Demers *et al.* reclutaron pacientes con EVC con deficiencias motoras moderadas [62]. Por otra parte, la mayoría de los pacientes reclutados por Caria *et al.*, Ramos-Murguialday *et al.* y Yuan presentan la lesión por EVC a nivel subcortical, lo que sugiere un daño mínimo o indirecto a nivel cortical [58][60][61]. Estos trabajos señalan una lateralización de las activaciones neuronales hacia el hemisferio ipsilesional posterior al programa de neu-

rorrehabilitación. En cambio, la mayoría de los pacientes reclutados por Young *et al*. presentan la EVC a nivel cortical y una lateralización contralesional post-terapia de las activaciones [59]. Además, los autores señalan que el área de la lesión es relativamente grande en la mayor parte de estos pacientes [59]. Esta diferencia sugiere que pacientes con una lesión cortical extensa requieren de un mayor reclutamiento del hemisferio contralesional para propiciar mejoras funcionales posterior a una EVC [80][81][82]. Asimismo, se ha reportado que pacientes con disfunciones motoras más severas, usualmente relacionadas a una lesión extensa, tienden a un mayor reclutamiento del hemisferio contralesional al intentar mover la extremidad superior afectada [80][82].

Por otra parte, distintos estudios han sugerido una relación entre el reclutamiento de un hemisferio cerebral, la neuromodulación y la recuperación funcional tras una EVC. La activación repetitiva de las sinapsis puede propiciar un refuerzo (PLP) o una reducción (DLP) de la eficacia en las conexiones sinápticas [83][84][85]. Estas activaciones repetitivas pueden ser propiciadas dentro de un programa de neurorrehabilitación, como una terapia ICC. Por ejemplo, se ha reportado que un buen pronóstico en la recuperación motora está asociado a aumentos en plasticidad por mecanismos similares a la PLP en el hemisferio ipsilesional y similares a la DLP en el hemisferio contralesional [82]. Además, se ha visto que el balance de la plasticidad por PLP en el hemisferio ipsilesional y de la plasticidad por DLP en el hemisferio contralesional puede predecir la recuperación motora 6 meses después del inicio de la EVC [86]. Este mecanismo podría explicar que pacientes con afectaciones motoras severas, usualmente con reclutamiento contralesional post-terapia, tienden a una menor recuperación funcional de extremidad superior que pacientes con deficiencias motoras moderadas [5]. Sin embargo, debido a la heterogeneidad de las poblaciones de pacientes con EVC estudiadas y a los resultados reportados, es necesario continuar investigando la relación de los mecanismos de neuroplasticidad con la recuperación funcional motora.

En conjunto, estos estudios muestran la relevancia de analizar cuantitativamente los cambios producidos por mecanismos de neuroplasticidad. Este análisis permite entender en mejor medida los efectos que las terapias convencionales o ICC para extremidad superior tienen en la neurorrehabilitación de los pacientes con EVC. Por esto, es de interés que este campo de investigación continúe desarrollándose.

Imagenología por tensor de difusión

En esta sección se presentan las bases teóricas de la ITD, métodos de análisis y métricas de integridad estructural de la neuroanatomía. Por último, se discuten los trabajos que cuantifican la neuroplasticidad, mediante métricas provenientes de la ITD, en pacientes con EVC posterior a un programa de rehabilitación para extremidad superior. En la Tabla 2 se muestra un resumen de los cuatro artículos incluidos en este apartado.

La ITD es una técnica ampliamente utilizada en la práctica clínica y brinda información acerca de la neuroanatomía [87]. Además, es susceptible al desplazamiento de moléculas de agua [87]. La difusión del agua no es aleatoria en tejidos humanos debido a las membranas celulares y otras barreras que impiden su libre movimiento. Por lo tanto, la ITD puede proveer información acerca de la magnitud y de la orientación del movimiento de agua [50]. Las membranas celulares de los axones y la mielina, orientadas de manera regular, actúan como barreras microestructurales a la difusión de agua. Esto genera una dependencia de orientación del movimiento de las moléculas de agua paralela a la orientación de las fibras de la materia blanca [37].

En la literatura, se han reportado parámetros necesarios en la adquisición de la ITD para describir adecuadamente el desplazamiento del agua. Por ejemplo, durante la adquisición se aplican dos gradientes magnéticos de amplitud alta. El valor *b* es un escalar que refleja el gradiente de difusión y está influenciado por la duración, la amplitud y el intervalo entre los gradientes magnéticos aplicados [90][91]. Mientras más altos sean

los valores *b*, mayor resolución tendrá el muestreo de la difusión de las moléculas de agua [91]. Comúnmente, en estudios con ITD se utiliza un valor *b* en el rango de 400 a 1500 s/mm², siendo el valor *b* de 1000 s/mm² el más utilizado [61][73][88][90][92]. Además, se necesita al menos una adquisición sin gradiente de difusión (*b*=0 s/mm²) y seis adquisiciones (direcciones) no colineales de imágenes con gradiente de difusión [91][93]. Generalmente, un mayor número de direcciones con gradiente de difusión produce una mejor representación del desplazamiento del agua [90]. Sin embargo, esto conlleva un aumento en el tiempo de adquisición [94].

La ITD utiliza el desplazamiento medido de las moléculas de agua como un sondeo que permite hacer inferencias de la neuroanatomía. Además, la información que produce la ITD es dominada por la anatomía y poco influenciada por la fisiología [37]. Cuando el agua se mueve libremente a lo largo de los axones, debido a la escasez de obstáculos contra su flujo, se produce una difusión anisotrópica, indicando una alta densidad de fibras orientadas en una misma dirección [37]. Las difusiones con mayor grado de anisotropía se encuentran en presencia de fibras altamente orientadas, como es el caso de los tractos [90]. Sin embargo, este flujo de agua se ve afectado en patologías como la EVC que, como se mencionó anteriormente, puede dañar directamente tractos de materia blanca además de causar degeneración *Walleriana* [38]. La información que otorga la ITD proporciona representaciones y métricas asociadas a las propiedades microestructurales de la materia blanca, lo que ayuda a comprender de mejor manera la extensión del daño producido por la EVC y su asociación con la pérdida (o posible recuperación) de la función motora de los pacientes [93].

TABLA 2. Resumen de los trabajos incluidos en esta revisión que utilizaron la ITD para cuantificar cambios de neuroplasticidad en pacientes con EVC tras recibir un programa de neurorrehabilitación.

Trabajos	Número de pacientes con EVC	Tipo de terapia proporcionada	Índice utilizado	Resultados relacionados a neuroplasticidad
Young *et al*. (2016) [88]	19	ICC	aAF	Correlación entre cambios en la aAF sobre una estimación del TCE con mejoras en la escala *Action Research Arm Test* (ARAT).
Caria *et al*. (2020) [73]	29	ICC	AF	Correlación entre mejoras en la escala clínica de Fugl-Meyer para extremidad superior y una disminución de la AF en la radiación talámica posterior contralesional y el esplenio del cuerpo calloso en el grupo experimental (*n* = 16).
Yuan *et al*. (2020) [61]	12	ICC	rAF	La rAF, calculada en un templete del TCE, fue correlacionada con aumentos en el puntaje de la escala clínica de Fugl-Meyer para extremidad superior.
Bhasin *et al*. (2021) [89]	20	Fisioterapia	rAF	Incrementos en la rAF sobre el área de la lesión correlacionados con el puntaje de la escala de Fugl-Meyer.

*aAF: Asimetría de anisotropía fraccional, AF: Anisotropía fraccional, ICC: Interfaz cerebro computadora, rAF: Proporción de AF, TCE: Tracto corticoespinal.

Una forma de analizar la información proporcionada por la resonancia magnética de difusión es mediante la tractografía, la cual es la reconstrucción por computadora de los tractos de materia blanca [95]. Es posible rastrear los tractos de manera no invasiva al seguir la dirección de flujo favorecida por las moléculas de agua vóxel a vóxel [90][96]. Esta reconstrucción se realiza mediante dos métodos principales [90]: 1) el determinístico, donde se estima la orientación más probable de las fibras en cada vóxel, y 2) el probabilístico, el cual se basa en la estimación de la incertidumbre de la orientación de las fibras. El método probabilístico es considerado como el más robusto, sin embargo, es computacionalmente exigente y requiere un alto tiempo de procesamiento [90][97]. La reconstrucción de un tracto inicia desde un punto de origen determinado ya sea por una RI predefinida para guiar el camino de la reconstrucción, o a nivel de vóxel para hacer una tractografía en todo el cerebro [98]. La reconstrucción se detiene mediante parámetros como umbrales de anisotropía (entre 0.1 y 0.3 para adultos) y de ángulo de giro (entre 40 y 70º), o al llegar a vóxeles de materia gris o líquido cefalorraquídeo [99].

En las Figuras 3a y 3b se muestran ejemplos de tractografías determinísticas, realizadas en el software del fabricante (Philips) del equipo de resonancia magnética utilizado en la adquisición, de los TCE de un paciente con EVC sobre un corte coronal de una imagen estructural T2-*flair*. La reconstrucción de los tractos tiene como origen una selección manual de RI en cada hemisferio y no cuenta con restricciones de término por ángulo o por tipo de tejido. En esta reconstrucción se pueden distinguir visualmente las diferencias morfológicas del TCE en el hemisferio ipsilesional (rojo) y contralesional (azul). La tractografía permite un análisis cualitativo y cuantitativo a lo largo del tracto reconstruido, sin embargo, no hay un método establecido para validar los resultados de la reconstrucción, la cual se ve afectada por ruido y artefactos en las imágenes [90][96]. Por otra parte, cabe mencionar que las Figuras 2 y 3 fueron generadas a partir de estudios de neuroimagen adquiridos de pacientes con EVC, quienes leyeron y firmaron un consentimiento informado previo a los estudios.

Otro método utilizado para cuantificar la información estructural brindada por la ITD es mediante el cálculo de métricas asociadas con propiedades de difusión en el tejido cerebral. El tensor de difusión (TD) es el método más utilizado para modelar la señal de difusión al descomponerla en eigenvalores y eigenvectores, lo que permite determinar la señal de desplazamiento de agua en un vóxel. Cada eigenvector representa un eje principal de difusión donde el eigenvalor correspondiente proporciona la magnitud de la difusión [90].

Entre las métricas que se pueden obtener a partir de la descomposición del TD se encuentran [90][99]: 1) la anisotropía fraccional (AF), representando el grado de anisotropía en la difusión [99]; 2) la difusividad media, la cual describe la magnitud de la difusión [99]; 3) la difusividad radial, representativa de la difusividad promedio perpendicular al primer eigenvector [100][101]; y 4) la difusividad axial, indicativa de la difusividad sobre la dirección dominante de difusión [100][101]. La mayor parte de los estudios se enfocan en la AF debido a que se considera que refleja el nivel de integridad de la materia blanca [50][92]. Esto permite, por ejemplo, analizar la estructura anatómica cerebral en pacientes con neuropatologías.

En las Figuras 3c y 3d se muestran ejemplos de mapas de AF de un paciente con EVC en el hemisferio derecho obtenidos tras el procesamiento de datos de ITD en la interfaz gráfica de usuario del software FSL (v6.0.4) [102] siguiendo la metodología de procesamiento de imágenes descrita en la guía del *toolbox* de análisis de resonancia magnética de difusión [103]. Aquí, los vóxeles con valores altos de AF se muestran en tonos claros mientras que vóxeles con valores bajos de AF se muestran en tonos oscuros. En estos mapas se observan valores disminuidos de la AF alrededor de la corona radiada anterior (CRA) derecha, región afectada por la EVC en

estos cortes axiales, con respecto a la CRA izquierda. Asimismo, se ha observado que valores disminuidos de la AF en el TCE están asociados a disfunciones motoras y que ésta es un buen predictor de la recuperación motora de extremidad superior de los pacientes con EVC en estudios clínicos [92][104]. Además, este índice es una métrica de alta sensibilidad [41][90]. La AF toma un valor de 0 cuando la difusión es completamente isotrópica y un valor de 1 cuando ésta es anisotrópica. La anisotropía incrementa en presencia de fibras altamente orientadas y disminuye en condiciones o patologías que afectan a la materia blanca, como en el caso de una EVC [90].

La AF, al igual que las otras métricas de difusión, se calcula sobre los tractos reconstruidos mediante tractografía, o en RI definidas ya sea por un experto clínico o en un atlas anatómico. Sin embargo, en estudios con pacientes con EVC es común hacer el cálculo de la AF basándose en RI preseleccionadas [89][104][105]. En la Figura 3e se muestra un ejemplo de RI definidas en el atlas anatómico *JHU ICBM-DTI-81 White Matter labels* [106], incluido en el software FSL [102], sobre un mapa de AF en vista coronal. Estas RI corresponden a las regiones cerebrales de la corona radiada superior, el brazo posterior de la cápsula interna (BPCI), el pedúnculo cerebral y las RI denominadas en el atlas como tracto corticoespinal [106]. Además, las RI pueden ser combinadas en cada hemisferio cerebral para formar una región objetivo de estudio. Por ejemplo, en la Figura 3e se muestra una combinación de las RI para crear una región representativa de cada TCE (TCE_{RI}).

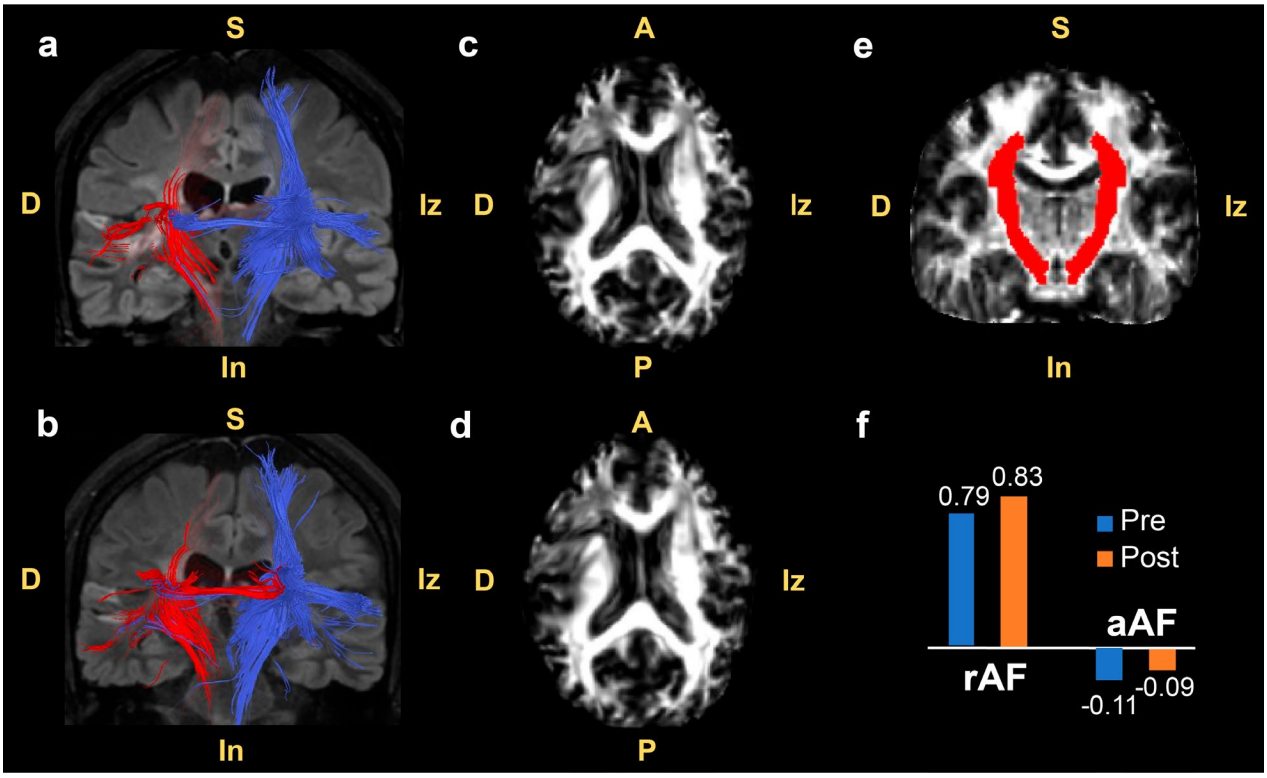

FIGURA 3. Imágenes por ITD de un paciente con EVC que recibió una terapia ICC para extremidad superior. (a) Corte coronal de tractografía previo al inicio de la terapia sobre una imagen estructural T2-*flair*. (b) Corte coronal de tractografía post-terapia sobre una imagen estructural T2-*flair*. (c) Corte axial de un mapa de anisotropía fraccional (AF) pre-terapia. (d) Corte axial de un mapa de AF post-terapia. (e) Vista coronal de las RI utilizadas para el cálculo de la proporción de AF (rAF) y de la asimetría de AF (aAF) sobre un mapa de AF. (f) Resultados de rAF y aAF pre-terapia (azul) y post-terapia (anaranjado). Figura de elaboración propia. S: superior, In: inferior, D: derecha, Iz: izquierda, A: anterior, P: posterior.

Los resultados de AF suelen ser reportados como índices de asimetría, tales como la proporción entre la AF (rAF) en los hemisferios ipsilesional (AF_{ipsi}) y contralesional (AF_{contra}), calculada como $rAF=AF_{ipsi}/AF_{contra}$, o como la asimetría de AF (aAF), definida como $aAF=(AF_{ipsi}-AF_{contra})/(AF_{ipsi}+AF_{contra})$ [90]. Estos índices son de gran utilidad para cuantificar las diferencias hemisféricas de la integridad de la materia blanca. Un valor de rAF de 1 representa una igualdad en la AF en ambos hemisferios, mientras que la aAF, de manera similar al IL, indica una mayor AF en el hemisferio ipsilesional o contralesional si ésta toma valores positivos o negativos, respectivamente [90].

En la Figura 3 se muestran ejemplos del uso e interpretación de estos índices de asimetría. En esta Figura se encuentran la tractografía (3a y 3b) y los mapas de AF (3c y 3d) de un paciente con EVC en el hemisferio derecho antes (3a y 3c) y después (3b y 3d) de recibir una terapia ICC para extremidad superior. El TCE ipsilesional reconstruido (rojo) muestra un aumento en grosor y longitud post-terapia, además de una mayor semejanza a la morfología del TCE contralesional (azul). Por otra parte, distinguir visualmente diferencias entre los mapas de AF pre-terapia y post-terapia representa un reto. De aquí la importancia del uso de los índices de rAF y aAF para cuantificar los posibles cambios en la integridad de la materia blanca posterior a una intervención. En la Figura 3f se encuentran los valores de rAF y aAF obtenidos con los mapas completos de AF del paciente con EVC pre-terapia (Figura 3c) y post-terapia (Figura 3d). Estos índices se calcularon en la plataforma MATLAB [78] con las fórmulas aritméticas presentadas anteriormente sobre las TCE_{RI} ejemplo de la Figura 3e, donde en ambas regiones se obtiene el valor promedio de AF para obtener así una métrica representativa en cada hemisferio. La rAF y la aAF muestran, respectivamente, un incremento y un decremento en magnitud post-terapia. Estos resultados indican que la integridad de la materia blanca del hemisferio ipsilesional sobre el TCE_{RI} se asemeja en mayor medida a aquella del hemisferio contralesional al finalizar la terapia ICC para extremidad superior. Esto sugiere un cambio neuroanatómico en el paciente con el programa de neurorrehabilitación.

Uno de los usos de los índices de asimetría de AF ha sido como herramienta de pronóstico. Okamoto *et al.* reportaron que mientras mayor sea la rAF en el BPCI al momento de admisión de pacientes con EVC, mayor podría ser el grado de recuperación en la función motora de extremidad superior [92]. De manera similar, Bhasin *et al.* indicaron que la rAF medida en la región de la lesión cerebral previo a recibir terapia física se correlacionó con el puntaje obtenido con la escala de Fugl-Meyer para extremidad superior (FM-ES) [89]. Sin embargo, hay pocos estudios que evalúan los cambios en la AF en pacientes con EVC a lo largo de un proceso de neurorrehabilitación para extremidad superior, lo cual podría proporcionar información relevante acerca de los cambios en neuroplasticidad de los pacientes.

En los estudios presentados en la Tabla 2 se empleó la AF como índice de neuroplasticidad en programas de terapia para extremidad superior tanto convencionales como experimentales que incorporan sistemas ICC. Bhasin *et al.* reportaron un aumento de la rAF en pacientes con EVC en etapa crónica tras recibir fisioterapia tradicional, indicando un aumento en la integridad de la materia blanca en el área de la lesión del hemisferio afectado [89]. Este incremento en la rAF se correlacionó significativamente con la mejora funcional de extremidad superior de los pacientes de acuerdo con las escalas clínicas de FM-ES y el índice de motricidad [89].

Tras proporcionar un programa de terapia ICC a 19 pacientes con EVC, Young *et al.* señalaron una correlación en el incremento de la AF del TCE contralesional con mejoras en la escala *Nine-Hole Peg Test* (9-HPT), además de una correlación entre cambios en la aAF, *i.e.* aumentos de la AF en el TCE contralesional con respecto a la AF del TCE ipsilesional, con mejoras en la escala *Action Research Arm Test* (ARAT) [88]. Caria *et al.*

proporcionaron terapias ICC a 16 pacientes con EVC, conformando su grupo experimental, y reportaron una correlación del aumento en el puntaje de la escala FM-ES con una disminución de la AF en el esplenio del cuerpo calloso y en la radiación talámica posterior contralesional post-terapia [73]. Además, se encontró una correlación positiva entre los cambios post-terapia y pre-terapia del IL calculado sobre la corteza motora (incluyendo la corteza motora primaria, la corteza premotora y la corteza somatosensorial primaria) y los cambios post-terapia y pre-terapia de la AF en las regiones anatómicas mencionadas anteriormente, lo que indica que la disminución de los valores de la AF en el esplenio y en la radiación talámica posterior contralesional está asociada a una lateralización ipsilesional de la activación neuronal en la corteza motora al mover la mano afectada [73]. Asimismo, en el trabajo de Yuan *et al.* se observó que la integridad estructural del TCE, cuantificada con la rAF, tiene una correlación positiva con la recuperación de la función motora de extremidad superior según la escala de FM-ES en pacientes con EVC que recibieron terapias ICC [61].

Los cambios reportados de los índices de asimetría de AF difieren entre los trabajos. Los pacientes reclutados por Young *et al.* presentan principalmente lesiones corticales y una mayor integridad de la materia blanca en el hemisferio contralesional post-terapia [88]. Esto ha sido asociado con una menor recuperación funcional de extremidad superior [80]. Sin embargo, Young *et al.* reportaron una correlación positiva del incremento de AF contralesional con una mejora funcional de extremidad superior con base en distintas escalas clínicas [88]. Esto sugiere que los cambios estructurales de neuroplasticidad generados en el hemisferio contralesional posterior a una terapia ICC, están relacionados con la mejora funcional en pacientes con lesiones corticales o severas. Por otra parte, Bhasin *et al.*, Caria *et al.* y Yuan *et al.* reclutaron pacientes con discapacidades motrices moderadas de extremidad superior o pacientes cuya lesión se encuentra principalmente a nivel subcortical [61][73][89].

Los resultados de estos trabajos sugieren que un programa de neurorrehabilitación proporcionado a este tipo de población puede propiciar un aumento en la integridad estructural ipsilesional, la cual fue asociada a una recuperación funcional de extremidad superior. Además, se ha reportado que el aumento de la integridad estructural del hemisferio ipsilesional produce una mayor recuperación motora que una mayor integridad estructural contralesional [7][80]. Los resultados presentados sugieren que los mecanismos de neuroplasticidad estructurales, como la proliferación axonal, sinaptogénesis o neurogénesis, propician un aumento en la integridad estructural de la materia blanca, lo que juega un rol en la recuperación motora de pacientes con EVC [21][22][23]. Además, el hemisferio cerebral principal sobre el cual estos mecanismos actúan podría estar definido por la ubicación y severidad de la lesión por la EVC [7]. Estos resultados muestran que la AF es una métrica de los mecanismos de neuroplasticidad en la recuperación motora de pacientes con EVC posterior a un proceso de neurorrehabilitación. Sin embargo, es necesario continuar estudiando estos mecanismos con distintas poblaciones de pacientes con EVC para comprender mejor el proceso de recuperación funcional.

Los trabajos incluidos en esta revisión indican que los pacientes con EVC muestran cambios neuroanatómicos tras recibir programas de terapia para extremidad superior como parte del proceso de neuroplasticidad que se produce. Además, estos cambios se han asociado a una mejora funcional motora de extremidad superior. Esto indica que es relevante continuar explorando la información proporcionada por la ITD para comprender el proceso de recuperación de los pacientes con EVC.

Limitaciones

La información que otorgan estas técnicas de neuroimagenología es relevante, sin embargo, existen ciertas limitaciones que son importantes de mencionar. Por ejemplo, el tiempo de escaneo puede ser largo en estudios con pacientes con EVC. Entre las secuencias reali-

zadas a pacientes con esta patología se encuentran la RMF, la ITD, secuencias estructurales, espectroscopía por resonancia magnética (RM), imagenología de perfusión y angiografía por RM [25][94] [107][108]. En promedio, estas secuencias tienen una duración aproximada de 15.5 min tanto en resonadores de 1.5-T como de 3-T, por lo que, un estudio que abarque 3 o 4 de estas secuencias podría tender a una duración de 1 hora [109]. Además, se ha reportado que pacientes con EVC presentan mayores movimientos de cabeza que sujetos sanos en estudios de RMF de 6 min de duración [110]. Esto produce una mayor cantidad de artefactos en las imágenes adquiridas que deben removerse. Por lo tanto, la duración total del estudio de imagenología debe mantenerse limitado para evitar fatiga y molestias en los pacientes [50][90][111].

Por otra parte, los estudios de RMF son comúnmente caracterizados por baja potencia estadística debido al tamaño limitado de la muestra y al gran número de comparaciones que se realizan [55][112]. Una forma de contrarrestar esto es mediante un diseño en bloques del paradigma de la RMF, el cual se ha utilizado ampliamente en estudios con pacientes con EVC. Además, el IL también tiene algunas limitaciones. La variabilidad existente en la fórmula utilizada en el cálculo del IL, particularmente la definición de lo que constituye un vóxel con activación significativa, dificulta la comparación de resultados entre distintos estudios con respecto a la lateralización de la actividad cerebral [46][75][77]. Sin embargo, se ha observado una tendencia en estudios que involucran lesiones cerebrales a utilizar el número de vóxeles que superan un umbral estadístico como métrica para el cálculo del IL debido a la robustez mostrada por este método [67][75].

Entre las limitaciones de la ITD se encuentra la estimación del TD donde se asume que la difusión asociada a las fibras dentro de un vóxel sigue una distribución gaussiana, representada por una sola dirección [41][90]. Sin embargo, esto no se cumple por la presencia de fibras cruzadas y múltiples orientaciones axonales [41][90]. A pesar de esto, las métricas de la ITD, particularmente la AF, tienen alta sensibilidad a cambios provocados por una EVC [89]. Además, múltiples estudios han utilizado esta técnica para tener una mejor comprensión y caracterizar los cambios que se producen posterior a la EVC, permitiendo medir los efectos de distintos protocolos de terapia [41]. La aAF, al igual que el IL, sufre de la variabilidad existente en la literatura en el cálculo de este índice [46]. Sin embargo, distintos estudios han asociado la aAF, al igual que la rAF, a cambios en escalas clínicas que reflejan la mejora funcional motora de extremidad superior de los pacientes con EVC [88][89].

Finalmente, la RMF y la ITD requieren de equipo y software especializados [71][102]. En general, estos estudios utilizan resonadores de 3-T, mientras que el software requerido para la adquisición y el procesamiento de imágenes tiene, usualmente, un costo elevado, especialmente las licencias propias del fabricante del equipo de resonancia [59][60][61][73][88][109]. En conjunto, estas limitaciones hacen que la RMF y la ITD se usen principalmente con fines de investigación.

Los detalles de los métodos de procesamiento de los estudios de neuroimagen y del cálculo de los índices están fuera del tópico de la presente revisión, lo cual se considerará para un trabajo futuro.

CONCLUSIONES

Las técnicas de RMF y de ITD se han posicionado como herramientas útiles en el estudio de la enfermedad vascular cerebral. Distintos estudios muestran que la RMF permite el análisis de las activaciones neuronales de los pacientes con EVC cuando éstos intentan mover su extremidad superior afectada. Además, el IL permite cuantificar los cambios producidos por mecanismos de neuroplasticidad que se presenten en la lateralización de estas activaciones tras un proceso de neurorrehabilitación. Por otra parte, la ITD es capaz

de otorgar información relevante acerca de la neuroanatomía de los pacientes con EVC y la asociación que ésta tiene con la posible recuperación funcional de los pacientes. La AF, al igual que los índices derivados de rAF y aAF, han probado ser métricas de alta sensibilidad a los cambios en la integridad de la materia blanca tras la EVC y posterior a un proceso de rehabilitación. La RMF y la ITD son de gran importancia en la investigación de los mecanismos de neuroplasticidad funcionales y estructurales involucrados en la recuperación de los pacientes con EVC. Ambas técnicas de neuroimagenología permiten comprender en mejor medida este proceso. De esta forma, se podrán diseñar y proporcionar mejores programas de neurorrehabilitación que beneficien a los pacientes con EVC.

DECLARACIÓN ÉTICA

Los datos utilizados para ilustrar los conceptos de las técnicas de neuroimagen fueron obtenidos de estudios de imagenología realizados a pacientes con EVC. Previo a los estudios, los pacientes leyeron y firmaron un consentimiento informado aprobado por el Comité de Ética del Instituto Nacional de Rehabilitación "Luis Guillermo Ibarra Ibarra" (número de registro 25/19AC), donde autorizaron el uso de sus imágenes en revistas científicas y se estableció el resguardo de sus datos por cuestiones de privacidad y confidencialidad.

AGRADECIMIENTOS

Los autores agradecen al Consejo Nacional de Humanidades, Ciencias y Tecnologías (CONAHCYT) por el financiamiento número SALUD-2018-02-B-S-45803. MERG agradece al CONAHCYT por la beca de doctorado 844633. Los autores agradecen al Dr. Álvaro Lomelí Rivas, al Dr. Marvin Merino Casas, al Dr. Rubén I. Cariño-Escobar, al Dr. Paul Carrillo-Mora y al Dr. Oscar Marrufo-Meléndez por su apoyo para la realización de estudios de resonancia magnética funcional.

CONFLICTO DE INTERESES

Los autores indican que no existe algún conflicto de interés.

CONTRIBUCIONES DE LOS AUTORES

M.E.R.G. conceptualizó el proyecto, participó en la recopilación y curación de datos, llevó a cabo análisis formales in silico, colaboró en el diseño y desarrollo de la metodología, contribuyó a la programación de software especializado y la visualización de resultados, y participó en la redacción de la primera versión del manuscrito. N.M.A. contribuyó a la recopilación de datos, proporcionó recursos computacionales e instrumentales y participó en la redacción, revisión y edición del manuscrito. S.G.M.A. realizó análisis formales, recopilación de datos y procesamiento de datos para análisis in silico mediante el uso de software especializado, y participó en la redacción, revisión y edición del manuscrito. B.S.C. colaboró en la recopilación, curación e interpretación de datos, llevó a cabo análisis de software y participó en la redacción, revisión y edición del manuscrito. T.R.R. participó en la recopilación y procesamiento de datos, el uso de software especializado y participó en la redacción, revisión y edición del manuscrito. V.H.A.J. participó en el procesamiento de la recopilación de datos, el uso de software especializado, y participó en la redacción, revisión y edición del manuscrito. R.V.C. conceptualizó el proyecto, diseñó y desarrolló la metodología, llevó a cabo la visualización de datos y participó en la redacción, revisión y edición del manuscrito. J.C.N. conceptualizó el proyecto, obtuvo financiamiento y recursos financieros, participó en la recopilación de datos y proporcionó pacientes y recursos computacionales, diseñó y desarrolló la metodología, contribuyó a la visualización de datos y resultados y participó en la redacción, revisión y edición del manuscrito. Todos los autores revisaron y aprobaron la versión final del manuscrito.

REFERENCIAS

[1] V. L. Feigin, B. A. Stark, C. O. Johnson, G. A. Roth, C. Bisignano, et al., "Global, regional, and national burden of stroke and its risk factors, 1990-2019: A systematic analysis for the Global Burden of Disease Study 2019," Lancet Neurol., vol. 20, no. 10, pp. 795-820, Oct. 2021, doi: https://doi.org/10.1016/S1474-4422(21)00252-0

[2] V. De la Cruz-Góngora, E. Chiquete, H. Gómez-Dantés, L. Cahuana-Hurtado, C. Cantú-Brito, "Trends in the burden of stroke in Mexico: A national and subnational analysis of the global burden of disease 1990-2019," Lancet Reg. Health Am., vol. 10, art. no. 100204, Jun. 2022, doi: https://doi.org/10.1016/j.lana.2022.100204

[3] C. Grefkes, G. R. Fink, "Recovery from stroke: current concepts and future perspectives.," Neurol. Res. Pract., vol. 2, art. no. 17, Jun. 2020, doi: https://doi.org/10.1186/s42466-020-00060-6

[4] B. H. Dobkin, "Clinical practice. Rehabilitation after stroke.," N. Engl. J. Med., vol. 352, pp. 1677-1684, Apr. 2005, doi: https://doi.org/10.1056/NEJMcp043511

[5] L. M. Carey, D. F. Abbott, G. F. Egan, et al., "Evolution of Brain Activation with Good and Poor Motor Recovery after Stroke," Neurorehabil. Neural Repair, vol. 20, no. 1, pp. 24-41, Mar. 2006, doi: https://doi.org/10.1177/1545968305283053

[6] R. Mane, T. Chouhan, C. Guan, "BCI for stroke rehabilitation: motor and beyond.," J. Neural Eng., vol. 17, no. 4, art. no. 41001, Aug. 2020, doi: https://doi.org/10.1088/1741-2552/aba162

[7] K. C. Dodd, V. A. Nair, and V. Prabhakaran, "Role of the Contralesional vs. Ipsilesional Hemisphere in Stroke Recovery," Front. Hum. Neurosci., vol. 11, art. no. 469, Sep. 2017, doi: https://doi.org/10.3389/fnhum.2017.00469

[8] L. Carey, A. Walsh, A. Adikari, P. Godin, et al., "Finding the Intersection of Neuroplasticity, Stroke Recovery, and Learning: Scope and Contributions to Stroke Rehabilitation.," Neural Plast., vol. 2019, art. no. 5232374, May. 2019, doi: https://doi.org/10.1155/2019/5232374

[9] S. C. Cramer, M. Sur, B. H. Dobkin, C. O'Brien, et al., "Harnessing neuroplasticity for clinical applications.," Brain, vol. 134, no. 6, pp. 1591-1609, Jun. 2011, doi: https://doi.org/10.1093/brain/awr039

[10] W. T. Greenough, J. E. Black, C. S. Wallace, "Experience and Brain Development," Child Dev., vol. 58, No. 3, pp. 539-559, Jun. 1987, doi: https://doi.org/10.2307/1130197

[11] Y. Chang, "Reorganization and plastic changes of the human brain associated with skill learning and expertise," Front. Hum. Neurosci., vol. 8, art. no. 35, 2014, doi: https://doi.org/10.3389/fnhum.2014.00035

[12] L. G. Ungerleider, J. Doyon, A. Karni, "Imaging Brain Plasticity during Motor Skill Learning," Neurobiol. Learn. Mem., vol. 78, no. 3, pp. 553-564, Nov. 2002, doi: https://doi.org/10.1006/nlme.2002.4091

[13] A. May, "Experience-dependent structural plasticity in the adult human brain," Trends Cogn. Sci., vol. 15, no. 10, pp. 475-482, Oct. 2011, doi: https://doi.org/10.1016/j.tics.2011.08.002

[14] N. Dancause S. Barbay, S. B. Frost, "Extensive Cortical Rewiring after Brain Injury," J. Neurosci., vol. 25, no. 44, pp. 10167-10179, Nov. 2005, doi: https://doi.org/10.1523/JNEUROSCI.3256-05.2005

[15] T. Murphy, D. Corbett, "Plasticity during stroke recovery: from synapse to behaviour," Nat. Rev. Neurosci., vol. 10, pp. 861-872, Dec. 2009, doi: https://doi.org/10.1038/nrn2735

[16] M. Pekna, M. Pekny, M. Nilsson, "Modulation of Neural Plasticity as a Basis for Stroke Rehabilitation," Stroke, vol. 43, no. 10, pp. 2819-2828, Oct. 2012, doi: https://doi.org/10.1161/STROKEAHA.112.654228

[17] T. V Bliss, T. Lømo, "Long-lasting potentiation of synaptic transmission in the dentate area of the anaesthetized rabbit following stimulation of the perforant path," J. Physiol., vol. 232, no. 2, pp. 331-356, Jul. 1973, doi: https://doi.org/10.1113/jphysiol.1973.sp010273

[18] R. A. Nicoll, "A Brief History of Long-Term Potentiation.," Neuron, vol. 93, no. 2, pp. 281-290, Jan. 2017, doi: https://doi.org/10.1016/j.neuron.2016.12.015

[19] S. Peineau, C. Taghibiglou, C. Bradley, T. P. Wong, L. Liu, J. Lu, et al., "LTP inhibits LTD in the Hippocampus via Regulation of GSK3beta," Neuron, vol. 53, no. 5, pp. 703-717, Mar. 2007, doi: https://doi.org/10.1016/j.neuron.2007.01.029

[20] A. Mancini, A. de Iure, B. Picconi, "Basic mechanisms of plasticity and learning," in Handbook of Clinical Neurology, A. Quartarone, M. F. Ghilardi, F. Boller, Eds., Straive, India: Elsevier, 2022, ch. 2, pp. 21-34, doi: https://doi.org/10.1016/B978-0-12-819410-2.00002-3

[21] S. C. Cramer, M. Chopp, "Recovery recapitulates ontogeny," Trends Neurosci., vol. 23, no. 6, pp. 265-271, Jun. 2000, doi: https://doi.org/10.1016/s0166-2236(00)01562-9

[22] T. Wieloch, K. Nikolich, "Mechanisms of neural plasticity following brain injury," Curr. Opin. Neurobiol., vol. 16, no. 3, pp. 258-264, Jun. 2006, doi: https://doi.org/10.1016/j.conb.2006.05.011

[23] S. T. Carmichael, "Emergent properties of neural repair: elemental biology to therapeutic concepts," Ann. Neurol., vol. 79, no. 6, pp. 895-906, Jun. 2016, doi: https://doi.org/10.1002/ana.24653

[24] A. Durukan, T. Tatlisumak, "Acute ischemic stroke: Overview of major experimental rodent models, pathophysiology, and therapy of focal cerebral ischemia," Pharmacol. Biochem. Behav., vol. 87, no. 1, pp. 179-197, May 2007, doi: https://doi.org/10.1016/j.pbb.2007.04.015

[25] L. A. Boyd, K. S. Hayward, N. S. Ward, et al., "Biomarkers of stroke recovery: Consensus-based core recommendations from the Stroke Recovery and Rehabilitation Roundtable," Int. J. Stroke, vol. 12, no. 5, pp. 480-493, Jul. 2017, doi: https://doi.org/10.1177/1747493017714176

[26] C. Grefkes, G. R. Fink, "Reorganization of cerebral networks after stroke: new insights from neuroimaging with connectivity approaches," Brain, vol. 134, no. 5, pp. 1264-1276, May 2011, doi: https://doi.org/10.1093/brain/awr033

[27] S. Ogawa, D. W. Tank, R. Menor, J. M. Ellermann, et al., "Intrinsic signal changes accompanying sensory stimulation: functional brain mapping with magnetic resonance imaging," Proc. Natl. Acad. Sci., vol. 89, no. 13, pp. 5951-5955, Jul. 1992, doi: https://doi.org/10.1073/pnas.89.13.5951

[28] D. Attwell, C. Iadecola, "The neural basis of functional brain imaging signals," Trends Neurosci., vol. 25, no. 12, pp. 621-625, Dec. 2002, doi: https://doi.org/10.1016/s0166-2236(02)02264-6

[29] A. Crofts, M. E. Kelly, C. L. Gibson, "Imaging Functional Recovery Following Ischemic Stroke: Clinical and Preclinical fMRI Studies," J. Neuroimaging, vol. 30, no. 1, pp. 5-14, Jan. 2020, doi: https://doi.org/10.1111/jon.12668

[30] N. S. Ward, M. M. Brown, A. J. Thompson, R. S. J. Frackowiak, "Neural correlates of motor recovery after stroke: a longitudinal fMRI study," Brain, vol. 126, no. 11, pp. 2476-2496, Nov. 2003, doi: https://doi.org/10.1093/brain/awg245

[31] D. A. Nowak, C. Grefkes, M. Dafotakis, S. Eickhoff, et al., "Effects of Low-Frequency Repetitive Transcranial Magnetic Stimulation of the Contralesional Primary Motor Cortex on Movement Kinematics and Neural Activity in Subcortical Stroke," Arch. Neurol., vol. 65, no. 6, pp. 741-747, Jun. 2008, doi: https://doi.org/10.1001/archneur.65.6.741

[32] A. K. Rehme, S. B. Eickhoff, C. Rottschy, G. R. Fink, C. Grefkes, "Activation likelihood estimation meta-analysis of motor-related neural activity after stroke," Neuroimage, vol. 59, no. 3, pp. 2771-2782, Feb. 2012, doi: https://doi.org/10.1016/j.neuroimage.2011.10.023

[33] A. K. Rehme, S. B. Eickhoff, L. E. Wang, G. R. Fink, C. Grefkes, "Dynamic causal modeling of cortical activity from the acute to the chronic stage after stroke," Neuroimage, vol. 55, no. 3, pp. 1147-1158, Apr. 2011, doi: https://doi.org/10.1016/j.neuroimage.2011.01.014

[34] A. K. Rehme, G. R. Fink, D. Y. von Cramon, C. Grefkes, "The Role of the Contralesional Motor Cortex for Motor Recovery in the Early Days after Stroke Assessed with Longitudinal fMRI," Cereb. Cortex, vol. 21, no. 4, pp. 756-768, Apr. 2011, doi: https://doi.org/10.1093/cercor/bhq140

[35] L. E. Wang, G. R. Fink, S. Diekhoff, A. K. Rehme, S. B. Eickhoff, C. Grefkes, "Noradrenergic enhancement improves motor network connectivity in stroke patients," Ann. Neurol., vol. 69, no. 2, pp. 375-388, Feb. 2011, doi: https://doi.org/10.1002/ana.22237

[36] C. Grefkes, G. R. Fink, "Connectivity-based approaches in stroke and recovery of function," Lancet Neurol., vol. 13, no. 2, pp. 206-216, Feb. 2014, doi: https://doi.org/10.1016/S1474-4422(13)70264-3

[37] S. Mori, J. Zhang, "Principles of Diffusion Tensor Imaging and Its Applications to Basic Neuroscience Research," Neuron, vol. 51, no. 5, pp. 527-539, Sep. 2006, doi: https://doi.org/10.1016/j.neuron.2006.08.012

[38] Y. J. Chen, S. A. Nabavizadeh, A. Vossough, S. Kumar, L. A. Loevner, S. Mohan, "Wallerian Degeneration Beyond the Corticospinal Tracts: Conventional and Advanced MRI Findings," J. Neuroimaging, vol. 27, no. 3, pp. 272-280, May 2017, doi: https://doi.org/10.1111/jon.12404

[39] J. Puig, G. Blasco, J. Daunis-I-Estadella, G. Thomalla, M. Castellanos, et al., "Decreased Corticospinal Tract Fractional Anisotropy Predicts Long-term Motor Outcome After Stroke," Stroke, vol. 44, no. 7, pp. 2016-2018, Jul. 2013, doi: https://doi.org/10.1161/STROKEAHA.111.000382

[40] J. Song, V. A. Nair, B. M. Young, L. M. Walton, et al., "DTI measures track and predict motor function outcomes in stroke rehabilitation utilizing BCI technology," Front. Hum. Neurosci., vol. 9, art. no. 195, Apr. 2015, doi: https://doi.org/10.3389/fnhum.2015.00195

[41] E. V. R. DiBella, A. Sharma, L. Richards, V. Prabhakaran, J. J. Majersik, and S. K. HashemizadehKolowri, "Beyond Diffusion Tensor MRI Methods for Improved Characterization of the Brain after Ischemic Stroke: A Review," AJNR Am. J. Neuroradiol., vol. 43, no. 5, pp. 661-669, May 2022, doi: https://doi.org/10.3174/ajnr.A7414

[42] W. Feng, J. Wang, P. Y. Chhatbar, C. Doughty, D. Landsittel, et al., "Corticospinal tract lesion load: An imaging biomarker for stroke motor outcomes," Ann. Neurol., vol. 78, no. 6, pp. 860-870, Dec. 2015, doi: https://doi.org/10.1002/ana.24510

[43] P. Kumar, A. K. Yadav, S. Misra, A. Kumar, K. Chakravarty, K. Prasad, "Prediction of upper extremity motor recovery after subacute intracerebral hemorrhage through diffusion tensor imaging: a systematic review and meta-analysis," Neuroradiology, vol. 58, no. 10, pp. 1043-1050, Oct. 2016, doi: https://doi.org/10.1007/s00234-016-1718-6

[44] P. Kumar, P. Kathuria, P. Nair, K. Prasad, "Prediction of Upper Limb Motor Recovery after Subacute Ischemic Stroke Using Diffusion Tensor Imaging: A Systematic Review and Meta-Analysis," J. Stroke, vol. 18, no. 1, pp. 50-59, Jan. 2016, doi: https://doi.org/10.5853/jos.2015.01186

[45] R. T. Pivik, R. J. Broughton, R. Coppola, R. J. Davidson, N. Fox, M. R. Nuwer, "Guidelines for the recording and quantitative analysis of electroencephalographic activity in research contexts," Psychophysiology, vol. 30, no. 6, pp. 547-558, Nov. 1993, doi: https://doi.org/10.1111/j.1469-8986.1993.tb02081.x

[46] M. L. Seghier, "Laterality index in functional MRI: methodological issues," Magn. Reson. Imaging, vol. 26, no. 5, pp. 594-601, Jun. 2008, doi: https://doi.org/10.1016/j.mri.2007.10.010

[47] J. E. Desmond, J. M. Sum, A. D. Wagner, J. B. Demb et al., "Functional MRI measurement of language lateralization in Wada-tested patients," Brain, vol. 118, no. 6, pp. 1411-1419, Dec. 1995, doi: https://doi.org/10.1093/brain/118.6.1411

[48] J. R. Binder, S. J. Swanson, T. A. Hammeke, G. L. Morris, et al., "Determination of language dominance using functional MRI: a comparison with the Wada test," Neurology, vol. 46, no. 4, pp. 978-984, Apr. 1996, doi: https://doi.org/10.1212/wnl.46.4.978

[49] C. Doughty, J. Wang, W. Feng, D. Hackney, E. Pani, G. Schlaug, "Detection and Predictive Value of Fractional Anisotropy Changes of the Corticospinal Tract in the Acute Phase of a Stroke," Stroke, vol. 47, no. 6, pp. 1520-1526, Jun. 2016, doi: https://doi.org/10.1161/STROKEAHA.115.012088

[50] J. Griauzde, A. Srinivasan, "Advanced Neuroimaging Techniques: Basic Principles and Clinical Applications," J. Neuroophthalmol., vol. 38, no. 1, pp. 101-114, Mar. 2018, doi: https://doi.org/10.1097/WNO.0000000000000539

[51] R. A. Poldrack, J. A. Mumford, T. E. Nichols, Handbook of Functional MRI Data Analysis. Cambridge, UK: Cambridge University Press, 2011, pp. 70.

[52] S. Saini, R. B. Frankel, D. D. Stark, J. T. Ferrucci, "Magnetism: a primer and review," AJR Am. J. Roentgenol., vol. 150, no. 4, pp. 735-743, Apr. 1988, doi: https://doi.org/10.2214/ajr.150.4.735

[53] S. Ogawa, T.-M. Lee, A. S. Nayak, P. Glynn, "Oxygenation-sensitive contrast in magnetic resonance image of rodent brain at high magnetic fields," Magn. Reson. Med., vol. 14, no. 1 pp. 68-78, Apr. 1990, doi: https://doi.org/10.1002/mrm.1910140108

[54] J. M. Soares, R. Magalhães, P. S. Moreira, A. Sousa, et al., "A Hitchhiker's Guide to Functional Magnetic Resonance Imaging," Front. Neurosci., vol. 10, art. no. 515 Nov. 2016, doi: https://doi.org/10.3389/fnins.2016.00515

[55] L. Hay, A. H. B. Duffy, S. J. Gilbert, M. A. Grealy, "Functional magnetic resonance imaging (fMRI) in design studies: Methodological considerations, challenges, and recommendations," Des. Stud., vol. 78, art. no. 101078, Jan. 2022, doi: https://doi.org/10.1016/j.destud.2021.101078

[56] S.-G. Kim, E. Rostrup, H. B. W. Larsson, S. Ogawa, O. B. Paulson, "Determination of relative CMRO2 from CBF and BOLD changes: Significant increase of oxygen consumption rate during visual stimulation," Magn. Reson. Med., vol. 41, no. 6, pp. 1152-1161, Jun. 1999, doi: https://doi.org/10.1002/(SICI)1522-2594(199906)41:6<1152::AID-MRM11>3.0.CO;2-T

[57] C. M. Bennett, M. B. Miller, "fMRI reliability: Influences of task and experimental design," Cogn. Affect. Behav. Neurosci., vol. 13, no. 4, pp. 690-702, 2013, doi: https://doi.org/10.3758/s13415-013-0195-1

[58] A. Caria, C. Weber, D. Brötz, A. Ramos, et al., "Chronic stroke recovery after combined BCI training and physiotherapy: A case report," Psychophysiology, vol. 48, no. 4 pp. 578-582, Apr. 2011, doi: https://doi.org/10.1111/j.1469-8986.2010.01117.x

[59] B. M. Young, Z. Nigogosyan, L. M. Walton, A. Remsik, et al., "Dose-response relationships using brain-computer interface technology impact stroke rehabilitation," Front. Hum. Neurosci., vol. 9, art. no. 361, Jun. 2015, doi: https://doi.org/10.3389/fnhum.2015.00361

[60] A. Ramos-Murguialday, M. R. Curado, D. Broetz, Ö. Yilmaz, et al., "Brain-Machine Interface in Chronic Stroke: Randomized Trial Long-Term Follow-up," Neurorehabil. Neural Repair, vol. 33, no. 3, pp. 188-198, Mar. 2019, doi: https://doi.org/10.1177/1545968319827573

[61] K. Yuan, X. Wang, C. Chen, C. C.-Y. Lau, et al., "Interhemispheric Functional Reorganization and its Structural Base After BCI-Guided Upper-Limb Training in Chronic Stroke," IEEE Trans. Neural Syst. Rehabilitation Eng., vol. 28, no. 11, pp. 2525-2536, Nov. 2020, doi: https://doi.org/10.1109/TNSRE.2020.3027955

[62] M. Demers, R. Varghese, C. Winstein, "Retrospective Analysis of Task-Specific Effects on Brain Activity After Stroke: A Pilot Study," Front. Hum. Neurosci., vol. 16, art. no. 871239, 2022, doi: https://doi.org/10.3389/fnhum.2022.871239

[63] S. E. Petersen, J. W. Dubis, "The mixed block/event-related design," Neuroimage, vol. 62, no. 2, pp. 1177-1184, Aug. 2012, doi: https://doi.org/10.1016/j.neuroimage.2011.09.084

[64] M. Welvaert, Y. Rosseel, "A Review of fMRI Simulation Studies," PLoS One, vol. 9, no. 7, art. no. e101953, Jul. 2014, doi: https://doi.org/10.1371/journal.pone.0101953

[65] J. Saunders, H. L. Carlson, F. Cortese, B. G. Goodyear, A. Kirton, "Imaging functional motor connectivity in hemiparetic children with perinatal stroke," Hum. Brain Mapp., vol. 40, no. 5, pp. 1632-1642, Apr. 2019, doi: https://doi.org/10.1002/hbm.24474

[66] G. Lioi, S. Bulet, M. Fleury, E. Bannier, et al., "A Multi-Target Motor Imagery Training Using Bimodal EEG-fMRI Neurofeedback: A Pilot Study in Chronic Stroke Patients," Front. Hum. Neurosci., vol. 14, art. no. 37, Feb. 2020, doi: https://doi.org/10.3389/fnhum.2020.00037

[67] S.-L. Liew, K. A. Garrison, K. L. Ito, P. Heydari, et al., "Laterality of Poststroke Cortical Motor Activity during Action Observation Is Related to Hemispheric Dominance," Neural Plast., vol. 2018, p. 3524960, May. 2018, doi: https://doi.org/10.1155/2018/3524960

[68] A. Errante, D. Saviola, M. Cantoni, K. Iannuzzelli, et al., "Effectiveness of action observation therapy based on virtual reality technology in the motor rehabilitation of paretic stroke patients: a randomized clinical trial," BMC Neurol., vol. 22, no. 1, art. no. 109, Mar. 2022, doi: https://doi.org/10.1186/s12883-022-02640-2

[69] J. B. Kroth, B. Handfas, G. Rodrigues, F. Zepeda, et al., "Effects of Repetitive Peripheral Sensory Stimulation in the Subacute and Chronic Phases After Stroke: Study Protocol for a Pilot Randomized Trial," Front. Neurol., vol. 13, art. no. 779128, Feb. 2022, doi: https://doi.org/10.3389/fneur.2022.779128

[70] A. Lasek-Bal, J. Kidoń, M. Błaszczyszyn, B. Stasiów, A. Żak, "BOLD fMRI signal in stroke patients and its importance for prognosis in the subacute disease period - Preliminary report," Neurol. Neurochir. Pol., vol. 52, no. 3, pp. 341-346, May. 2018, doi: https://doi.org/10.1016/j.pjnns.2017.12.006

[71] W. Penny, K. Friston, J. Ashburner, S. Kiebel, T. Nichols, Eds., Statistical Parametric Mapping: The Analysis of Functional Brain Images. London, UK: Academic Press, 2007 pp. 5.

[72] J. Ashburner, G. Barnes, C.-C. Chen, G. Flandin, et al. SPM12 Manual. (2021). Accessed: Jun. 10, 2023. [Online]. Available: https://www.fil.ion.ucl.ac.uk/spm/doc/spm12_manual.pdf

[73] A. Caria, J. L. D. da Rocha, G. Gallitto, N. Birbaumer, R. Sitaram, A. R. Murguialday, "Brain-Machine Interface Induced Morpho-Functional Remodeling of the Neural Motor System in Severe Chronic Stroke," Neurotherapeutics, vol. 17, no. 2, pp. 635-650, Apr. 2020, doi: https://doi.org/10.1007/s13311-019-00816-2

[74] A. Ramos-Murguialday, D. Broetz, M. Rea, L. Läer, et al., "Brain-machine interface in chronic stroke rehabilitation: A controlled study," Ann. Neurol., vol. 74, no. 1, pp. 100-108, Jul. 2013, doi: https://doi.org/10.1002/ana.23879

[75] A. Jansen, R. Menke, J. Sommer, A. F. Förster, et al., "The assessment of hemispheric lateralization in functional MRI—Robustness and reproducibility," Neuroimage, vol. 33, no. 1, pp. 204-217, Oct. 2006, doi: https://doi.org/10.1016/j.neuroimage.2006.06.019

[76] E. T. Rolls, C.-C. Huang, C.-P. Lin, J. Feng, M. Joliot, "Automated anatomical labelling atlas 3," Neuroimage, vol. 206, art. no. 116189, Feb. 2020, doi: https://doi.org/10.1016/j.neuroimage.2019.116189

[77] M. Wilke, K. Lidzba, "LI-tool: A new toolbox to assess lateralization in functional MR-data," J. Neurosci. Methods, vol. 163, no. 1, pp. 128-136, Jun. 2007, doi: https://doi.org/10.1016/j.jneumeth.2007.01.026

[78] MATLAB 9.11.0. (2001). The MathWorks, Inc. Accessed: Jun. 10, 2023. [Online]. Available: https://www.mathworks.com

[79] S. Vulliemoz, O. Raineteau, D. Jabaudon, "Reaching beyond the midline: why are human brains cross wired?," Lancet Neurol., vol. 4, no. 2, pp. 87-99, Feb. 2005, doi: https://doi.org/10.1016/S1474-4422(05)00990-7

[80] C. M. Stinear, P. A. Barber, P. R. Smale, J. P. Coxon, M. K. Fleming, W. D. Byblow, "Functional potential in chronic stroke patients depends on corticospinal tract integrity," Brain, vol. 130, no. 1, pp. 170-180, Jan. 2007, doi: https://doi.org/10.1093/brain/awl333

[81] G. Schlaug, S. Marchina, C. Y. Wan, "The Use of Non-invasive Brain Stimulation Techniques to Facilitate Recovery from Post-stroke Aphasia," Neuropsychol. Rev., vol. 21, no. 3, pp. 288-301, Sep. 2011, doi: https://doi.org/10.1007/s11065-011-9181-y

[82] G. Di Pino, G. Pellegrino, G. Assenza, F. Capone, et al., "Modulation of brain plasticity in stroke: a novel model for neurorehabilitation," Nat. Rev. Neurol., vol. 10, no. 10, pp. 597-608, Oct. 2014, doi: https://doi.org/10.1038/nrneurol.2014.162

[83] J. C. Magee, D. Johnston, "A Synaptically Controlled, Associative Signal for Hebbian Plasticity in Hippocampal Neurons," Science, vol. 275, no. 5297, pp. 209-213, Jan. 1997, doi: https://doi.org/10.1126/science.275.5297.209

[84] G.-Q. Bi, M.-M. Poo, "Synaptic Modifications in Cultured Hippocampal Neurons: Dependence on Spike Timing, Synaptic Strength, and Postsynaptic Cell Type," J. Neurosci., vol. 18, no. 24, pp. 10464-10472, Dec. 1998, doi: https://doi.org/10.1523/JNEUROSCI.18-24-10464.1998

[85] G. Q. Bi and M. M. Poo, "Synaptic Modification by Correlated Activity: Hebb's Postulate Revisited," Annu. Rev. Neurosci., vol. 24, pp. 139-166, 2001, doi: https://doi.org/10.1146/annurev.neuro.24.1.139

[86] V. Di Lazzaro, P. Profice, F. Capone, P. Pasqualetti, et al., "Motor Cortex Plasticity Predicts Recovery in Acute Stroke," Cereb. Cortex, vol. 20, no. 7, pp. 1523-1528, Jul. 2010, doi: https://doi.org/10.1093/cercor/bhp216

[87] N. J. J. Beauchamp, A. M. Ulug, T. J. Passe, P. C. van Zijl, "MR diffusion imaging in stroke: review and controversies," Radiographics, vol. 18, no. 5, pp. 1265-1269, Sep. 1998, doi: https://doi.org/10.1148/radiographics.18.5.9747619

[88] B. M. Young, J. M. Stamm, J. Song, A. B. Remsik, et al., "Brain-Computer Interface Training after Stroke Affects Patterns of Brain-Behavior Relationships in Corticospinal Motor Fibers," Front. Hum. Neurosci., vol. 10, art. no. 457, Sep. 2016, doi: https://doi.org/10.3389/fnhum.2016.00457

[89] A. Bhasin, P. Srivastava, S. S. Kumaran, "Correlation of DTI-Derived Measures to Therapy-Mediated Recovery after Stroke: Preliminary Findings," Neurol. India, vol. 69, no. 5, pp. 1210-1216, Oct. 2021 [Online]. Available: https://www.neurologyindia.com/text.asp?2021/69/5/1210/329584

[90] L. M. Moura, R. Luccas, J. P. Q. de Paiva, E. Amaro et al., "Diffusion Tensor Imaging Biomarkers to Predict Motor Outcomes in Stroke: A Narrative Review," Front. Neurol., vol. 10, art. no. 445, May 2019, doi: https://doi.org/10.3389/fneur.2019.00445

[91] M. Descoteaux, C. Poupon, "Diffusion-Weighted MRI", in Comprehensive Biomedical Physics, vol. 3, D. Belkić, K. Belkić, Eds., Oxford, United Kingdom: Elsevier, 2014, pp. 81-97.

[92] Y. Okamoto, D. Ishii, S. Yamamoto, M. Wakatabi, et al., "Relationship Between Motor Function, DTI, and Neurophysiological Parameters in Patients with Stroke in the Recovery Rehabilitation unit," J. Stroke Cerebrovasc. Dis., vol. 30, no. 8, art. no. 105889, Aug. 2021, doi: https://doi.org/10.1016/j.jstrokecerebrovasdis.2021.105889

[93] D. Le Bihan, J.-F. Mangin, C. Poupon, C. A. Clark, et al., "Diffusion tensor imaging: Concepts and applications," J. Magn. Reson. Imaging, vol. 13, no. 4, pp. 534-546, Apr. 2001, doi: https://doi.org/10.1002/jmri.1076

[94] B. J. Macintosh, S. J. Graham, "Magnetic resonance imaging to visualize stroke and characterize stroke recovery: a review," Front. Neurol., vol. 4, art. no. 60, May 2013, doi: https://doi.org/10.3389/fneur.2013.00060

[95] K. H. Maier-Hein, P. F. Neher, J.-C. Houde, M. A. Côté, et al., "The challenge of mapping the human connectome based on diffusion tractography," Nat. Commun., vol. 8, no. 1, art. no. 1349, Nov. 2017, doi: https://doi.org/10.1038/s41467-017-01285-x

[96] W. Van Hecke, L. Emsell, and S. Sunaert, Eds. Diffusion Tensor Imaging: A Practical Handbook. New York, U.S.: Springer New York, 2015, pp. 205.

[97] J.-D. Tournier, F. Calamante, A. Connelly, "MRtrix: Diffusion tractography in crossing fiber regions," Int. J. Imaging Syst. Technol., vol. 22, pp. 53-66, Feb. 2012, doi: https://doi.org/10.1002/ima.22005

[98] D. Wassermann, N. Makris, Y. Rathi, M. Shenton, R. Kikinis, M. Kubicki, C. F. Westin, "The white matter query language: a novel approach for describing human white matter anatomy," Brain Struct. Funct., vol. 221, no. 9, pp. 4705-4721, Jan. 2016, doi: https://doi.org/10.1007/s00429-015-1179-4

[99] J. M. Soares, P. Marques, V. Alves, N. Sousa, "A hitchhiker's guide to diffusion tensor imaging," Front. Neurosci., vol. 7, art. no. 31, Mar. 2013, doi: https://doi.org/10.3389/fnins.2013.00031

[100] S.-K. Song, S.-W. Sun, M. J. Ramsbottom, C. Chang, J. Russell, A. H. Cross, "Dysmyelination Revealed through MRI as Increased Radial (but Unchanged Axial) Diffusion of Water," Neuroimage, vol. 17, no. 3, pp. 1429-1436, Nov. 2002, doi: https://doi.org/10.1006/nimg.2002.1267

[101] C. A. M. Wheeler-Kingshott, M. Cercignani, "About "axial" and "radial" diffusivities," Magn. Reson. Med., vol. 61, no. 5, pp. 1255-1260, May 2009, doi: https://doi.org/10.1002/mrm.21965

[102] M. Jenkinson, C. F. Beckmann, T. E. J. Behrens, M. W. Woolrich, S. M. Smith, "FSL," Neuroimage, vol. 62, no. 2, pp. 782-790, Aug. 2012, doi: https://doi.org/10.1016/j.neuroimage.2011.09.015

[103] Analysis Group, FDT/UserGuide. (2022). Accessed: Jun. 10, 2023. [Online]. Available: https://fsl.fmrib.ox.ac.uk/fsl/fslwiki/FDT/UserGuide#DTIFIT

[104] T. Koyama, Y. Uchiyama, K. Domen, "Outcome in Stroke Patients Is Associated with Age and Fractional Anisotropy in the Cerebral Peduncles: A Multivariate Regression Study," Prog. Rehabil. Med., vol. 5, art. no. 20200006, 2020, doi: https://doi.org/10.2490/prm.20200006

[105] J. Chen, M. Liu, D. Sun, Y. Jin, T. Wang, C. Ren, "Effectiveness and neural mechanisms of home-based telerehabilitation in patients with stroke based on fMRI and DTI: A study protocol for a randomized controlled trial," Medicine, vol. 97, no. 3, art. no. e9605, Jan. 2018, doi: https://doi.org/10.1097/MD.0000000000009605

[106] S. Mori, K. Oishi, H. Jiang, L. Jiang, et al., "Stereotaxic white matter atlas based on diffusion tensor imaging in an ICBM template," Neuroimage, vol. 40, no. 2, pp. 570-582, Apr. 2008, doi: https://doi.org/10.1016/j.neuroimage.2007.12.035

[107] J. C. Eliassen, E. L. Boespflug, M. Lamy, J. Allendorfer, W.-J. Chu, J. P. Szaflarski, "Brain-Mapping Techniques for Evaluating Poststroke Recovery and Rehabilitation: A Review," Top. Stroke Rehabil., vol. 15, no. 5, pp. 427-450, 2008, doi: https://doi.org/10.1310/tsr1505-427

[108] R. G. González, "Clinical MRI of acute ischemic stroke," J. Magn. Reson. Imaging, vol. 36, no. 2, pp. 259-271, Aug. 2012, doi: https://doi.org/10.1002/jmri.23595

[109] J. M. Wardlaw, W. Brindle, A. M. Casado, K. Shuler, et al., "A systematic review of the utility of 1.5 versus 3 Tesla magnetic resonance brain imaging in clinical practice and research," Eur. Radiol., vol. 22, no. 11, pp. 2295-2303, Nov. 2012, doi: https://doi.org/10.1007/s00330-012-2500-8

[110] E. Seto, G. Sela, W. E. Mcllroy, S. E. Black, et al., "Quantifying Head Motion Associated with Motor Tasks Used in fMRI," Neuroimage, vol. 14, no. 2, pp. 284-297, Aug. 2001, doi: https://doi.org/10.1006/nimg.2001.0829

[111] M. Veldsman, T. Cumming, A. Brodtmann, "Beyond BOLD: Optimizing functional imaging in stroke populations," Hum. Brain Mapp., vol. 36, no. 4, pp. 1620-1636, Apr. 2015, doi: https://doi.org/10.1002/hbm.22711

[112] Q. Guo, G. Hall, M. Mckinnon, R. Goeree, E. Pullenayegum, "Setting sample size using cost efficiency in fMRI studies," Open Access Med. Stat., vol. 2, pp. 33-41, May 2012, doi: https://doi.org/10.2147/OAMS.S30830

REVIEW ARTICLE

VOL. 44 | NO. 2 | **MAY - AUGUST 2023** | PP 74-96

Revista Mexicana de Ingeniería Biomédica

dx.doi.org/10.17488/RMIB.44.2.6

E-LOCATION ID: 1359

Novel Studies in the Designs of Natural, Synthetic, and Compound Hydrogels with Biomedical Applications

Novedosos Estudios en el Diseño de Hidrogeles Naturales, Sintéticos y Compuestos con Aplicaciones Biomédicas

Claudia Gabriela Cuéllar Gaona[1], *María Cristina Ibarra Alonso*[1], *Rosa Idalia Narro Céspedes*[1]
María Maura Téllez Rosas[1], *Ricardo Reyna Martínez*[1], *Miriam Paulina Luévanos Escareño*[1]

[1]Universidad Autónoma de Coahuila, Coahuila - México

ABSTRACT

Hydrogels are gaining widespread popularity in the biomedical field due to their extraordinary properties, such as biocompatibility, biodegradability, zero toxicity, easy processing, and similarity to physiological tissue. They have applications in controlled drug release, wound dressing, tissue engineering, and regenerative medicine. Among these applications, hydrogels as a controlled drug delivery system stands out, which releases active substances in precise amounts and at specific times. To explore the latest advances in the design of hydrogels, a literature review of articles published in indexed scientific journals, in Scopus and Science Direct, was carried out. This review aimed to discover and describe the most innovative hydrogel research with applications in the biomedical field; hydrogels synthesized with polymers of different origins were selected, such as; i. Natural (dextran, agarose, chitosan, etc.); ii. Synthetic (polyacrylamide, polyethylene glycol, polyvinyl alcohol, etc.); iii. Composites (interpenetrants, hybrid crosslinkers, nanocomposites, etc.). Comparative analysis revealed that hydrogels with composite materials show the most promise. These composite hydrogels combine the advantages of different polymers or incorporate additional components, offering enhanced properties and functionalities. In summary, hydrogels are versatile biomaterials with immense potential in biomedicine. Their unique properties make them suitable for diverse applications. However, innovative designs and formulations must continue to be explored to further advance the capabilities of hydrogels and expand their biomedical applications.

KEYWORDS: drug delivery system, hydrogel, regenerative medicine, wound repair

RESUMEN

Los hidrogeles están ganando una extensa popularidad en el campo biomédico gracias a que presentan propiedades extraordinarias como biocompatibilidad, biodegradabilidad, nula toxicidad, fácil procesamiento, y similitud con el tejido fisiológico. tienen aplicaciones en la liberación controlada de fármacos, el vendaje de heridas, la ingeniería de tejidos y la medicina regenerativa. Entre estas aplicaciones, destaca el uso de hidrogeles como sistema de administración controlada de fármacos, que liberan sustancias activas en cantidades precisas y en momentos concretos. Para explorar los últimos avances en el diseño de hidrogeles, se realizó una revisión bibliográfica de artículos publicados en revistas científicas indexadas, en Scopus y Science Direct. El objetivo de esta revisión fue descubrir y describir las investigaciones de hidrogeles más innovadoras con aplicaciones en el campo biomédico, se seleccionaron hidrogeles sintetizados con polímeros de diferente índole como; i. Naturales (dextrano, agarosa, quitosano, etc.); ii. Sintéticos (poliacrilamida, polietilenglicol, alcohol polivinílico, etc); iii. Compuestos (interpenetrantes, reticulantes híbridos, nanocompuestos, etc.). El análisis comparativo reveló que los hidrogeles que utilizan materiales compuestos son los más prometedores. Estos hidrogeles compuestos combinan las ventajas de distintos polímeros o incorporan componentes adicionales, ofreciendo propiedades y funcionalidades mejoradas. En resumen, los hidrogeles son biomateriales versátiles con un inmenso potencial en biomedicina. Sus propiedades únicas los hacen adecuados para diversas aplicaciones, sin embargo, se debe seguir explorando diseños y formulaciones innovadores para seguir avanzando en las capacidades de los hidrogeles y ampliar sus aplicaciones biomédicas.

PALABRAS CLAVE: hidrogel, medicina regenerativa, sistema de liberación de fármacos, reparación de heridas

Corresponding author

TO: **Rosa Idalia Narro Céspedes**
INSTITUTION: **Universidad Autónoma de Coahuila**
ADDRESS: **Blvd. Venustiano Carranza S/N, Col.República Oriente, C.P. 25280 Saltillo, Coahuila - México**
EMAIL: **rinarro@uadec.edu.mx**

Received:

3 June 2023

Accepted:

12 July 2023

INTRODUCTION

Hydrogels are soft polymeric materials formed by three-dimensional networks that have a high content of water or biological fluid while maintaining their structure without dissolution [1][2], in addition to being biodegradable, biocompatible, and flexible thanks to the water content that makes them very similar to natural tissue [3][4][5][6][7]. They can have a variety of applications in different areas, such as agriculture, biomedicine, or food. However, one of the most researched approaches in recent years is the use of hydrogels in biomedicine, as they provide a versatile platform for the supply of drugs, wound dressings, engineering tissue, and regenerative medicine, such as being applied in cartilage regeneration and as scaffolds for cell proliferation and growth [8].

In recent years, a significant focus has been put on the development of controlled-release drug delivery systems, since in conventional delivery systems, the dose of the drug increases dramatically in the blood and then decreases, causing organ toxicity and body tissues before the drug, reaches the target site [9]. The controlled drug delivery system must provide the correct amount of the active substance to the desired site within a specified period [10]. There has been a significant boom in the application of hydrogels as drug delivery vehicles since their three-dimensional network allows them to retain liquids, which helps them to encapsulate hydrophilic drugs and release them in a controlled way. The basic growth factor of fibroblasts is widely used (bFGF) since it is a hydrophilic drug that can be incorporated into hydrogels to repair damaged tissue since it has the property of attracting cells and fibroblasts to the site of injury; it also helps in angiogenesis and metabolism [11].

Different presentations of dressings are used for wound healing, including gauze, gels, hydrogels, foams, hydrocolloids, etc. Within these presentations, hydrogels are the most promising for wound treatment since they can retain large amounts of liquid inside, providing a moist wound environment, removing exudates, preventing infection, and providing a suitable environment for wound healing tissue regeneration [11] [12].

This review explores and describes the most innovative research on the use of hydrogels in the biomedical field, mainly for controlled-release drug applications, wound dressings, and tissue engineering, opening an overview of new composite hydrogels, which improve the properties of conventional hydrogels designed from natural or synthetic polymers. It also aims to open the reader's view toward designing new smart hydrogels with more unique properties that aid in rapid and effective patient recovery.

MATERIALS AND METHODS

A review of the literature of articles related to the design of hydrogels was carried out. Investigations were chosen in which hydrogels were made from natural, synthetic, or composites. These articles selected for this review were published in scientific journals indexed in Scopus and Science Direct. No limit was selected for the publication date. However, articles published in the last 5 years mainly provide information on the most recent advances in this field.

The following parameter was determined for selecting the articles: obtaining hydrogels based on natural, synthetic, or composite sources with promising results to be used exclusively in medical applications.

RESULTS AND DISCUSSIONS

Hydrogel structure and crosslinkin strategies

The mesh size and molecular weight of the crosslinked polymer chain are essential properties of the hydrogel at the molecular level [11]. The final application of the hydrogel generally determines the strategy for

selecting crosslinking. They can be prepared by physical or chemical crosslinking, and the first ones are formed by ionic bonds, hydrogen bonds, or Van der Waals forces [13], which makes hydrogels dynamic, while in chemical crosslinking, hydrogels are formed by covalent bonds, which gives them better stability [14] [15]. Different molecules have been used to crosslink such networks as dialdehydes, diisocyanate, and diacrylate, among others [4]. Among the most widely used crosslinking agents are glutaraldehyde, poly(itaconic acid) and genipin [16]. Genipin is 5,000 to 10,000 times less toxic than glutaraldehyde, although its price is high [4]. Another way to crosslink relatively stable hydrogels is by enzymatic crosslinking. The most important advantages of this type of crosslinking are that hydrogels have a greater cytocompatibility than chemical crosslinking, the possibility of kinetic manipulation of gel formation by controlling the concentration of enzymes, and the gel time is fast, and strong covalent bonds are formed. Transglutaminase and horseradish peroxidase are the enzymes most used for manufacturing and crosslinking hydrogels [17].

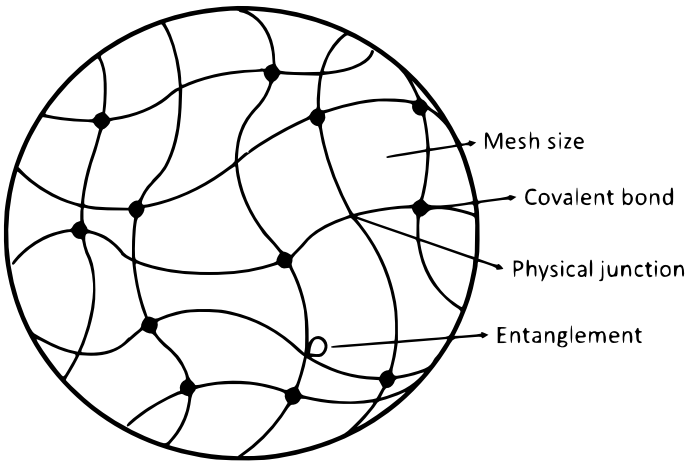

FIGURE 1. **Hydrogel structure at the molecular level. Adapted from [11].**

The degree and speed of swelling in the hydrogel depend on the crosslinking density and the concentration of the polymer. The swelling of the hydrogel has three stages: 1) Water joins the hydrophilic group, 2) the interaction of water with hydrophobic groups, and 3) free water in equilibrium, water fills the spaces gaps [11]. Denser crosslinked materials swell less compared to more freely crosslinked hydrogels. Another property determined during the crosslinking stage is porosity which determines the ability to adequately exchange nutrients and debris for the encapsulated cells [12]. Figure 1 shows the hydrogel structure at the molecular level presenting the mess size and the two main types of crosslinking: covalent bonds (chemical crosslinking) and non-covalent bonds (physical crosslinking).

Classification of hydrogels according to the type of material

Hydrogels can be classified as natural, synthetic, and composite, depending on the type of material with which they are formed [18]. Hydrogels based on natural polymers have physicochemical and biological characteristics that make them interesting for biomedical applications, such as biocompatible, biodegradable, non-toxic, and promoting cell adhesion [4][5]. Among these applications are used as controlled release drug delivery systems (hydrogels sensitive to stimuli such as pH changes; in response, the hydrogel swelling percentages vary, causing the release of drug molecules), wound dressings (used due to their ability to absorb wound exudate while allowing oxygen to pass to the wound site) [19][20]. Natural biopolymers are generally polysaccharides and proteins such as -dextran, hyaluronic acid, alginate, agarose, pectin, cellulose, carrageenan, or chitosan. On the other hand, synthetic polymers include polyethylene glycol (PEG) and polyacrylamide [12]. These polymers are promising candidates for preparing hydrogels because they form hydrophilic gels that retain water or biological fluids without collapsing their structure and are biocompatible and biodegradable [5][9][14]. In addition, hydrogels can improve their mechanical and adhesive properties through crosslinking concentration and additives, improving or optimizing their functionality for various applications. [13][21]. Composite hydrogels are a combination of a natural polymer with a synthetic one that

gives the hydrogel both mechanical and biological properties [11] since the use of synthetic materials gives it better mechanical resistance properties while using of biological materials gives the compound hydrogel biological properties that allow it to be self-healing [12]. Table 1 presents the classification of hydrogels according to the type of material with which they have been synthesized, the materials most used to synthesize hydrogels, and their applications in biomedicine and properties.

TABLE 1. Classification of hydrogels with their applications and properties.

Hydrogel	Material and Application	Properties
Natural	**Dextran:** Tissue engineering, drug administration	Biocompatible, biodegradable, non-toxic
	Hyaluronic acid: Tissue engineering, drug administration	Biocompatible, biodegradable, non-immunogenic, high viscoelasticity
	Alginate: Wound healing, drug administration	Biocompatible, biodegradable, non-immunogenic, crosslinking with divalent cations
	Gelatin: Bone regeneration., wound management	Biocompatible, biodegradable, non-toxic, good adhesiveness
	Agarose: Cell growth and adhesion, drug administration	Biocompatible, biodegradable, self-gelling
	Chitosan: Tissue engineering, drug administration, wound dressing	Biocompatible, biodegradable, non-toxic, non-allergic, bioavailable
	Xylene: Skincare, drug administration, bone regeneration	Biocompatible, biodegradable, non-toxic, anti-inflammatory, antioxidant, and anticancer effects
	Silk fibroin: Wound healing	Biocompatible, biodegradable, good mechanical properties, hardness, and stability
Synthetics	**Polyacrylamide:** Cartilage regeneration, tissue engineering	Controllable hardness, a high degree of swelling
	Poly (N-isopropyl acrylamide): Drug administration, medical diagnosis	Temperature-induced sol-gel transition ability
	Polyethylene glycol: Drug administration, tissue engineering	Good mechanical properties
	Poly (methyl methacrylate-co-methacrylic acid): Cartilage regeneration, tissue engineering	Biocompatible, hydrophilic
	Pluronic diacrylate: Cell growth and proliferation	Biocompatible, hydrophilic, self-gelling
	Polyvinyl alcohol: Wound healing, regenerative medicine	Controllable hardness, a high degree of swelling
Composites	**Interpenetrating polymer networks:** Wound healing	Biocompatible, good mechanical properties
	Crosslinking hybrids: Wound healing	7 Biocompatible, good mechanical properties
	Nanocomposites: Wound healing, cell growth, and proliferation	Biocompatible, good mechanical properties

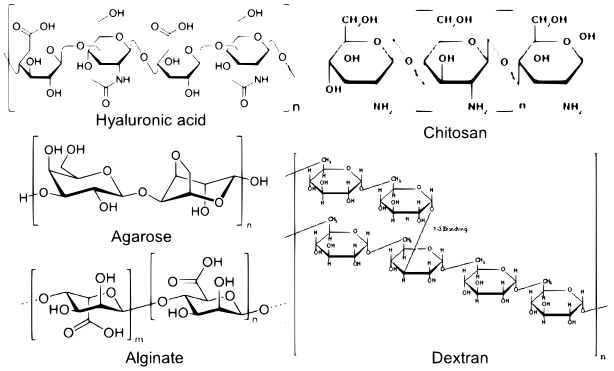

FIGURE 2. Structure of the natural hydrogels used for the biomedical area.

Natural hydrogels

Natural hydrogels are made from natural polymers

(alginate, chitosan, hyaluronic acid) or proteins (gelatin, silk fibroin) [22]. They have zero toxicity, biodegradability, and biocompatibility [23], making them promising candidates for biomedical applications such as tissue engineering, drug administration, etc. The most significant limitation of natural hydrogels is their poor stability, so their use decreases in applications where high-resistance hydrogels are required [24]. Figure 2 shows the structures of the most applied natural hydrogels in biomedicine. Table 2 shows the advantages and disadvantages of natural hydrogels.

TABLE 2. Advantages and disadvantages of natural hydrogels used in the biomedical area.

Hydrogel material	Advantages	Disadvantages
Dextran	Biocompatible, biodegradable, non-toxic	Low biological activity
Hyaluronic acid	Biocompatible, biodegradable, non-immunogenic, high viscoelasticity	Low mechanical properties
Alginate	Biocompatible, biodegradable, non-immunogenic, crosslinking with divalent cations	Low tensile strength, limited mechanical properties
Gelatin	Biocompatible, biodegradable, non-toxic, good adhesiveness	Requires chemical agents as crosslinking agents to stabilize
Agarose	Biocompatible, biodegradable, self-gelling	Not present bioactivity for cell proliferation
Chitosan	Biocompatible, biodegradable, non-toxic, non-allergic, bioavailable	Low mechanical properties
Xylene	Biocompatible, biodegradable, non-toxic, anti-inflammatory, antioxidant, and anticancer effects	Low mechanical properties
Silk fibroin	Biocompatible, biodegradable, good mechanical properties, hardness, and stability	From wake and brittle biomaterials

Dextran hydrogels

Dextran is a carbohydrate biopolymer, which breaks down in specific physical environments without any effect on cell viability [25], is produced by bacterial species from sucrose or by chemical synthesis, is non-toxic, it is also biocompatible and biodegradable [5][26], it promotes wound healing due to the existence of specific glucan receptors in human fibroblasts where glucan stimulates the expression of fibroblasts that help cell proliferation [27], the disadvantage of dextran is that they have relatively low biological activity, but it can be improved with the incorporation of another polymer capable of improving said activity [28]. Also, they have low load capacity and ease of deformation, which restricts their use for hard-tissue engineering applications [25]. However, the hydroxyl groups that dextran presents can be oxidized, alkylated, and esterified to obtain various derivatives, which are expected to be beneficial in the design of new polymeric materials in which various properties can be controlled, for example, the degradation rate [29][30]. Solomevich *et al.*, 2019, designed a hydrogel based on a dextran phosphate derivative with the final drug release application for local tumor chemotherapy. Dextran phosphate hydrogels were loaded with prospidine. Hydrogels are sensitive to pH thanks to phosphate groups; in a low-pH environment, the swelling was significantly less than in a neutral environment. Tests for drug release showed that prospidine was released depending on the pH of the external media, and the loaded hydrogels were able to inhibit the proliferation of cancer cells depending on the dose delivered. Hence, the application of the hydrogel was successful with an effective antitumor [29].

On the other hand, Ghaffari *et al.* 2020, synthesized dextran hydrogels with the incorporation of nanoparticles of β-nanocrystalline tricalcium phosphate (β-TCP) as scaffolds for bone tissue engineering and reported that the effect of β-TCP improved the activity exhibiting an increased ability to interact with body fluids and specifically produced active sites for cell anchoring and mineral precipitation in vitro [28]. Dong-Soo *et al.* 2022,

prepared a hydrogel matrix by introducing a functional group capable of forming crosslinks between natural polymers to create a basis for preparing a favorable microenvironment for cell adaptation in biotissues. The modified dextran hydrogel polymer was designed to mimic the extracellular matrix conditions as a scaffold. The results showed that the functional groups of the polymers helped with self-assembly due to intermolecular interactions. The dextran residues in the molecular structure of the hydrogel helped to keep the scaffold self-assembled by undergoing interactions due to Van der Waals forces, electrostatic forces, and the ability to form intramolecular hydrogen bonds [31]. Jintao *et al.* 2023, designed injectable hydrogels modified with dextran and gallic acid to accelerate wound healing by scavenging reactive oxygen species (ROS) in burn and combined radiation injuries. These composites showed good self-healing ability, excellent injectability, strong antioxidant activity, and favorable biocompatibility. In addition, they exhibited excellent antibacterial properties, which facilitated wound healing [32].

Hyaluronic Acid Hydrogels

Hyaluronic acid is a natural unbranched polysaccharide part of the extracellular matrix of human tissue. It is highly hydrated and negatively charged, consisting of glucuronic acid and N-acetylglucosamine; it is biocompatible, biodegradable, non-immunogenic, high viscoelastic, and high-water holding capacity [17] [33][34]. It is currently used for wound healing, cell augmentation and proliferation, angiogenesis, and drug delivery [22]. Menezes *et al.* 2020, manufactured a collagen-based hydrogel (extracted from the skin of Nile tilapia fish) / hyaluronic acid with 1-ethyl-3- (3-dimethyl aminopropyl) carbodiimide(EDC) and NHS as crosslinking agents, the hydrogel presented a robust reticulated network with high potential for its use in tissue engineering [33]. Luo *et al.* 2020, synthesized a hyaluronic acid hydrogel loaded with 5-fluorouracil, cisplatin, and paclitaxel to function as a multi-drug delivery system. *In vivo* studies in mice presenting with colorectal peritoneal carcinomatosis showed that the hydrogel decreased the formation of ascites, inhibited tumor growth and metastasis in the liver and lungs, and also prolonged the survival time of the mice; therefore, the hyaluronic acid hydrogel is a promising tool in the treatment of colorectal peritoneal carcinomatosis [35]. In 2023, Weinqian *et al.* synthesized in situ an injectable hydrogel with good swelling resistance using hyaluronic acid and aldehyde β-cyclodextrin (ACD) via Schiff base reaction for long-term controlled drug release. They concluded that hyaluronic acid-based injectable hydrogel prepared by Schiff base reaction provides a new option for long-term controlled drug release in the course of disease treatment from a material perspective [36]. Nam-Gyun *et al.* 2023, fabricated a hydrogel with fast self-healing properties and high antibacterial activity by testing various proportions of hyaluronic acid and pectin mixture using Fe^{3+} as a crosslinker. The proposed hydrogel demonstrated antibacterial activity against *Staphylococcus aureus* and *Pseudomonas aeruginosa* due to the release of Fe^{3+} during the hydrogel degradation process without being toxic to human dermal fibroblast cells. These results suggest that the proposed hyaluronic acid/PT hydrogel holds great promise for tissue regeneration [37].

Alginate hydrogels

Alginate is a natural linear and anionic glycan [38] [39], it is extracted from brown algae, but it is also produced by *Azotobacter* and *Pseudomonas* bacteria [22]; it can absorb wound exudate, so it has been widely used as a wound dressing, as well as providing protection to the wound against bacterial load, providing a humid environment and helping the formation of granulation tissue causing faster wound closure. It is also biocompatible, biodegradable, non-immunogenic, and has controlled release properties [40][41]. It can crosslink with divalent cations such as Calcium (Ca^{2+}) [38] or Magnesium (Mg^{2+}) [37]. Despite their efficient application in wound healing, they have the disadvantage of having low tensile strength and limited mechanical properties [40]. Zhang *et al.* 2019, manufactured a hydrogel for the

controlled release of dexamethasone sodium phosphate (Dexp). The hydrogel was formed based on alginate with the crosslinking of Ca^{2+}. The *in vivo* pharmacological analysis indicated that the hydrogel significantly improved the bioavailability of the drug since the hybrid hydrogel had a slower drug release rate than the hydrogel without alginate [42]. In another study, Abbasi *et al.* 2020, also synthesized a hydrogel with a final application of wound dressing, using a combination of a thermosensitive polymer (formulated for accelerated wound healing), sodium alginate, which due to its properties, is being widely used in wound healing, and polyvinyl alcohol (PVA) as a crosslinker. The crosslinking of the chosen materials showed the hydrogel's good tensile strength, mechanical properties, and pharmaceutical viability and efficacy in wound healing [40]. Sun *et al.* 2020, made a sulfanilamide-loaded alginate hydrogel using a combination of Ca^{2+} ions and crosslinked with glutaraldehyde that helped it to have an improved mechanical resistance, which had the adjustable fluid absorption capacity and controlled release of the drug, improved cell adhesion and proliferation without cytotoxicity, making it promise to be used as a wound dressing [43]. In another study, Yang *et al.* 2023, fabricated an alginate hydrogel loaded with chitosan nanoparticles and Fumaria officinalis extract, which was evaluated for its wound healing capacity compared to a commercial product with that function. The hydrogel was tested on diabetic rats' wounds, obtaining a promising dressing, and carrying out the healing process with comparable results to the commercial product tested [44].

Gelatin hydrogels

Gelatin is a biocompatible and biodegradable polymer derived through the physical or chemical partial hydrolysis of native collagen in bone, tendon, and skin. It has attractive characteristics such as low cost, colorless and non-toxic adhesiveness [45][46]. Generally speaking, there are two types of gelatin, Type A, processed by acid collagen treatment, and Type B, obtained by alkaline hydrolysis [17]. The aqueous gelatin solution spontaneously forms a hydrogel when it is cooled by the molecules that form a triple helix, but at physiological temperature, it returns to the liquid state, so chemical agents such as crosslinking agents are required to stabilize the hydrogel [47]. Anamizu and Tabata 2019, designed an injectable hydrogel based on the physicochemical interaction between gelatin/alginate/ Fe^{3+} to evaluate cells encapsulated in hydrogels and evaluated whether the cells were able to survive, proliferate and carry out osteogenic differentiation. The cells were encapsulated by the hydrogel and injected into the posterior subcutis of mice. The percentage of cells retained at the injected site was higher than those injected in a phosphate buffer suspension, so the cells were successfully transplanted with the hydrogel for bone regeneration [48]. Takei *et al.* 2020, manufactured a hydrophobically modified gelatin hydrogel to form a physical crosslink that would stabilize the hydrogel and limit chemical agents' use as crosslinking agents. The researchers loaded the hydrogel with two drugs, one with basic fibroblast growth factor (bFGF) (hydrophilic drug) and the other with fluorescein sodium (hydrophobic drug). *In vivo* tests showed that bFGF is released gradually as the hydrogel breaks down, aiding therapeutic angiogenesis. The same result occurred with fluorescein sodium, which proposes the hydrogel as a drug delivery system that can release both hydrophilic and hydrophobic drugs controllably [47]. Gonzalez-Ulloa *et al.* developed and characterized polymeric hydrogels based on gelatin and collagen. Different studies were performed to evaluate their mechanical, thermal, and microstructural properties and biocompatibility. The results showed that hydrogels formed from the mixture of collagen and gelatin retain, to a large extent, the good viscoelastic properties of collagen while showing low levels of cytotoxicity and hemocompatibility. However, due to the nature of the materials used, the thermal characteristics are not ideal for use in biomedicine, so further studies are required to overcome these drawbacks [49].

Agarose hydrogels

Agarose is a carbohydrate with self-gelling properties

and is converted into a gel without the need for chemical crosslinking agents [50][51]; it is composed of 1-4-anhydrous-α derivatives -1-galactose linked to 1,4 and derivatives of β-D-galactose linked to 1,3, which is extracted from seaweed [52]. It is soluble in water at temperatures above 65 °C, and depending on the molecular weight and functional groups, it gels between 17 °C and 40 °C. Once the agarose gel is stable, it cannot swell or liquefy until heated to 65 °C. [53]. Agarose produces mechanically robust networks with long-term stability and is widely used in hydrogels as a rigid component to improve the mechanical properties of hydrogels. Agarose chains can generate porous scaffolds that allow cell mobility and transport oxygen and nutrients to cells embedded in the hydrogel matrix. However, agarose hydrogels have the disadvantage of not having bioactivity to promote binding and cell proliferation [54]. Topuz *et al.* 2018, developed agarose hydrogels incorporating 2D anisotropic nano silicates (Laponite), which enhanced the bioactivity of the hydrogel by aiding cell growth and proliferation, finding that nano silicates do not affect the structure of the hydrogel but revealed greater incorporation of fibroblasts, which is never seen in pure agarose hydrogels [54]. In another investigation, Yuan *et al.* 2018, also made agarose hydrogels, incorporating Konjac glucomannan (KGM) to improve the properties of the agarose hydrogel, the hydrogel was loaded with the drug ciprofloxacin, and its release behavior was evaluated. KGM was able to significantly reduce the hardness and stiffness of hydrogels. It also improved agarose hydrogels' encapsulation, drug loading efficiency, and sustained release ability [52]. Qi *et al.*, 2019, successfully built an agarose-based hydrogel and introduced salt to the hydrogel matrix. Only these natural biopolymers were used without the help of chemical crosslinkers or monomers. The hydrogel resulted in good biocompatibility, serving as a cellular framework because it supports cell adhesion and growth [55]. Patiño-Vargas *et al.* 2022, synthesized a human agarose/plasma hydrogel as a wound-healing dressing. In this work, they varied the concentrations of agarose in hydrogels: 0 %, 0.5 %, 1 %, 1.5 %, and 2 % (w / v), to evaluate the activity of fibroblasts present in the hydrogel, obtaining that fibroblasts propagate faster at low concentrations of agarose present in the hydrogel [56].

Chitosan hydrogels

Chitosan, a partially deacetylated chitin product, is a natural polyamine saccharide made up of two common sugars, glucosamine, and N-acetylglucosamine, that has attracted attention because it is non-toxic, odorless, non-allergenic, biocompatible, biodegradable and bioavailable [4][6][9][57][58][59][60][61][62]. These characteristics make chitosan be used as a vehicle for drug delivery, in tissue engineering, and as a dressing in wound healing due to its anticancer, antimicrobial, and antioxidant properties [60][63][64]. Low molecular weight chitosan can protect RNA from degradation by inhibiting the RNAse. Chitosan has a primary amino group and needs to be dissolved in an acidic medium to protonate its amino group and have a positive charge [18]. Songkroh *et al.* 2015, manufactured a hydrogel with a new surgical approach as a sealant for treating biological reduction in lung volume. This chitosan-based hydrogel was crosslinked with genipin and loaded with sodium orthophosphate hydrate ($Na_3PO_4 \cdot 12H_2O$); the hydrogel was evaluated in Chinese dogs, presented good mechanical resistance, and proved to be promising as a lung sealant [65]. For their part, Dehghan-Banani *et al.* 2020, formed a modified chitosan hydrogel using N-(β-maleimidopropyloxy) succinimide ester (BMPS), incorporating ketogenic (KGN) to promote the chondrogenesis of stem cells in the hydrogel, suggesting a solution for the regeneration of cartilage defects in the form of an injectable platform [66]. In another investigation, Thongchai *et al.* 2020, obtained a hydrogel based on chitosan and collagen using tetraethyl orthosilicate as a crosslinking agent; the purpose of the hydrogel was to be loaded with caffeic acid as a controlled drug delivery system, which was satisfactory since caffeic acid decreased the degradation behavior of the hydrogel, gradually releasing over 8 hours. The antioxidant properties of the hydrogel demonstrated potential utility

for cosmetic and pharmaceutical research [67]. Wang *et al.* 2023 prepared an injectable chitosan hydrogel with catechol and 4-glutenolic acid to prevent swelling and promote wound healing. The hydrogel showed antimicrobial efficacy against *Escherichia coli* and *Staphylococcus aureus*. In vitro evaluation showed that the hydrogels contributed to coagulation by absorbing red blood cells and platelets. In vivo, evaluation in mice showed that they stimulated fibroblast migration and epithelialization, which may be a promising option for wound healing treatment [68].

Xylene hydrogels

Xylene is one of nature's most abundant hemicellulosic polysaccharides, a predominant by-product of chemical and mechanical pulps [45]. Xylene hydrogels have biodegradability and non-toxicity properties. They have anti-inflammatory effects, immune functionality, antioxidant, and anticancer. They are used as carriers of biological and pharmacological macromolecules [2]. Gami *et al.* 2020, prepared xylene and β-cyclodextrin based hydrogels using ethylene glycol diglycidyl ether (EDGE) as crosslinking chemical; the hydrogels were loaded with curcumin and 5-fluorouracil to analyze their release kinetics, having promising applications as a drug delivery system [2]. Fu *et al.* 2020, made a hydrogel mainly of dialdehyde xylene (DAX) and gelatin; DAX was produced by direct oxidation of the xylene obtained from a viscous fiber mill and was used as a crosslinker to allow the formation of a network of 3D gel, glycerol, and nicotinamide were introduced to adjust the texture and function of the hydrogel. The hydrogel was a promising skincare application and a strategy for manufacturing crosslinked hydrogels from biomass [45]. Gutiérrez-Hernández *et al.* 2023, evaluated a xylene hydrogel mixed with functionalized multi-walled carbon nanotubes (MWCNTs) with biomedical applications as a scaffold for *in vitro* culture of osteoblastic cells. The results show that the developed hydrogels have a high potential to be bionanomaterials for bone regeneration due to increased cell viability, proliferation, and adhesion [69].

Silk fibroin hydrogels

Some lepidopteran larvae manufacture silk. Silk is made of two proteins: fibroin is the central protein covered by sericin, similar to glue. Silk fibroin is a natural copolymer formed by hydrophobic and hydrophilic segments that provide it with hardness and stability; it is also biocompatible, biodegradable, with good mechanical properties, relatively low molecular weight, and acceptable immunogenicity, which makes it attractive in tissue engineering [17][70]. It is also widely used in preparing controlled-release drug delivery systems, biosensors, and wound repair [71]. Despite having good mechanical properties, most biomaterials made from silk fibroin are usually weak and brittle [71]. Li *et al.* 2020, manufactured a hydrogel based on silk fibroin from cocoons of *Bombyx mori* to evaluate the therapeutic effects of the hydrogel on hypertrophic scars on the ears of white rabbits from New Zealand; the results obtained showed that the hydrogel had favorable biocompatibility, and hypertrophic scars showed a decrease in scar color in addition to a reduction in thickness [72]. For their part, Wang *et al.* 2023, developed a silk fibroin-based hydrogel for use in the controlled release of miR-29a nanoparticles, aiding peripheral nerve regeneration. The results indicated that the silk fibroin hydrogels promoted myelination and neuronal differentiation of PC12 cells. This indicates a potential application as a nerve guidance conduit in peripheral nerve repair [73].

Synthetic hydrogels

Synthetic hydrogels are formed from synthetic polymers such as polyacrylamide, polyethylene glycol, and polyvinyl alcohol, among others. They are candidates in various implantable devices, including controlled-release drug depots and tissue engineering [74]. They exhibit good mechanical strength; however, the human body recognizes synthetic materials as foreign materials, provoking an immune response. Its properties can be improved by redesigning the hydrogel, as with controlled degradation or alterations in crosslinking density [75]. There are several methods to produce synthetic

hydrogels, such as photopolymerization or crosslinking by chemical agents; these two methods are the most used to synthesize hydrogels with biomedical applications [74]. Figure 3 shows the structures of the most applied synthetic hydrogels in biomedicine. Table 3 shows the advantages and disadvantages of synthetic hydrogels.

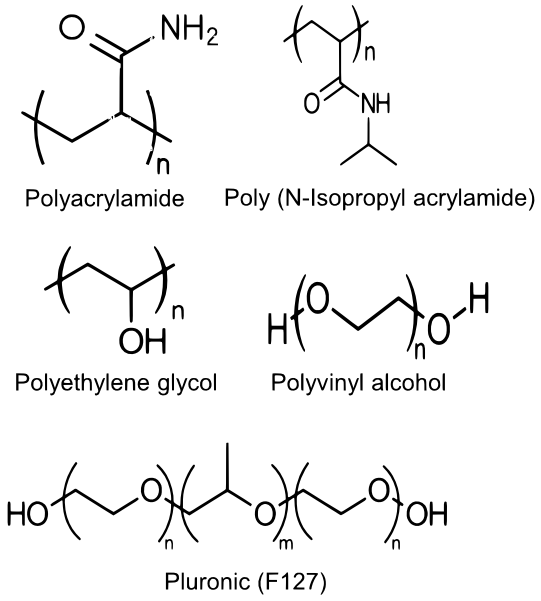

FIGURE 3. Structure of the synthetic hydrogels used for the biomedical area.

TABLE 3. Advantages and disadvantages of synthetic hydrogels used in the biomedical area.

Hydrogel material	Advantages	Disadvantages
Poly acrylamide	Controllable hardness, a high degree of swelling	Brittleness, low biodegradability
Poly (N-isopropyl acrylamide)	Temperature-induced sol-gel transition ability	Low biological activity
Pluronic (F127)	Good mechanical properties	Low biological activity
Polyethylene glycol	Biocompatible, hydrophilic	Limited metabolism in the human body
Polyvinyl alcohol	Biocompatible, hydrophilic, self-gelling	Minimal cellular and protein adhesion

Polyacrylamide hydrogels

Polyacrylamide is a polymer that can be synthesized from the acrylamide monomer in an aqueous solution with the addition of N, N' methylene bisacrylamide (crosslinking agent), ammonium persulfate (photothermal initiator), N, N, N ', N' - tetramethylene diamine (crosslinking accelerator) [52]. It has been extensively studied for its compatible applications as a hydrogel [76] [77][78]. It is a type of hydrogel with easily controllable hardness; polyacrylamide allows the hydrogel to form quickly and has a high degree of swelling; the disadvantages are brittleness and low biodegradability [79]. Depending on the application of the hydrogel, the properties can be adjusted by altering the synthesis conditions, polymerizing it with other monomers, or chemically modifying the hydrogel [22]. McClure and Wang 2017 evaluated a 4 % polyacrylamide hydrogel to investigate its effect on horses with natural osteoarthritis. 28 horses with the disease were evaluated, obtaining that 23 horses reduced the problem and could walk better on day 45 of the evaluation. The mechanism of action that causes improvement when walking is unknown, but it is attributed to the fact that the viscosity of the hydrogel polyacrylamide is similar to that of normal synovial fluid at 37 °C. Polyacrylamide can protect the cartilage surface in horses with osteoarthritis, allowing quality fibrocartilaginous healing [80]. Chen *et al.* 2023, prepared a hydrogel with a double polyacrylamide network, to which they introduced carboxymethyl chitosan, exhibiting excellent mechanical properties and stability. The carboxymethyl chitosan provided the hydrogel with antibacterial and biocompatible properties, resulting in a hydrogel with promising applications as an implantable biosensor [81].

Poly (N-isopropyl acrylamide) hydrogels

It is the most studied synthetic polymer with a polar peptide group in the side chain. This polymer forms a thermo-reversible/thermo-responsive hydrogel. This property allows the hydrogel to act according to the temperature at which it is found; at low temperatures, it is in a liquid state and gradually transforms into a

semi-solid gel as the temperature increases [82]. This phenomenon occurs when the aqueous solution of poly (N-isopropyl acrylamide) (PNIPAM) below 30-32 °C remains hydrated, but phase separation occurs when heated above 32 °C, forming a two-phase system. The polymer will precipitate out of a clear solution. The polymer-rich phase is insoluble in water. This temperature-induced sol-gel transition is a reversible process [52][83]. This property makes it suitable for drug delivery; applying a PNIPAM-based gel on the skin can increase drug retention in the epidermis and reduce drug penetration into the skin [84]. Shivshetty *et al.* 2022, developed a poly(N -isopropyl acrylamide) hydrogel used for etiologic diagnosis of corneal infection of bacteria and fungi without using a microbiology laboratory. This research was carried out on ex vivo rabbit eyes infected with the microorganisms *Staphylococcus aureus, Pseudomonas aeruginosa,* and *Candida albicans*. They found with this work a hydrogel easy to use and with potential in the diagnosis of infected eyes since the hydrogel was able to collect the three microorganisms only 30 minutes after being in place. These results were confirmed by conventional microbiology techniques and fluorescence signals [85]. Damonte *et al.* in 2023 developed a work whose objective was to improve the properties of poly(N-isopropyl acrylamide) (PNIPAAm)-based hydrogels in terms of mechanical characteristics and functionality by combining the polymer with a star-shaped tetra functional polycaprolactone (PCL), which was synthesized ad-hoc and introduced into the reaction mixture. This work developed novel PNIPAAm-based hydrogels with high mechanical strength, the ability to interact with positively charged molecules with tunable kinetic release and swelling ratio, biocompatibility, and thermo-reactivity [86].

Polyethylene glycol hydrogels

It is one of the best synthetic polymers widely used in biomedicine. It is highly hydrophilic and has excellent biocompatibility; the kidney and liver are metabolized in the human body and remove the complete polymer chains according to their molecular weight. The kidney eliminates it if its weight is <30 kDa and the liver if its weight is > 30 kDa. Only polyethylene glycol with a molecular weight <50 kDa is considered for use in biomedicine to ensure its complete elimination from the human body [52]. Janse van Rensburg *et al.* 2017, synthesized a polyethylene glycol (PEG) hydrogel that contained heparin (Hep) and heparan sulfate (HS) and loaded with growth factors to be administered in a controlled way and thus can improve angiogenesis in applications of tissue regeneration. These hydrogels were able to release heparin and growth factors on a sustained basis to increase the vascularization of scaffolds *in vivo*. These hydrogels are potentially valuable for tissue engineering or regenerative medicine applications where the hydrogel is required to be anti-thrombogenic [87]. In another study, Navaratman *et al.* 2020, evaluated a PEG hydrogel in patients undergoing proton beam radiotherapy to treat prostate cancer. Seventy-two patients with the disease were evaluated, of whom 51 patients had the hydrogel placed before radiation; after introducing the hydrogel, the prostate-rectum separation was measured and correlated with the rectal radiation dose and toxicity rectal. The result showed a 42.2 % decrease in the rectal radiation dose in patients with the hydrogel due to the degree of sagittal separation from the midline created by the PEG hydrogel [88]. In 2023, Fan *et al.* fabricated PEG-based synthetic hydrogels with placenta powder for application in tissue engineering. PEG hydrogels with placenta powder and pristine hydrogels were evaluated. All hydrogels showed *in vitro* viability greater than 91%. The hydrogels with placenta powder showed bioactivity, as cell adhesion and proliferation were propagated, while the pristine hydrogels remained bioinert. The bioactivity property makes the hydrogels promising for applications in tissue regeneration [89].

Poly (methylmethacrylate-co-methacrylic acid) hydrogels

It is a polymer of hydrophobic nature, used in drug delivery and tissue engineering; however, one of its main applications is as a biomaterial for bone tissue; it

has the advantages of being easy to process and low cost [90]. Jiménez *et al.*, 2020, created a hydrogel based on poly (methylmethacrylate-co-methacrylic acid), using poly (ethylene glycol) diacrylate and polyethylene glycol as a sporogenous agent as a crosslinking agent; *In vitro* and *in vivo* biological tests showed that the chondrocytes grown in the hydrogel were capable of producing an extracellular matrix similar to hyaline cartilage and that it can promote cell proliferation, being an optimal candidate for cartilage tissue regeneration and as scaffolds in osteoarthritis treatment [91].

Pluronic diacrylate hydrogels

Pluronic diacrylate is a nonionic, water-soluble, biocompatible copolymer that can form solid hydrogels after chemical crosslinking and release drugs and active substances. It self-assembles in the presence of polar and non-polar solvents, making it useful for forming hard materials and bone nanocomposites [92]. Bao *et al.* 2020, made a hydrogel scaffold composed of nanoparticles of calcium carbonate (nanoCaCO3)/multiple hydro cyclone diacrylates (F127-DA) as an option for bone regeneration. Control of the nano space distribution of the $CaCO_3$ in the hydrogel matrix improved and regulated the mechanical properties and also acted as an intelligent source of calcium by promoting a weakly acidic environment at the bone defect site. The hydrogel obtained a gradient distribution of Ca^{2+} in its matrix, which promoted the scaffold's migration, cell growth, and osteogenic capacity, achieving controllable bone regeneration. [93]. In another study, Li e*t al.* 2023, fabricated a hydrogel based on methacrylate gelatin (GelMA)/ F127DA and Pluronic F127 aldehyde (AF127) micelles and type I collagen, applied to repair the damaged cornea. Multiple crosslinking imparts toughness to the hydrogel. White male rabbits underwent lamellar keratoplasty to evaluate the hydrogel, where the lamella was removed, and the hydrogels were applied and spread as a thin film. The evaluation was carried out for 4 weeks, resulting in a regeneration of the corneal stroma, so it has great potential for ophthalmic surgeries [94].

Polyvinyl alcohol hydrogels (PVA)

Polyvinyl alcohol is a synthetic hydrophilic biocompatible polymer with a high affinity for water, processability, and minimal cell and protein adhesion. It is used in various pharmaceutical applications, such as drug delivery, scaffolding, contact lenses, dialysis membranes, and artificial cartilage [95]. Chunshom *et al.* 2018, manufactured a hydrogel based on polyvinyl alcohol and bacterial cellulose, with which hydrogen bonds were formed along with the crosslinked hydrogel network. The hydrogel showed outstanding swelling, the presence of bacterial cellulose had an essential effect on pore size, and it presented high water absorption [96]. Shefa *et al.*, 2020, implemented a polyvinyl alcohol hydrogel (PVA) for its gelling capacity and oxidized cellulose nanofiber to improve porosity, loaded with curcumin to treat skin wounds, curcumin had to be solubilized in pluronic (F127) to solve the hydrophobicity problem it presents. A freeze-thaw process physically crosslinked the hydrogel; as the concentration of PVA increased, the viscosity also increased. In vitro tests revealed that L929 fibroblast cells absorbed curcumin, improving wound healing [97]. Huang *et al.* 2023, developed a PVA hydrogel used in regenerative medicine as a cell releaser. Evaluations showed that the hydrogel was biocompatible with stem cells, but more importantly, stem cells cultured within the hydrogel showed high viability, making the hydrogel an interesting tool in regenerative medicine [98].

Composite hydrogels

The high-water content in the hydrogel can represent a disadvantage because water swells the hydrogel's three-dimensional network, thus reducing mechanical resistance. To prepare high-resistance hydrogels, researchers have considered the introduction of different energy dissipation mechanisms in the last decades in hydrogels. The new type of compound hydrogels has significantly improved mechanical resistance and has obtained other characteristics such as self-healing and electrical conductivity. The following compound hydrogel types have been designed: interpenetrating

polymer networks (IPNs), hybrid crosslinking hydrogels, nanocomposite hydrogels, and hydrogels composed of macromolecular microspheres [13].

Interpenetrating polymer networks

According to IUPAC, an interpenetrating polymer (IPN) has at least one pair of partially interlocking networks, but there is no covalent bond between the networks. The most representative characteristic is phase separation, which is why heterogeneous phases are formed. The IPN hydrogels can respond to stimuli such as temperature, pH, electricity, and magnetic field since the networks have different characteristics from the hydrogel. The first network is rigid and gives it firmness and rigidity; the second network presents a low degree of crosslinking and functions to fill the gaps in the first network [13]. Kim *et al.*, 2018, synthesized hydrogels of interpenetrating polymer networks composed of poly (N-isopropyl acrylamide) (PNIPAM) and hyaluronic acid to administer luteolin in a controlled way for psoriasis disease. They first prepared a primary network with PNIPAM. The secondary network was hyaluronic acid and divinyl sulfone (DVS) as a crosslinking agent (Figure 4). The hydrogels were loaded with luteolin. The results showed that the hydrogel did not show cytotoxicity regardless of the concentration of the crosslinking agent; it was able to incorporate 48.2 % of luteolin and to release this drug while inflammation was produced, hydrogels were considered powerful candidates for the relief of psoriasis when inhibiting hyperproliferation of keratinocytes present in the epidermis [83]. For their part, Zhang *et al.* 2020, developed an interpenetrating network hydrogel based on polyacrylamide and serine. Polyacrylamide was the basis for the hydrogel due to its easily controllable hardness and a high degree of swelling, while sericin provided antibacterial, antioxidant, and anticancer properties, stimulating cell growth and wound healing. They used hydrogen peroxide (H_2O_2) as a chemical crosslinking agent and horseradish peroxidase as a catalyst to apply it as a dressing for skin repair due to its highly transparent, biocompatible, and bioactive properties. The hydrogel was successfully synthesized without presenting cytotoxicity and with good adhesiveness and proliferation in cell culture in mouse skin fibroblasts [79]. In 2023, Sanchez-Cid *et al.* fabricated a chitosan-based hydrogel with a semi-IPN network by dissolving chitosan in glacial acetic acid and then adding synthetic polymers crosslinked with the chitosan solution. UV light was used to form the semi-IPN network. The results reported that the degree of crosslinking affects the properties of the resulting hydrogel. As the monomer is increased, the degree of crosslinking increases; however, it decreases the wettability and hinders the formation of the hydrogel. This study concluded that a hydrogel with adequate properties is obtained if a 1/1 ratio is used, potentially for future applications in tissue engineering or drug delivery [99].

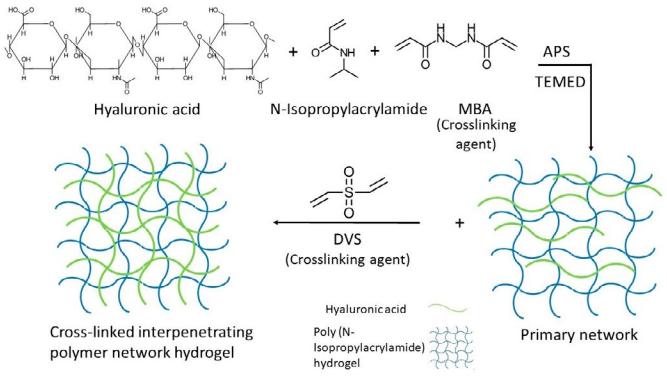

FIGURE 4. Schematic representation of an interpenetrating network hydrogel formed based on hyaluronic acid and poly (N-isopropyl acrylamide). Adapted from [13].

Hybrid crosslinking hydrogels

Covalent crosslinks and non-covalent crosslinks characterize it. Correct covalent crosslinking helps improve the hydrogel's mechanical strength, while proper non-covalent crosslinking allows the hydrogel to dissipate much energy during the deformation process [13]. Xue *et al.*, 2019, designed a hydrogel with a double physical-chemical network. The hydrogel was formed by mixing chitosan and acrylamide separately in deionized water. To continue mixing both solutions, then

liquid matrigel was added. The acrylamide and matrigel monomers formed a hybrid hydrogel by radical polymerization and physical crosslinking. The hydrogel exhibited good characteristics such as low cytotoxicity, high swelling, good stretching, and compression. The results of the in vivo tests showed that the hydrogel improved skin regeneration and consequently significantly favored wound healing [100]. In other research, Zhang et al., 2018 made an adhesive hydrogel using a hybrid crosslinking strategy. To the polyacrylamide-based hydrogel, adenine and MBA were introduced by free radical polymerization, and a hybrid network of crosslinking hydrogel was formed; adenine could generate intermolecular hydrogen-adenine bonds- Adenine and MBA served as a chemical crosslinker to form covalent bonds. The hydrogel exhibited excellent adhesiveness and toughness, capable of adhering to various surfaces of biological materials and tissues [101]. Gong *et al.* 2023, developed a gallic acid-agarose-based double network hydrogel with potential applications in wound healing. The hydrogel exhibited excellent porosity, good water retention, antimicrobial effect, and biocompatibility in vitro, while in vivo tests accelerated wound healing [102].

Nanocomposite hydrogels

Nanocomposite hydrogels are obtained by combining inorganic nanoparticles with organic polymers. Commonly used nanoparticles are silica, graphene, and silver. There are five methods to achieve a uniform distribution of nanoparticles in a hydrogel:

1) Formation of a hydrogel directly by the suspension of nanoparticles
2) Nanoparticles physically embedded in a pregelatinized hydrogel matrix
3) Formation of a hydrogel within pregelatinized nanoparticles
4) Formation of a hydrogel with nanoparticles mediated as crosslinkers
5) Formation of a hydrogel by adding a mixture of unique molecules of gellingagent

Many nanoparticles have attractive biological activities such as antioxidant, antimicrobial, antiangiogenic, anti-inflammatory, and antiplatelet properties [13]. Various types of silver, particularly silver halides, have superior bacterial properties. Pasaribu *et al.* 2018, synthesized a self-healing hydrogel based on polyacrylic acid (PAA), crosslinked with Al^{3+}, incorporating silver chloride nanoparticles; the resulting hydrogel had good antibacterial properties against Escherichia coli and improved the proliferation of L929 mouse fibroblast cells, this hydrogel could be suitable for self-healing applications [103]. On the other hand, Narayanan *et al.* 2019, made a *Lysinibacillus sphaericus* reduced graphene oxide (L-rGO) -polyacrylamide nanocomposite polymeric hydrogel, used as a scaffold to support the growth and proliferation of fibroblasts in the skin. Hydrogels were prepared using acrylamide, MBA as the crosslinking agent, and ammonium persulfate as the initiator. The results showed that hydrogels are biocompatible with human skin fibroblasts, providing an ideal extracellular matrix for the growth of human cells in tissue engineering [104]. Kumar and Kaur, 2019, prepared a polyvinyl alcohol/chitosan nanocomposite hydrogel incorporating silver nanoparticles. Adding more chitosan produces a high swelling, and adding silver nanoparticles provides mechanical resistance and flexibility. The PVA/chitosan nanocomposite hydrogels and silver nanoparticles are antimicrobial against *Staphylococcus aureus* and *Escherichia coli*, which makes them beneficial for wound dressings [105]. In another study, Chen *et al.* 2023, synthesized carboxylated polyvinyl alcohol nanocomposite hydrogels by photopolymerizing PVAGMACOOH and hydroxyapatite at nanoscale to increase cell adhesion. The carboxylated polyvinyl alcohol nanocomposite hydrogels exhibited excellent compressive strength and tensile strength. The introduction of nanoscale hydroxyapatite significantly improved the cytocompatibility and cell adhesion of the hydrogels [106]. Almajidi *et al.* 2023, In their research, they developed a novel nanocomposite scaffold based on a natural chitosan gelatin hydrogel (CS-Ge) by incorporating synthetic polyvinyl alco-

hol (PVA) and MnFe layered double hydroxides (LDH) to increase biological activity. Biological tests performed showed healthy cell line cell viability higher than 95 % after 48 and 72 h. In addition, the nanocomposite demonstrated high antibacterial activity against *Pseudomonas aeruginosa* bacterial biofilm, as confirmed through Anti-biofilm assays. In addition, mechanical tests revealed that the storage modulus was higher than the loss modulus (G'/G" > 1), confirming the appropriate elastic state of the nanocomposite [107].

Hydrogels are composed of microspheres

For the preparation of these compound hydrogels, microspheres are used as initiators and crosslinking agents; these microspheres trigger a large amount of polymerized monomers on the surface of the macromolecules to obtain the hydrogel compounds of high-resistance microspheres. The structure of this type of hydrogel is more regular. The mechanical resistance of these hydrogels depends on the following factors: the initiation time of the radicals, the concentration of the macromolecular monomers and microspheres, and the initiation temperature [13]. Imaizumi *et al.* 2019, designed a gelatin microsphere hydrogel as a scaffold to be loaded with bFGF (basic fibroblast growth factor with a short half-life) for slow release in the vocal cords as a preventive approach to minimize the risk of tumor growth. BFGF is a chemoattractant for endothelial cells and fibroblasts, and it also stimulates angiogenesis, metabolism, and extracellular matrix deposition. This investigation used bovine bone collagen to isolate gelatin through an alkaline process and crosslinking with glutaraldehyde. The study was conducted on Japanese white rabbits, where the gelatin hydrogel microspheres were injected into the injured vocal cords. To avoid leakage to the microspheres, a gelling material was added 4 to 5 minutes after mixing; if more time were allowed to gel, the needle would become clogged. The volume to be injected was careful not to cause excessive tissue swelling to avoid obstructing the airways of the rabbits. As the gelatin hydrogel microspheres were degraded, they released bFGF. The results demonstrated the regenerative potential of the growth factor contained in biodegradable gelatin hydrogel microspheres as a drug delivery system applied immediately after vocal cord injury due to the interaction of bFGF with cells that modulate the environment of the wound. The bFGF significantly helped to repair the injured vocal cords; however, hoe repaired cords do not return as whole strings [108]. Xiang-Ping *et al.*, 2023, fabricated agarose and alginate (Ag/Al) based hydrogel microspheres for stem cell encapsulation. The hydrogel obtained was required to degrade, releasing the stem cells at the desired site. This was achieved for at least 10 days, when the stem cells survived without needing nutrients or temperature control, making this hydrogel a promising device for cell-based transport and therapy [109].

Plasma modified hydrogels

Hydrogels can be used as screens during treatment with cold plasma at atmospheric pressure, or they can also be used as reservoirs for gases generated by liquid plasma, such as oxygen and nitrogen. Complex research is required to assess possible modifications to polymers in solution when exposed to cold plasma reactivity. The primary products of plasma hydrogel treatment are free radicals, unsaturated organic compounds, crosslinks between polymers, products of polymer chain destruction, and gas-phase products. The radical formation is mainly due to the impact of electrons and UV radiation. The efficacy of plasma treatment is related to generating reactive oxygen and nitrogen species in biological tissues or liquids [110]. Cyganowski *et al.*, 2019, produced a new gold nanoparticle catalyst (AuNP), synthesized by direct current cold plasma glow discharge, applied to a hydrogel used in the catalytic reduction of 4-nitrophenol (4- NP) to 4-aminophenol (4-AP), which is a fundamental substance in the elaboration of several drugs (Figure 5). Chemically synthesizing AuNPs by providing and controlling NP size was difficult but solved using cold plasma at atmospheric pressure. The results obtained

showed that the AuNPs had an average size of 7 nm, so the size could be controlled without altering the polymer matrix where they were found. The hydrogel prepared with AuNP completely reduced 4-NP to 4-AP (Figure 5) [111].

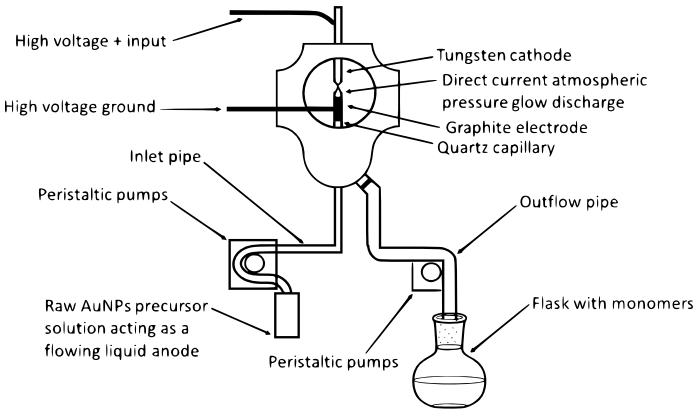

FIGURE 5. **The schematization of the plasma reactor. Adapted from [111].**

Future directions

Science has evolved, and although various hydrogels are still manufactured with only one polymeric material with good properties, the development of hydrogels currently focuses on compound hydrogels that have had a more extraordinary upswing than conventional hydrogels due to the deficiency that the material presents. It can be supplemented with another polymer so that the designed hydrogel can provide excellent mechanical and biological properties. Compound hydrogels are potential candidates for application in many fields, especially biomedical ones. The primary commitment of these new hydrogels is to comply with the requirements to be used in physiological tissues, improving their biocompatibility, biodegradability, zero toxicity properties, and increasing their mechanical properties. Achieving this continues to be a significant challenge for researchers in the coming years, so this review provides a guide for constructing hydrogels according to their final application.

CONCLUSIONS

Despite the significant progress in biomedicine, there are still many areas of opportunity to advance in the research of hydrogels to be candidates for applications in this field. Before choosing the design of the hydrogel, we should think about the final application that will have such hydrogel, as well as take into account what biological and mechanical properties are the most important that present the hydrogel to be used in wound healing, tissue engineering, regenerative medicine or for the controlled release of drugs, which any of these applications remains a significant challenge, due to the high complexity of recovery in an injured organ or wound, as well as to improve the controlled release of drugs since the traditional release can cause toxicity in an undesired site. Hydrogel is a promising dressing material due to its excellent biocompatibility, high water retention, and immune cell activation to accelerate wound healing. They have also been successfully used for scaffolding in tissue engineering. Hydrogels based on a single polymer, either natural or synthetic, continue to be widely used; however, composite hydrogels are now being heavily investigated, as using two or more polymers confers a wide range of biological and mechanical properties to the hydrogel.

ACKNOWLEDGMENTS

The authors thank the Mexican Council of Science and Technology (CONACYT), for the grant awarded to Claudia Gabriela Cuéllar Gaona, with CVU number 618041, for their doctoral studies.

AUTHOR CONTRIBUTIONS

C.G.C.G. reviewed literature and participated in the writing and editing of the original manuscript. M.C.I.A. prepared the tables and performed the drafting of the manuscript. R.I.N.C. participated in the review, editing and the validation of the final version of the manuscript. R.R.M. elaborated the figures and performed the

drafting of the manuscript. M.M.T.R. participated in the review and editing of the different stages of the manuscript. M.P.L.E. translated the manuscript to English language. All authors reviewed and approved the final version of the manuscript.

REFERENCIAS

[1] J. A. Cortés, J. E. Puig, J. A. Morales, E. Mendizábal, "Thermosensitive nanostructured hydrogels synthesized by inverse microemulsion polymerization," Rev. Mex. Ing. Quim., vol. 10, no. 3, pp. 513-520, 2011. [Online]. Available: https://www.scielo.org.mx/pdf/rmiq/v10n3/v10n3a16.pdf

[2] P. Gami, D. Kundu, S. D. Seera, T. Banerjee, "Chemically cross-linked xylan-β-Cyclodextrin hydrogel for the in vitro delivery of curcumin and 5-Fluorouracil," Int. J. Biol. Macromol., vol. 158, pp. 18-31, Sep. 2020, doi: https://doi.org/10.1016/j.ijbiomac.2020.04.237

[3] N. Guo, L. Zhang, J. Wang, S. Wang, Y. Zou, X. Wang, "Novel fabrication of morphology tailored nanostructures with Gelatin/Chitosan Co-polymeric bio-composited hydrogel system to accelerate bone fracture healing and hard tissue nursing care management," Process. Biochem., vol. 90, pp. 177-183, Mar. 2020, doi: https://doi.org/10.1016/j.procbio.2019.11.016

[4] M. Martínez-Martínez, G. Rodríguez-Berna, M. Bermejo, I. González-Alvarez, M. González-Alvarez, V. Merino, "Covalently crosslinked organophosphorus derivatives-chitosan hydrogel as a drug delivery system for oral administration of camptothecin," Eur. J. Pharm. Biopharm., vol. 136, pp. 174-183, Mar. 2019, doi: https://doi.org/10.1016/j.ejpb.2019.01.009

[5] J. Qu, Y. Liang, M. Shi, B. Guo, Y. Gao, Z. Yin, "Biocompatible conductive hydrogels based on dextran and aniline trimer as electro-responsive drug delivery system for localized drug release," Int. J. Biol. Macromol., vol. 140, pp. 255-264, Nov. 2019, doi: https://doi.org/10.1016/j.ijbiomac.2019.08.120

[6] S. Omidi, M. Pirhayati, A. Kakanejadifard, "Co-delivery of doxorubicin and curcumin by a pH-sensitive, injectable, and in situ hydrogels composed of chitosan, graphene, and cellulose nanowhisker," Carbohydr. Polym., vol. 231, art. no. 115745, Mar. 2020, doi: https://doi.org/10.1016/j.carbpol.2019.115745

[7] T. Takei, R. Yoshihara, S. Danjo, Y. Fukuhara, et al., "Hydrophobically-modified gelatin hydrogel as a carrier for charged hydrophilic drugs and hydrophobic drugs," Int. J. Biol. Macromol., vol. 149, pp. 140-147, Apr. 2020, doi: https://doi.org/10.1016/j.ijbiomac.2020.01.227

[8] C. A. Dreiss, "Hydrogel design strategies for drug delivery," Curr. Opin. Colloid Interface Sci., vol. 48, pp. 1-17, Aug. 2020, doi: https://doi.org/10.1016/j.cocis.2020.02.001

[9] M. S. Amini-Fazl, R. Mohammadi, K. Kheiri, "5-Fluorouracil loaded chitosan/polyacrylic acid/Fe3O4 magnetic nanocomposite hydrogel as a potential anticancer drug delivery system," Int. J. Biol. Macromol., vol. 132, pp. 506-513, Jul. 2019, doi: https://doi.org/10.1016/j.ijbiomac.2019.04.005

[10] G. F. B. Almeida, M. R. Cardoso, D. C. Zancanela, L. L. Bernarde, et al., "Controlled drug delivery system by fs-laser micromachined biocompatible rubber latex membranes," Appl. Surf. Sci., vol. 506, art. no. 144762, Mar. 2020, doi: https://doi.org/10.1016/j.apsusc.2019.144762

[11] S. H. Aswathy, U. Narendrakumar, I. Manjubala, "Commercial hydrogels for biomedical applications," Heliyon, vol. 6, no. 4, art. no. e03719, Apr. 2020, doi: https://doi.org/10.1016/j.heliyon.2020.e03719

[12] M. Tenje, F. Cantoni, A. M. Porras-Hernández, S. S. Searle, et al., "A practical guide to microfabrication and patterning of hydrogels for biomimetic cell culture scaffolds," Organs-on-a-Chip, art. no. 100003, Dec. 2020, doi: https://doi.org/10.1016/j.ooc.2020.100003

[13] J. Xiang, L. Shen, Y. Hong, "Status and future scope of hydrogels in wound healing: Synthesis, materials, and evaluation," Eur. Polym. J., vol. 130, art. no. 109609, May 2020, doi: https://doi.org/10.1016/j.eurpolymj.2020.109609

[14] S. Ata, A. Rasool, A. Islam, I. Bibi, et al., "Loading of Cefixime to pH-sensitive chitosan-based hydrogel and investigation of controlled release kinetics," Int. J. Biol. Macromol., pp. 1236-1244, Jul. 2020, doi: https://doi.org/10.1016/j.ijbiomac.2019.11.091

[15] Y. Qiao, S. Xu, T. Zhu, N. Tang, X. Bai, C. Zheng, "Preparation of printable double-network hydrogels with rapid self-healing and high elasticity based on hyaluronic acid for controlled drug release," Polymer, art. no. 121994, Jan. 2020, doi: https://doi.org/10.1016/j.polymer.2019.121994

[16] L. de Y. Pozzo, T. F. da Conceição, A. Spinelli, N. Scharnagl, "Chitosan coatings crosslinked with genipin for corrosion protection of AZ31 magnesium alloy sheets," Carbohydr. Polym., vol. 181, pp. 71-77, Feb. 2018, doi: https://doi.org/10.1016/j.carbpol.2017.10.055

[17] H. Samadian, H. Maleki, A. Fathollahi, M. Salehi, et al., "Naturally occurring biological macromolecules-based hydrogels: Potential biomaterials for peripheral nerve regeneration," Int. J. Biol. Macromol., vol. 154, pp. 795-817, Jul. 2020, doi: https://doi.org/10.1016/j.ijbiomac.2020.03.155

[18] M. Farrag, S, Abri, N. Leipzig, "pH-dependent RNA isolation from cells encapsulated in chitosan-based biomaterials," Int. J. Biol. Macromol., vol. 146, pp. 422-430, Mar. 2020, doi: https://doi.org/10.1016/j.ijbiomac.2019.12.263

[19] N. A. O'Connor, M. Jitianu, G. Nunez, Q. Picard, et al., "Dextran hydrogels by crosslinking with amino acid diamines and their viscoelastic properties," Int. J. Biol. Macromol., vol. 111, pp. 370-378, May 2018, doi: https://doi.org/10.1016/j.ijbiomac.2018.01.042

[20] M. C. Stanciu, M. Nichifor, "Influence of dextran hydrogel characteristics on adsorption capacity for anionic dyes," Carbohydr. Polym., vol. 199, pp. 75-83, Nov. 2018, doi: https://doi.org/10.1016/j.carbpol.2018.07.011

[21] J. E. Lee, W. H. Seung, H. K. Chae, J. P. Seong, P. Suk-Hee, K. Tae Hee, "In-situ ionic crosslinking of 3D bioprinted cell-hydrogel constructs for mechanical reinforcement and improved cell growth," Biomater. Adv., vol. 147, art. no. 213322, Apr. 2023, doi: https://doi.org/10.1016/j.bioadv.2023.213322

[22] D. A. Gyles, L. D. Castro, J. O. Carréra Silva, R. M. Ribeiro-Costa, "A review of the designs and prominent biomedical advances of natural and synthetic hydrogel formulations," Eur. Polym. J., vol. 88, pp. 373-392, Mar. 2017, doi: https://doi.org/10.1016/j.eurpolymj.2017.01.027

[23] L. Li, F. Yu, L. Zheng, R. Wang, et al., "Natural hydrogels for cartilage regeneration: Modification, preparation, and application," J. Orthop. Trans., vol. 17, pp. 26-41, Apr. 2019, doi: https://doi.org/10.1016/j.jot.2018.09.003

[24] Z, Liu, Z. Tang, L. Zhu, S. Lu, et al., "Natural protein-based hydrogels with high strength and rapid self-recovery," Int. J. Biol. Macromol., vol. 141, pp. 108-116, Dec. 2019, doi: https://doi.org/10.1016/j.ijbiomac.2019.08.258

[25] P. Nikpour, H. Salimi-Kenari, F. Fahimipour, S. M. Rabbie, M. Imani, E. Dashtimoghadam, L. Tayebi, "Dextran hydrogels incorporated with bioactive glass-ceramic: Nanocomposite scaffolds for bone tissue engineering," Carbohydr. Polym., vol. 190, pp. 281-294, Jun. 2018, doi: https://doi.org/10.1016/j.carbpol.2018.02.083

[26] M. Zhang, Y. Huang, W. Pan, X. Tong, et al., "Polydopamine-incorporated dextran hydrogel drug carrier with the tailorable structure for wound healing," Carbohydr. Polym., vol. 253, art. no. 117213, Feb. 2021, doi: https://doi.org/10.1016/j.carbpol.2020.117213

[27] C. Zheng, C. Liu, H. Chen, N. Wang, X. Liu, G. Sun, W. Qiao, "Effective wound dressing based on Poly (vinyl alcohol)/Dextran-aldehyde composite hydrogel," Int. J. Biol. Macromol., vol. 132, pp. 1098-1105, Jul. 2019, doi: https://doi.org/10.1016/j.ijbiomac.2019.04.038

[28] R. Ghaffari, H. Salimi-Kenari, F. Fahimipour, S. M. Rabbie, H. Adeli, E. Dashtimoghadam, "Fabrication and characterization of dextran/nanocrystalline β-tricalcium phosphate nanocomposite hydrogel scaffolds," Int. J. Biol. Macromol., vol. 148, pp. 434-448, Apr. 2020, doi: https://doi.org/10.1016/j.ijbiomac.2020.01.112

[29] S. O. Solomevich, P. M. Bychkovsky, T. L. Yurkshtovich, N. V. Golub, P. Y. Mirchuk, M. Y. Revtovich, A. I. Shmak, "Biodegradable pH-sensitive prospidine-loaded dextran phosphate-based hydrogels for local tumor therapy," Carbohydr. Polym., vol. 226, art. no. 115308, Dec. 2019, doi: https://doi.org/10.1016/j.carbpol.2019.115308

[30] P. Nonsuwan, A. Matsugami, F. Hayashi, S.-H. Hyon, K. Matsumura, "Controlling the degradation of an oxidized dextran-based hydrogel independent of the mechanical properties," Carbohydr. Polym., vol. 204, pp. 131-141, Jan. 2019, doi: https://doi.org/10.1016/j.carbpol.2018.09.081

[31] D.-S. Kang, S.-Y. Yang, C.-Y. Lee, "Fabrication of innocuous hydrogel scaffolds based on modified dextran for biotissues," Carbohydr. Res., vol. 522, art. no. 108699, Dec. 2022, doi: https://doi.org/10.1016/j.carres.2022.108699

[32] J. Shen, W. Jiao, Z. Chen, C. Wang, et al., "Injectable multifunctional chitosan/dextran-based hydrogel accelerates wound healing in combined radiation and burn injury," Carbohydr. Polym., vol. 316, art. no. 121024, Sep. 2023, doi: https://doi.org/10.1016/j.carbpol.2023.121024

[33] M. D. L. L. R. Menezes, H. L. Ribeiro, F. O. M. D. S. Abreu, J. P. A. Feitosa, M. S. M. S. Filho, "Optimization of the collagen extraction from Nile tilapia skin (Oreochromis niloticus) and its hydrogel with hyaluronic acid," Colloids Surf. B, vol. 189, art. no. 110852, May 2020, doi: https://doi.org/10.1016/j.colsurfb.2020.110852

[34] Y. Fang, L. Shi, Z. Duan, S. Rohani, "Hyaluronic acid hydrogels, as a biological macromolecule-based platform for stem cells delivery and their fate control: A review," Int. J. Biol. Macromol., vol. 189, pp. 554-566, Oct. 2021, doi: https://doi.org/10.1016/j.ijbiomac.2021.08.140

[35] J. Luo, Z. Wu, Y. Lu, K. Xiong, et al., "Intraperitoneal administration of biocompatible hyaluronic acid hydrogel containing multi-chemotherapeutic agents for the treatment of colorectal peritoneal carcinomatosis," Int. J. Biol. Macromol., vol. 152, pp. 718-726, Jun. 2020, doi: https://doi.org/10.1016/j.ijbiomac.2020.02.326

[36] W. Wang, D. Shi, Y. Zhang, W. Li, et al., "An injectable hydrogel based on hyaluronic acid prepared by Schiff base for long-term controlled drug releasee," Int. J. Biol. Macromol., vol. 245, art. no. 125341, Aug. 2023, doi: https://doi.org/10.1016/j.ijbiomac.2023.125341

[37] N.-G. Kim, P. Chandika, S.-C. Kim, D.-H. Won, et al., "Fabrication and characterization of ferric ion cross-linked hyaluronic acid/pectin-based injectable hydrogel with antibacterial ability," Polymer, vol. 271, art. no. 125808, Apr. 2023, doi: https://doi.org/10.1016/j.polymer.2023.125808

[38] S.R Batool, M. A. Nazeer, D. Ekinci, A. Sahin, S. Kizilel, "Multifunctional alginate-based hydrogel with reversible cross-linking for controlled therapeutics delivery," Int. J. Biol. Macromol., vol. 150, pp. 315-325, May 2020, doi: https://doi.org/10.1016/j.ijbiomac.2020.02.042

[39] B. M. Millán-Olvera, B. García-Gaitán, I. Ruiz-Aguilar, M. Flores-Castañeda, N. Ríos-Donato, J. L. García-Rivas, "Obtención y caracterización de perlas de Alginato-imidacloprid y alginato-bifentrina," Afinidad, vol. 77, art. no. 590, 2020. [Online]. Available: https://raco.cat/index.php/afinidad/article/view/371257

[40] A. R. Abbasi, M. Sohail, M. U. Minhas, T. Khaliq, M. Kousar, S. Khan, Z. Hussain, A. Munir, "Bioinspired sodium alginate-based thermosensitive hydrogel membranes for accelerated wound healing," Int. J. Biol. Macromol., vol. 155, pp. 751-765, Jul. 2020 doi: https://doi.org/10.1016/j.ijbiomac.2020.03.248

[41] A. Remes, D. Basha, T. Puehler, C. Borowski, et al., "Alginate hydrogel polymers enable efficient delivery of a vascular-targeted AAV vector into aortic tissue," Mol. Ther. Methods Clin. Dev., vol. 21, pp. 83-93, Jun. 2021, doi: https://doi.org/10.1016/j.omtm.2021.02.017

[42] R. Zhang, L. Lei, Q. Song, X. Li, "Calcium ion cross-linking alginate/dexamethasone sodium phosphate hybrid hydrogel for extended drug release," Colloids Surf. B, vol. 175, pp. 569-575, Mar. 2019, doi: https://doi.org/10.1016/j.colsurfb.2018.11.083

[43] X. Sun, C. Ma, W. Gong, Y. Ma, Y. Ding, L. Liu, "Biological properties of sulfanilamide-loaded alginate hydrogel fibers based on ionic and chemical crosslinking for wound dressings," Int. J. Biol. Macromol., vol. 157, pp. 522-529, Aug. 2020, doi: https://doi.org/10.1016/j.ijbiomac.2020.04.210

[44] X. Yang, W. Mo, Y. Shi, X. Fang, Y. Xu, X. He, Y. Xu, "Fumaria officinalis-loaded chitosan nanoparticles dispersed in an alginate hydrogel promote diabetic wounds healing by upregulating VEGF, TGF-β, and b-FGF genes: A preclinical investigation," Helyon, vol. 9, no. 7, art. no. e17704, Jul. 2023, doi: https://doi.org/10.1016/j.heliyon.2023.e17704

[45] G.-Q. Fu, S.-C. Zhang, G.-G. Chen, X. Hao, J. Bian, F. Peng, "Xylan-based hydrogels for potential skincare application," Int. J. Biol. Macromol., vol. 158, pp. 244-250, Sep. 2020, doi: https://doi.org/10.1016/j.ijbiomac.2020.04.235

[46] S. Sharifi, M. M. Islam, H. Sharifi, R. Islam, et al., "Tuning gelatin-based hydrogel towards bioadhesive ocular tissue engineering applications," Bioact. Mater., vol. 6, no. 11, pp. 3947-3961, Nov. 2021, doi: https://doi.org/10.1016/j.bioactmat.2021.03.042

[47] T. Takei, R. Yoshihara, S. Danjo, Y. Fukuhara, et al., "Hydrophobically-modified gelatin hydrogel as a carrier for charged hydrophilic drugs and hydrophobic drugs," Int. J. Biol. Macromol., vol. 149, pp. 140-147, Apr. 2020, doi: https://doi.org/10.1016/j.ijbiomac.2020.01.227

[48] M. Anamizu, Y. Tabata, "Design of injectable hydrogels of gelatin and alginate with ferric ions for cell transplantation," Acta Biomater., vol. 100, pp. 184-190, Dec. 2019, doi: https://doi.org/10.1016/j.actbio.2019.10.001

[49] G. González-Ulloa, M. Jiménez-Rosado, M. Rafii-El-Idrissi Benhnia, A. Romero, E. Ruiz-Mateos, F.J. Ostos, V. Perez-Puyana, "Hybrid polymeric Hydrogel-based biomaterials with potential applications in regenerative medicine," J. Mol. Liq., vol. 384, art. no. 122224, Aug. 2023, doi: https://doi.org/10.1016/j.molliq.2023.122224

[50] A. Alehosseini, E.-M. Gomez del Pulgar, M. J. Fabra, L. G. Gómez-Mascaraque, et al., "Agarose-based freeze-dried capsules prepared by the oil-induced biphasic hydrogel particle formation approach for the protection of sensitive probiotic bacteria," Food Hydrocoll., vol. 87, pp. 487-496, Feb. 2019, doi: https://doi.org/10.1016/j.foodhyd.2018.08.032

[51] B. Bagheri, P. Zarrintaj, S. S. Surwase, N. Baheiraei, et al., "Self-gelling electroactive hydrogels based on chitosan-aniline oligomers/agarose for neural tissue engineering with on-demand drug release," Colloids Surf. B, vol. 184, art. no. 110549, Dec. 2019, doi: https://doi.org/10.1016/j.colsurfb.2019.110549

[52] Y. Yuan, L. Wang, R.-J. Mu, J. Gong, et al., "Effects of konjac glucomannan on the structure, properties, and drug release characteristics of agarose hydrogels," Carbohydr. Polym., vol. 190, pp. 196-203, Jun. 2018, doi: https://doi.org/10.1016/j.carbpol.2018.02.049

[53] J. Li, C. Wu, P. K. Chu, M. Gelinsky, "3D printing of hydrogels: Rational design strategies and emerging biomedical applications," Mater. Sci. Eng. R. Rep., vol. 140, art. no. 100543, Apr. 2020, doi: https://doi.org/10.1016/j.mser.2020.100543

[54] F. Topuz, A. Nadernezhad, O. S. Caliskan, Y. Z. Menceloglu, B. Kac, "Nanosilicate embedded agarose hydrogels with improved bioactivity," Carbohydr. Polym., vol. 201, pp. 105-112, Dec. 2018, doi: https://doi.org/10.1016/j.carbpol.2018.08.032

[55] X. Qi, T. Su, X. Tong, W. Xiong, et al., "Facile formation of sale can/agarose hydrogels with tunable structural properties for cell culture," Carbohydr. Polym., vol. 224, art. no. 115208, Nov. 2019, doi: https://doi.org/10.1016/j.carbpol.2019.115208

[56] M.I. Patiño Vargas, F.D. Martinez-Garcia, F. Offens, N.Y. Becerra, et al., Viscoelastic properties of plasma-agarose hydrogels dictate favorable fibroblast responses for skin tissue engineering applications," Biomater. Adv., vol. 139, art. no. 212967, Aug. 2022, doi: https://doi.org/10.1016/j.bioadv.2022.212967

[57] R. García-González, R. E. Zavala-Arce, P. Ávila-Pérez, B. García-Gaitán, J. L. González-Chávez, C. Muro-Urista, G. Luna-Bárcenas, "Síntesis y caracterización de un material criogénico a partir de quitosano y celulosa," Afinidad, vol. 71, art. no. 567, 2014. [Online]. Available: https://raco.cat/index.php/afinidad/article/view/281148/368860

[58] J. O. Gonçalves, J. P. Santos, E. C. Rios, M. M. Crispim, G. L. Dotto, L. A. A. Pinto, "Development of chitosan-based hybrid hydrogels for dyes removal from an aqueous binary system," J. Mol. Liq., vol. 225, pp. 265-270, Jun. 2019, doi: https://doi.org/10.1016/j.molliq.2016.11.067

[59] K. Kaur, R. Jindal, "Comparative study on the behavior of Chitosan-Gelatin based Hydrogel and nanocomposite ion exchanger synthesized under microwave conditions towards photocatalytic removal of cationic dyes," Carbohydr. Polym., vol. 207, pp. 398-410, Mar. 2019, doi: https://doi.org/10.1016/j.carbpol.2018.12.002

[60] M. Imran, M. Sajwan, B. Alsuwayt, M. Asif, "Synthesis, characterization, and anticoagulant activity of chitosan derivatives," Saudi Pharm. J., vol. 28, no. 1, pp. 25-32, Jan. 2020, doi: https://doi.org/10.1016/j.jsps.2019.11.003

[61] P. S. Pauletto, J. O. Gonçalves, L. A. A. Pinto, G. L. Dotto, N. P. G. Salau, "Single and competitive dye adsorption onto chitosan-based hybrid hydrogels using artificial neural network modeling," J. Colloid Interface Sci., vol. 560, pp. 722-729, Feb. 2020, doi: https://doi.org/10.1016/j.jcis.2019.10.106

[62] L. Quihui-Cota, G. G. Morales-Figueroa, E. Valbuena-Gregorio, J. C. Campos-García, N. P. Silva-Beltrán, M. A. López-Mata, "Membrana de Quitosano con Aceites Esenciales de Romero y Árbol de Té: Potencial como Biomaterial," Rev. Mex. Ing. Biomed., vol. 38, no. 1, pp. 255 -264, Jan. 2017, doi: https://doi.org/10.17488/RMIB.38.1.20

[63] A. M. Heimbuck, T. R. Priddy-Arrington, B. J. Sawyer, M. E. Caldorera-Moore, "Effects of post-processing methods on chitosan-genipin hydrogel properties," Mater. Sci. Eng. C, vol. 98, pp. 612-618, May 2019, doi: https://doi.org/10.1016/j.msec.2018.12.119

[64] H. Tashakkorian, V. Hasantabar, A. Mostafazadeh, M. Golpour, "Transparent chitosan-based nanocomposite hydrogel: Synthesis, thermophysical characterization, cell adhesion, and viability assay," Int. J. Biol. Macromol., vol. 144, pp. 715-724, Feb. 2020, doi: https://doi.org/10.1016/j.ijbiomac.2019.10.157

[65] T. Songkroh, H. Xie, W. Yu, G. Lv, et al., "Erratum to: In situ forming chitosan-based hydrogel as a lung sealant for biological lung volume reduction," Sci. Bull., vol. 60, no. 2, pp. 235-240, Jan. 2015, doi: https://doi.org/10.1007/S11434-014-0548-3

[66] D. Dehghan-Baniani, Y. Chen, D. Wang, R. Bagheri, A. Solouk, H. Wu, "Injectable in situ forming kartogenin-loaded chitosan hydrogel with tunable rheological properties for cartilage tissue engineering," Colloids Surf. B, vol. 192, art. no. 111059, Aug. 2020, doi: https://doi.org/10.1016/j.colsurfb.2020.111059

[67] K. Thongchai, P. Chuysinuan, T. Thanyacharoen, S. Techasakul, S. Ummartyotin, "Characterization, release, and antioxidant activity of caffeic acid-loaded collagen and chitosan hydrogel composites," J. Mater. Res. Technol., vol. 9, no. 3, pp. 6512-6520, May 2020, doi: https://doi.org/10.1016/j.jmrt.2020.04.036

[68] J. Wang, W. Xu, W. Zhang, J. Da, et al., "UV cross-linked injectable non-swelling dihydrocaffeic acid grafted chitosan hydrogel for promoting wound healing," Carbohydr. Polym., vol. 314, art. no. 120926, Aug. 2023, doi: https://doi.org/10.1016/j.carbpol.2023.120926

[69] J. M. Gutiérrez-Hernández, C. Castorena-Alejandro, D. M. Escobar-García, A. Escalante, et al., "In vitro evaluation of spruce xylan/MWCNTs hydrogel scaffolds for bone regeneration," Mater. Today. Commun., vol. 35, art. no. 106070, Jun. 2023, doi: https://doi.org/10.1016/j.mtcomm.2023.106070

[70] Y. Kambe, "Functionalization of silk fibroin-based biomaterials for tissue engineering," Polym. J., vol. 53, Jul. 2021, doi: https://doi.org/10.1038/s41428-021-00536-5

[71] Z. Li, J. Song, J. Zhang, K. Hao, et al., "Topical application of silk fibroin-based hydrogel in preventing hypertrophic scars," Colloids Surf. B, vol. 186, art. no. 110735, Feb. 2020, doi: https://doi.org/10.1016/j.colsurfb.2019.110735

[72] D. Gaviria Arias, L. C. Caballero Mendez, "Fibroin from silkworm (Bombix mori L.) as biomaterial used in regenerative medicine process based on tissue engineering," Rev. Méd. Risaralda, vol. 21, no. 1, pp. 38-47, 2015. [Online]. Available: http://www.scielo.org.co/pdf/rmri/v21n1/v21n1a08.pdf

[73] H. Wang, H. Wan, Q. Wang, Y. Ma, G. Su, X. Cao, H. Gao, "Engineered multifunctional silk fibroin/gelatin hydrogel conduit loaded with miR-29a@ZIF-8 nanoparticles for peripheral nerve regeneration," Smart Mater. Med., vol. 4, pp. 480-496, 2023, doi: https://doi.org/10.1016/j.smaim.2023.02.002

[74] L. D. Amer, L. S. Saleh, C. Walker, S. Thomas, W. J. Janssen, S. Alper, S. J. Bryant, "Inflammation via myeloid differentiation primary response gene 88 signaling mediates the fibrotic response to implantable synthetic poly(ethylene glycol) hydrogels," Acta Biomater., vol. 100, pp. 105-117, Dec. 2019, doi: https://doi.org/10.1016/j.actbio.2019.09.043

[75] M. Guvendiren, J. A. Burdick, "Engineering synthetic hydrogel microenvironments to instruct stem cells," Curr. Opin. Biotechnol., vol. 24, no. 5, pp. 841-846, Oct. 2013, doi: https://doi.org/10.1016/j.copbio.2013.03.009

[76] R. Cruz-Acuña, A. J. García, "Synthetic hydrogels mimicking basement membrane matrices to promote cell-matrix interactions," Matrix Biol., vol. 57-58, pp. 324-333, Jan. 2017, doi: https://doi.org/10.1016/j.matbio.2016.06.002

[77] N. S. Alghunaim, "Characterization of selenium oxide nanofiller effect on the spectroscopic and thermal properties of Cs/PAM nanocomposites," J. Mater. Res. Technol., vol. 9, no. 3, pp. 3502-3510, 2020, doi: https://doi.org/10.1016/j.jmrt.2020.01.087

[78] D. Zhao, M. Feng, L. Zhang, B. He, X. Chen, J. Sun, "Facile synthesis of self-healing and layered sodium alginate/polyacrylamide hydrogel promoted by dynamic hydrogen bond," Carbohydr. Polym., vol. 256, art. no. 117580, Mar. 2021, doi: https://doi.org/10.1016/j.carbpol.2020.117580

[79] Y. Zhang, H. Chen, Y. Li, A. Fang, et al., "A transparent sericin-polyacrylamide interpenetrating network hydrogel as visualized dressing material," Polym. Test., vol. 87, art. no. 106517, Jul. 2020, doi: https://doi.org/10.1016/j.polymertesting.2020.106517

[80] S. R. McClure, C. Wang, "A Preliminary Field Trial Evaluating the Efficacy of 4% Polyacrylamide Hydrogel in Horses With Osteoarthritis," J. Equine Vet. Sci., vol. 54, pp. 98-102, Jul. 2017, doi: https://doi.org/10.1016/j.jevs.2017.02.019

[81] Y. Chen, X. Fan, X. Liu, C. Meng, et al., "Highly stretchable, adhesive and antibacterial double-network hydrogels toward flexible strain sensor," Polym. Test., vol. 124, art. no. 108087, Jul. 2023, doi: https://doi.org/10.1016/j.polymertesting.2023.108087

[82] Z. Liu, W. Tang, J. Liu, Y. Han, et al., "A novel sprayable thermosensitive hydrogel coupled with zinc modified metformin promotes the healing of skin wound," Bioact. Mater., vol. 20, pp. 610-626, Feb. 2023, doi: https://doi.org/10.1016/j.bioactmat.2022.06.008

[83] A. R. Kim, S. L. Lee, S. N. Park, "Properties and in vitro drug release of pH- and temperature-sensitive double cross-linked interpenetrating polymer network hydrogels based on hyaluronic acid/poly (N-isopropyl acrylamide) for transdermal delivery of luteolin," Int. J. Biol. Macromol., vol. 118, pp. 731-740, Oct. 2018 doi: https://doi.org/10.1016/j.ijbiomac.2018.06.061

[84] M. Martinez-Moro, J. Jenczyk, J. M. Giussi, S. Jurga, S. E. Moya, "Kinetics of the thermal response of poly(N-isopropylacrylamide co methacrylic acid) hydrogel microparticles under different environmental stimuli: A time-lapse NMR study," J. Colloid Interface Sci., vol. 580, pp. 439-448, Nov. 2020, doi: https://doi.org/10.1016/j.jcis.2020.07.049

[85] N. Shivshetty, T. Swift, A. Pinnock, D. Pownall, et al., "Evaluation of ligand modified poly (N-Isopropyl acrylamide) hydrogel for etiological diagnosis of corneal infection," Exp. Eye Res., vol. 214, art. no. 108881, Jan. 2022, doi: https://doi.org/10.1016/j.exer.2021.108881

[86] G. Damonte, M. Cozzani, D. Di Lisa, L. Pastorino, A. Mariani, O. Monticelli, "Mechanically-reinforced biocompatible hydrogels based on poly(N-isopropylacrylamide) and star-shaped polycaprolactones," Eur. Polym. J., vol. 195, art. no. 112239, Aug. 2023, doi: https://doi.org/10.1016/j.eurpolymj.2023.112239

[87] A. Janse van Rensburg, N. H. Davies, A. Oosthuysen, C. Chokoza, P. Zilla, D. Bezuidenhout, "Improved vascularization of porous scaffolds through growth factor delivery from heparinized polyethylene glycol hydrogels," Acta Biomater., vol. 49, pp. 89-100, Feb. 2017, doi: https://doi.org/10.1016/j.actbio.2016.11.036

[88] A. Navaratnam, J. Cumsky, H. Abdul-Mushin, J. Gagneur, et al., "Assessment of Polyethylene Glycol Hydrogel Spacer and Its Effect on Rectal Radiation Dose in Prostate Cancer Patients Receiving Proton Beam Radiation Therapy," Adv. Radiat. Oncol., vol. 5, no. 1, pp. 92-100, Sep. 2019, doi: https://doi.org/10.1016/j.adro.2019.08.007

[89] Y. Fan, M. Lüchow, A. Badria, D. J. Hutchinson, M. Malkoch, "Placenta Powder-Infused Thiol-Ene PEG Hydrogels as Potential Tissue Engineering Scaffolds," Biomacromolecules, vol. 24, no. 4, pp. 1617-1626, 2023, doi: https://doi.org/10.1021/acs.biomac.2c01355

[90] T.-M. De Witte, A. M. Wagner, L. E. Fratila-Apachitei, A. A. Zadpoor, N. A. Peppas, "Degradable Poly(Methyl Methacrylate)-co-Methacrylic Acid Nanoparticles for Controlled Delivery of Growth Factors for Bone Regeneration," Tissue Eng. Part A, vol. 26, no. 23-24. pp. 1226-1242, Dec. 2020, doi: https://doi.org/10.1089/ten.tea.2020.0010

[91] G. Jiménez, S. Venkateswaran, E. López-Ruiz, M. Perán, et al., "A soft 3D polyacrylate hydrogel recapitulates the cartilage niche and allows growth-factor free tissue engineering of human articular cartilage," Acta Biomater., vol. 90, pp. 146-156, May 2019, doi: https://doi.org/10.1016/j.actbio.2019.03.040

[92] A. Stepulane, K. Ahlgren, A. Rodriguez-Palomo, A. K. Rajasekharan, M. Andersson, "Lyotropic liquid crystal elastomers for drug delivery," Colloids Surf. B, vol. 226, art. no. 113304, Jun. 2023, doi: https://doi.org/10.1016/j.colsurfb.2023.113304

[93] Z. Bao, Z. Gu, J. Xu, M. Zhao, G. Liu, J. Wu, "Acid-responsive composite hydrogel platform with space-controllable stiffness and calcium supply for enhanced bone regeneration," Chem. Eng. J., vol. 396, art. no. 125353, Sep. 2020, doi: https://doi.org/10.1016/j.cej.2020.125353

[94] M. Li, R. Wei, C. Liu, H. Fang, et al., "A "T.E.S.T." hydrogel bioadhesive assisted by corneal cross-linking for in situ sutureless corneal repair," Bioact. Mater., vol. 25, pp. 333-346, Jul. 2023, doi: https://doi.org/10.1016/j.bioactmat.2023.02.006

[95] A. S. Montaser, M. Rehan, M. E. El-Naggar, "pH-Thermosensitive hydrogel based on polyvinyl alcohol/sodium alginate/N-isopropyl acrylamide composite for treating re-infected wounds," Int. J. Biol. Macromol., vol. 124, pp. 1016-1024, Mar. 2019, doi: https://doi.org/10.1016/j.ijbiomac.2018.11.252

[96] N. Chunshom, P. Chuysinuan, S. Techasakul, S. Ummartyotin, "Dried-state bacterial cellulose (Acetobacter xylinum) and polyvinyl-alcohol-based hydrogel: An approach to a personal care material," J. Sci. Adv. Mater. Dev., vol. 3, no. 3, pp. 296-302, Sep. 2018, doi: https://doi.org/10.1016/j.jsamd.2018.06.004

[97] A. A. Shefa, T. Sultana, M. K. Park, S. Y. Lee, J.-G. Gwon, B.-T. Lee, "Curcumin incorporation into an oxidized cellulose nanofiber-polyvinyl alcohol hydrogel system promotes wound healing," Mater. Des., vol. 186, art. no. 108313, Jan. 2020, doi: https://doi.org/10.1016/j.matdes.2019.108313

[98] Z. Huang, X. Xiao, X. Jiang, S. Yang, et al., "Preparation and evaluation of a temperature-responsive methylcellulose/polyvinyl alcohol hydrogel for stem cell encapsulation," vol. 119, art. no. 107936, Feb. 2023, doi: https://doi.org/10.1016/j.polymertesting.2023.107936

[99] P. Sánchez-Cid, A. Romero, M.J. Díaz, M.V. de-Paz, V. Perez-Puyana, "Chitosan-based hydrogels obtained via photoinitiated click polymer IPN reaction," J. Mol. Liq., vol. 379, art. no. 121735, Jun. 2023, doi: https://doi.org/10.1016/j.molliq.2023.121735

[100] H. Xue, L. Hu, Y. Xiong, X. Zhu, et al., "Quaternized chitosan-Matrigel-polyacrylamide hydrogels as a wound dressing for wound repair and regeneration," Carbohydr. Polym., vol. 226, art. no. 115302, Dec. 2019, doi: https://doi.org/10.1016/j.carbpol.2019.115302

[101] Q. Zhang, X. Liu, X. Ren, L. Duan, G. Gao, "Adenine-mediated adhesive and tough hydrogel based on hybrid crosslinking," Eur. Polym. J., vol. 106, pp. 139-147, Sep. 2018, doi: https://doi.org/10.1016/j.eurpolymj.2018.07.018

[102] W. Gong, R. Wang, H. Huang, Y. Hou, et al., "Construction of double network hydrogels using agarose and gallic acid with antibacterial and anti-inflammatory properties for wound healing," Int. J. Biol. Macromol., vol. 227, pp. 698-710, Feb. 2023, doi: https://doi.org/10.1016/j.ijbiomac.2022.12.085

[103] S. P. Pasaribu, M. Ginting, I. Masmur, J. Kaban, Hestina, "Silver chloride nanoparticles embedded in self-healing hydrogels with biocompatible and antibacterial properties," J. Mol. Liq., vol. 310, art. no. 113263, Jul. 2020, doi: https://doi.org/10.1016/j.molliq.2020.113263

[104] K. B. Narayanan, S. M. Choi, S. S. Han, "Biofabrication of Lysinibacillus sphaericus-reduced graphene oxide in three-dimensional polyacrylamide/carbon nanocomposite hydrogels for skin tissue engineering," Colloids Surf. B, vol. 181, pp. 539-548, Sep. 2019, doi: https://doi.org/10.1016/j.colsurfb.2019.06.007

[105] A. Kumar, H. Kaur, "Sprayed in-situ synthesis of polyvinyl alcohol/chitosan loaded silver nanocomposite hydrogel for improved antibacterial effects," Int. J. Biol. Macromol., vol. 145, pp. 950-964, Feb. 2020, doi: https://doi.org/10.1016/j.ijbiomac.2019.09.186

[106] X. Chen, M. Zhang, D. Zhu, J. Zhang, et al., "Photocrosslinkable carboxylated polyvinyl alcohol nanocomposite hydrogels with enhanced compressive strength and cell adhesion," Eur. Polym. J., vol. 196, art. no. 112252, Sep. 2023, doi: https://doi.org/10.1016/j.eurpolymj.2023.112252

[107] Y. Q. Almajidi, S. S. Abdullaev, B. G. Alani, E. A. M. Saleh, et al., "Chitosan-gelatin hydrogel incorporating polyvinyl alcohol and MnFe double-layered hydroxide nanocomposites with biological activity," Int. J. Biol. Macromol., vol. 246, art. no. 125566, Aug. 2023, doi: https://doi.org/10.1016/j.ijbiomac.2023.125566

[108] M. Imaizumi, R. Nakamura, Y. Nakaegawa, B. T. Dirja, et al., "Regenerative potential of basic fibroblast growth factor contained in biodegradable gelatin hydrogel microspheres applied following vocal fold injury: Early effect on tissue repair in a rabbit model," Braz. J. Otorhinolaryngol., vol. 87, no. 3, pp. 274-282, May 2021, doi: https://doi.org/10.1016/j.bjorl.2019.09.003

[109] M. K. Xiang Ping, H. W. Zhi, N.S. Aziz, N. A. Hadri, N. F. Ghazalli, N. Yusop, "Optimization of agarose-alginate hydrogel bead components for encapsulation and transportation of stem cells," J. Taibah Univ. Medical Sci., vol. 18, no. 1, pp. 104-116, Feb. 2023, doi: https://doi.org/10.1016/j.jtumed.2022.08.009

[110] I. Hamouda, C. Labay, M. P. Ginebra, E. Nicol, C. Canal, "Investigating the atmospheric pressure plasma jet modification of a photo-cross-linkable hydrogel," Polymer, vol. 192, art. no. 122308, Mar. 2020, doi: https://doi.org/10.1016/j.polymer.2020.122308

[111] P. Cyganowski, D. Jermakowicz-Bartkowiak, P. Jamroz, P. Pohl, A. Dzimitrowicz, "Hydrogel-based nanocomposite catalyst containing uncoated gold nanoparticles synthesized using cold atmospheric pressure plasma for the catalytic decomposition of 4-nitrophenol," Colloids Surf. A, vol. 582, art. no. 123886, Dec. 2019, doi: https://doi.org/10.1016/j.colsurfa.2019.123886